AFWL-TR-65-94

CURRENTS INDUCED IN CABLES IN THE EARTH BY A CONTINUOUS-WAVE ELECTROMAGNETIC FIELD

Donald R. Marston, 1Lt, USAF
William R. Graham, 1Lt, USAF

[redacted]

TECHNICAL REPORT NO. AFWL-TR-65-94

May 1966

AIR FORCE WEAPONS LABORATORY
Research and Technology Division
Air Force Systems Command
Kirtland Air Force Base
New Mexico

AFWL-TR-65-94

Research and Technology Division
AIR FORCE WEAPONS LABORATORY
Air Force Systems Command
Kirtland Air Force Base
New Mexico

CURRENTS INDUCED IN CABLES IN THE EARTH BY A CONTINUOUS-WAVE ELECTROMAGNETIC FIELD

Donald R. Marston, 1Lt, USAF

William R. Graham, 1Lt, USAF

TECHNICAL REPORT NO. AFWL-TR-65-94

Distribution of this document is unlimited.

FOREWORD

This report was prepared under Program Element 7.60.06.01.D, Project 5710, Task 571004. Inclusive dates of research were January 1964 through June 1965. The report was submitted by the authors 1 April 1966.

The authors wish to thank Dr. C. E. Long and Major W. D. Henderson for their assistance in the preparation of this report.

This report has been reviewed and is approved.

Donald R. Marston

DONALD R. MARSTON
1Lt USAF
Project Officer

Donald A. Dowler for

CLYDE C. REYNOLDS
Lt Colonel USAF
Chief, Physics Branch

William H. Stephens

WILLIAM H. STEPHENS
Colonel USAF
Chief, Research Division

ABSTRACT

The problem under examination is the determination of the currents induced by a distributed continuous-wave electromagnetic field in a conducting wire buried in the earth.

Transmission line theory is shown to provide a suitable approximation for studying this problem. A program for machine computation, utilizing this theory, was written to calculate the induced current. The special cases examined are: a bare wire with open circuit terminations, an insulated wire with either open circuit terminations or grounded terminations, and a wire encased in a high-conductivity coating with open circuit terminations.

The theoretical calculations are compared with experimental results obtained by Stanford Research Institute. The comparison of the theoretical and experimental results indicates that predictions of practical value can be made by using the transmission-line model.

This page intentionally left blank.

CONTENTS

ILLUSTRATIONS

ILLUSTRATIONS (cont'd)

ABBREVIATIONS AND SYMBOLS

Abbreviations

CW	continuous wave
TM	transverse magnetic field
TE	transverse electric field
EM	electromagnetic
cps	cycles per second
kc, kcs	kilocycles per second (10^3 cps)
Mc, Mcs	megacycles per second (10^6 cps)
pf	picofarad (10^{-12} farad)

Coordinate Systems (all lengths in meters, all angles in radians)

x,y,z	rectangular coordinate system
r,θ,z	cylindrical coordinate system used with wire analysis
r_c,θ_c,z_c	cylindrical coordinate system used with antenna analysis
r_s	spherical distance coordinate used at antenna base or wire termination
r'_s, θ'_s, ϕ_s	spherical coordinate system used in antenna analysis
z_c, z	cylindrical or rectangular coordinate along wire axis
x,y,v	used as dummy variables (for integrations, etc.)
$\frac{\partial}{\partial t}$	partial derivative wrt time (second^{-1})
$\vec{\nabla}$	the spacial derivative vector (meter^{-1})
$\vec{d\ell}$	a differential line element along a given path
$\vec{ds}$	a differential area element with direction perpendicular to the plane of the surface (meter^2).

Constants

Π	3.14159265
γ	1.781
i	$\sqrt{-1}$
μ_o	$4\Pi \times 10^{-7}$ henries/meter
ε_o	$10^{-9}/36\Pi$ farads/meter

ABBREVIATIONS AND SYMBOLS (cont'd)

Known Dimensions (meters)

a	wire radius
b	radius of the outer conductor of a coaxial transmission line
t	thickness of the insulation
a'	radius of the grounding rod for the wire termination
l'	length of the grounding rod for the wire termination
h'	height of the monopole antenna

Electrical Characteristics of the Media

μ_j	magnetic permeability (henries/meter)
σ_j	conductivity (mhos/meter)
ε_j	dielectric permittivity (farads/meter)
k_j	propagation constant for a given EM wave in the medium (meters^{-1})
δ_j	a skin depth for a given EM wave in the medium (meters)
j=0	pertains to air (or free space)
j=1	pertains to the metal of the wire
j=2	pertains to the earth material
j=3	pertains to the insulation (or covering) material
η_G	characteristics impedance of the earth (ohms)

Electrical Characteristics of the Wire

Z_o	characteristic impedance of the equivalent transmission line representing the wire (ohms)
Z	the longitudinal impedance per unit length of the wire (ohms/meter)
Z_t	the transverse impedance of the wire (ohm-meters)
Y_t	the transverse admittance per unit length of the wire (mhos/meter)
Z_L	the inductive impedance per unit length of the wire (ohms/meter)
Z_s	the skin impedance (surface impedance) per unit length of the wire (ohms/meter)
Γ,h	the propagation constant for the currents in the wire (meter^{-1})
L_o	the inductance per unit length of the wire (henry/meter)
L'	the total inductance per unit length of the wire, including skin inductance (henry/meter)
R	the resistance per unit length of the wire (ohms/meter)
G'	the total conductive admittance per unit length of the wire (mhos/meter)

ABBREVIATIONS AND SYMBOLS (cont'd)

C' — the total capacitance per unit length of the wire (farad/meter)

R_i — the resistance of the wire covering (ohm-meters)

G_i — the conductive admittance per unit length of the wire covering (mhos/meter)

R_g — the resistance to ground of the wire from outside its covering (ohm-meter)

G_g — the conductive admittance per unit length to ground of the wire from outside its covering (mhos/meter)

C_i — the capacitance per unit length of the wire covering (farads/meter)

C_g — the capacitance per unit length to ground of the wire from outside its covering (farads/meter)

Z_e — the impedance of a given grounding technique at a wire termination (ohms)

Z_1, Z_2 — the given impedances at the two wire terminations, used to determine the reflection coefficients (ohms)

K, L — the reflection coefficients at each of the two wire terminations

<u>Currents and Fields</u>

$\vec{\Pi}$, Π_q — the Hertz vector and its component in the q direction (volt-meters)

$\vec{B}$, B_q — the magnetic flux density (webers/meter^2)

$\vec{H}$, H_q — the magnetic field intensity (ampere-turns/meter)

$\vec{E}$, E_q — the electric field intensity (volts/meter)

E_o, E_{zo} — the electric field component that induces the current on a given wire (volts/meter)(this field is measured in the <u>absence</u> of the wire)

Φ — the magnetic flux per unit length generated by the wire current (webers)

I, I_z — the current in the wire at a given point (amperes)

V, V_r — the voltage wrt ground of a point on the wire (volts)

I_e — the current at a given wire termination (amperes) (used to determine Z_e)

V_e — the voltage wrt ground at a given wire termination (volts) (used to determine Z_e)

I_o — the base current in the monopole antenna (amperes)

$F(z)$ — the integral term in the expression for induced cable currents in a wire

Others

ω	the frequency of a given field or current (radians/second)
a_n^i, a_n^e	the constants for the nth order fields (internal and external respectively) produced by a current in a wire
λ_i	$\sqrt{k_i^2 - h^2}$
u	$\lambda_1 a$
ν	$\lambda_2 a$
$Z_n(x)$	an nth order cylinder function of argument x
$J_n(x)$	an nth order Bessel function of argument x
$H_n^{(1)}(x)$	an nth order Hankel function of the first kind, argument x
G(x)	the exponential integral function of argument x

$$Z_n'(x) = \frac{dZ_n(x)}{dx}$$

This page intentionally left blank.

SECTION I

INTRODUCTION

Currents induced in conductors in the ground have long been a problem of interest to those who must protect long power and communication cables from the high-current pulses created by a lightning stroke (ref. 1). In recent years the high-energy electromagnetic pulse created by a nuclear detonation has created another source of danger to these cables, especially those power and communication cables associated with a military defense system (ref. 2). To protect against these highly disruptive currents adequately and economically, we must understand the theory of the production of these currents. This study is the first step of a theory to determine the currents induced in long cables by pulsed electromagnetic fields.

This paper will derive theoretically a general method for calculating the currents induced in a finite length of conductor, which is lying on the surface of the earth or buried approximately parallel to the earth-air interface, by a continuous-wave (CW) distributed electric field parallel to the conductor. This theory for CW field-induced cable currents will then be compared with data obtained from current measurements on a cable in the field of a vertical dipole antenna (ref. 3). The limitations in the practical use of this theory will be presented, with examples of these limitations taken from the comparison of the theory with the data.

SECTION II

THEORY

A basic difficulty is encountered when we try to solve general classes of electromagnetic boundary value problems involving time-varying fields. General solutions to static-field boundary values problems governed by Laplace's equation are found by the technique of separation of variables (ref. 4). However, with time-varying fields, solving the vector wave equation using the separation of variables technique in general is very difficult.

The Fields Near a Cylindrical Wire

The vector wave equation reduces to the more tractable scalar wave equation when all of the electromagnetic fields are expressed in terms of their rectangular components. Each field component independently satisfies the scalar wave equation. This method will be used to determine the fields in and near a solid cylindrical conductor of infinite length buried in a medium of infinite extent (ref. 5).

A convenient field variable to use as the unknown for finding the fields around a conductor buried in the earth is the Hertz vector, $\vec{\Pi}$ (ref 6). There are two ways in which the electric and magnetic fields may be related to the Hertz vector. In the first relation, the Hertz vector $\vec{\Pi}_{(1)}$ is related to the fields $\vec{E}_{(1)}$ and $\vec{H}_{(1)}$ by the equations

$$\begin{aligned} \vec{E}_{(1)} &= \vec{\nabla} \times \vec{\nabla} \times \vec{\Pi}_{(1)} \\ \vec{H}_{(1)} &= \left(\sigma + \epsilon\frac{\partial}{\partial t}\right)\vec{\nabla} \times \vec{\Pi}_{(1)} \end{aligned} \qquad (1)$$

The second equally valid relation, among $\vec{\Pi}_{(2)}$, $\vec{E}_{(2)}$, and $\vec{H}_{(2)}$, is

$$\begin{aligned} E_{(2)} &= -\mu\frac{\partial}{\partial t}\left(\vec{\nabla} \times \vec{\Pi}_{(2)}\right) \\ H_{(2)} &= \vec{\nabla} \times \vec{\nabla} \times \vec{\Pi}_{(2)} \end{aligned} \qquad (2)$$

In source-free regions of space, both $\vec{\Pi}_{(1)}$ and $\vec{\Pi}_{(2)}$ satisfy the same vector wave equation

$$\vec{\nabla} \times \vec{\nabla} \times \vec{\Pi} - \vec{\nabla}(\vec{\nabla}\cdot\vec{\Pi}) + \mu\left(\epsilon \frac{\partial}{\partial t} - \sigma\right)\frac{\partial \vec{\Pi}}{\partial t} = 0 \tag{3}$$

If we represent $\vec{\Pi}$* in rectangular coordinates, then equation (3) reduces to the scalar wave equation for each rectangular component of $\vec{\Pi}$. If we furthermore set $\Pi_x = \Pi_y = 0$, then each of the "partial" fields defined by equations (1) and (2) becomes a function of a single scalar variable: $\Pi_{(1)}$ for the first partial field, and $\Pi_{(2)}$ for the second partial field. Linear combinations of these partial fields are still of such generality that the boundary conditions for any highly conducting cylinder of infinite length embedded in a homogeneous dielectric** of infinite extent can be satisfied. The demonstration of this fact follows.

Let us direct our attention to CW fields, and write Π_z in the form#

$$\Pi_z = R(r)\,\Theta(\theta)\,e^{i(\omega t \mp hz)} \tag{4}$$

the form of waves propagating along the cylinder. Then in the usual manner of solution by separation of variables we obtain

$$\Pi_z = \left[\sum_{-\infty}^{\infty} a_n e^{in\theta}\, Z_n\left(\sqrt{k^2 - h^2}\,r\right)\right] e^{i(\omega t \mp hz)} \tag{5}$$

where Z_n is a linear combination of the Bessel and Neumann functions (ref. 4 and 5).

Now we may find the fields by performing the operations indicated in equations (1) and (2). After we have performed these operations, we must remember that inside the cylinder there must be no contribution from the Neumann function, since Neumann functions diverge at the origin. Furthermore, to have the proper variation at large distances from the origin, the fields outside the cylinder must involve the combination of the Bessel and Neumann functions which make up the Hankel function of the first kind, $H_n^{(1)}$, representing outward-traveling cylindrical waves.

---

*The unsubscripted $\vec{\Pi}$ represents both $\vec{\Pi}_{(1)}$ and $\vec{\Pi}_{(2)}$.

**By "dielectric" we mean in general a medium described by both ϵ and σ; a lossy dielectric.

#Any solution to the scalar wave equation can be decomposed into a sum over ω of terms of the form shown in equation (4).

Therefore, the fields must have the form inside the cylinder

$$E_r^i = \sum_{n=-\infty}^{\infty} \left[- \frac{ih}{\lambda_1} J_n'(\lambda_1 r) a_{(1)n}^i - \frac{\omega\mu_1 n}{r\lambda_1^2} J_n(\lambda_1 r) a_{(2)n}^i \right] F_n$$

$$E_\theta^i = \sum_{n=-\infty}^{\infty} \left[- \frac{nh}{\lambda_1^2 r} J_n(\lambda_1 r) a_{(1)n}^i + \frac{i\omega\mu_1}{\lambda_1} J_n'(\lambda_1 r) a_{(2)n}^i \right] F_n$$

$$E_z^i = \sum_{n=-\infty}^{\infty} \left[J_n(\lambda_1 r) a_{(1)n}^i \right] F_n$$

$$H_r^i = \sum_{n=-\infty}^{\infty} \left[\frac{nk_1^2}{\lambda_1^2 \omega\mu_1 r} J_n(\lambda_1 r) a_{(1)n}^i - \frac{ih}{\lambda_1} J_n'(\lambda_1 r) a_{(2)n}^i \right] F_n \tag{6}$$

$$H_\theta^i = \sum_{n=-\infty}^{\infty} \left[- \frac{ik_1^2}{\omega\mu_1\lambda_1} J_n'(\lambda_1 r) a_{(1)n}^i - \frac{nh}{r\lambda_1^2} J_n(\lambda_1 r) a_{(2)n}^i \right] F_n$$

$$H_z^i = \sum_{n=-\infty}^{\infty} \left[J_n(\lambda_1 r) a_{(2)n}^i \right] F_n$$

and, outside the cylinder,

$$E_r^e = \sum_{n=-\infty}^{\infty} \left[-\frac{ih}{\lambda_2} H_n^{(1)'}(\lambda_2 r) a_{(1)n}^e - \frac{\omega\mu_2 n}{r\lambda_2^2} H_n^{(1)}(\lambda_2 r) a_{(2)n}^e \right] F_n$$

$$E_\theta^e = \sum_{n=-\infty}^{\infty} \left[-\frac{nh}{\lambda_2^2 r} H_n^{(1)}(\lambda_2 r) a_{(1)n}^e + \frac{i\omega\mu_2}{\lambda_2} H_n^{(1)'}(\lambda_2 r) a_{(2)n}^e \right] F_n$$

$$E_z^e = \sum_{n=-\infty}^{\infty} \left[H_n^{(1)}(\lambda_2 r) a_{(1)n}^e \right] F_n \tag{7}$$

$$H_r^e = \sum_{n=-\infty}^{\infty} \left[\frac{nk_2^2}{\omega\mu_2\lambda_2^2} H_n^{(1)}(\lambda_2 r) a_{(1)n}^e - \frac{ih}{\lambda_2} H_n^{(1)'}(\lambda_2 r) a_{(2)n}^e \right] F_n$$

$$H_\theta^e = \sum_{n=-\infty}^{\infty} \left[-\frac{ik_2^2}{\omega\mu_2\lambda_2} H_n^{(1)'}(\lambda_2 r) a_{(1)n}^e - \frac{nh}{\lambda_2^2 r} H_n^{(1)}(\lambda_2 r) a_{(2)n}^e \right] F_n$$

$$H_z^e = \sum_{n=-\infty}^{\infty} \left[H_n^{(1)}(\lambda_2 r) a_{(2)n}^e \right] F_n$$

where $\lambda_1^2 = k_1^2 - h^2$

$\lambda_2^2 = k_2^2 - h^2$

$k_1 = [-i\omega\mu_1(\sigma_1 + i\omega\varepsilon_1)]^{1/2}$, the propagation constant in the wire

$k_2 = [-i\omega\mu_2(\sigma_2 + i\omega\varepsilon_2)]^{1/2}$, the propagation constant in the surrounding medium

$$J_n'(x) = \frac{d\, J_n(x)}{dx} \tag{8}$$

$$H_n^{(1)'}(x) = \frac{d\, H_n^{(1)}(x)}{dx}$$

and $F_n = e^{i(\omega t - hz - n\theta)}$

The fields must satisfy the boundary conditions at the interface between the cylinder and the surrounding medium. These boundary conditions require that the tangential components of the electric field and the tangential components of the magnetic field be continuous across the interface. These conditions are expressed mathematically by the relations

$$\frac{nh}{u^2} J_n(u) a^i_{(1)n} - \frac{i\omega\mu_1}{u} J'_n(u) a^i_{(2)n} = \frac{nh}{\nu^2} H^{(1)}_n(\nu) a^e_{(1)n} - \frac{i\omega\mu_2}{\nu} H^{(1)'}_n(\nu) a^e_{(2)n}$$

$$J_n(u) a^i_{(1)n} = H^{(1)}_n(\nu) a^e_{(1)n}$$

$$\tag{9}$$

$$\frac{ik_1{}^2}{\omega\mu_1 u} J'_n(u) a^i_{(1)n} + \frac{nh}{u^2} J_n(u) a^i_{(2)n} = \frac{ik_2{}^2}{\omega\mu_2 \nu} H^{(1)'}_n(\nu) a^e_{(1)n} + \frac{nh}{\nu^2} H^{(1)}_n(\nu) a^e_{(2)n}$$

$$J_n(u) a^i_{(2)n} = H^{(1)}_n(\nu) a^e_{(2)n}$$

where $u = \lambda_1 a$

$\nu = \lambda_2 a$

and a is the radius of the metal cylinder.

We shall now state without proof two facts essential to the development of the solution. These facts are discussed at length elsewhere (ref. 5). Both of the facts relate to the solutions we have found only if the cylinder is a good conductor, such as a metal.

a. If the cylinder is a good conductor, then all fields resulting from $\Pi_{(2)}$ are highly attenuated and can be neglected for our purposes.

b. If the cylinder is a good conductor, all fields resulting from $\Pi_{(1)}$ are highly attenuated except that mode for which n=o, the axially symmetric mode. From these approximations it can be seen that $\Pi_{(1)}$ generates a magnetic field which only has components transverse to the axis of the cylinder ($\Pi_{(2)}$ generates a transverse <u>electric</u> field). $\Pi_{(1)}$ fields are sometimes called TM, or transverse magnetic, fields, and $\Pi_{(2)}$ fields TE, or transverse electric, fields (ref. 5).

With n=o, and with the $\Pi_{(2)}$ modes neglected*, equations (9) reduce to**

$$J_o(u)a_o^i = H_o^{(1)}(\nu)a_o^e$$

$$\frac{k_1^{\,2}}{\mu_1 u} J_1(u)a_o^i = \frac{k_2^{\,2}}{\mu_2 \nu} H_1^{(1)}(\nu)a_o^e \tag{10}$$

Combining these equations we obtain

$$\frac{k_1^{\,2}}{\mu_1 u}\frac{J_1(u)}{J_o(u)} = \frac{k_2^{\,2}}{\mu_2 \nu}\frac{H_1^{(1)}(\nu)}{H_o^{(1)}(\nu)} \tag{11}$$

For large values of the wire conductivity σ_1 it is usually a good approximation that

$$|u| = |k_1 a| >> 1 \tag{12}$$

(this means that the cylinder radius is much greater than a skin depth in the cylinder). With these approximations, we may use the asymptotic expansion of the Bessel functions, giving

$$\frac{J_1(u)}{J_o(u)} \cong i \tag{13}$$

Outside the cylinder, the approximations that may be made are somewhat different. h is equal to k_2 when the cylinder conductivity is infinite, and close to k_2 when the cylinder conductivity is large. Therefore, $\nu \equiv a\sqrt{k_2^{\,2} - h^2}$ in magnitude is usually << 1.

When this is the case, we may use the asymptotic expansion for small arguments, (refs. 4 and 5)

---

*From this point, we will denote $a_{(1)o}$ by a_o.

**Remember that $\frac{dZ_o(x)}{dx} = -Z_1(x)$ for the above cylinder functions.

$$H_o^{(1)}(\nu) \cong \frac{2i}{\Pi} \ln\left(\frac{\gamma\nu}{2i}\right)$$

$$H_1^{(1)}(\nu) \cong -\frac{2i}{\Pi\nu} \tag{14}$$

where $\gamma \cong 1.781$

Putting these expansions into equation (11) gives us the equation which determines ν and therefore h;

$$\nu^2 \ln \frac{\gamma\nu}{2i} = i \frac{\mu_1}{\mu_2} \frac{k_2{}^2 a}{k_1} \tag{15}$$

This transcendental equation may be solved for ν by interation, using for a good initial guess the value -20 for

$$\ln\xi = \ln\left(\frac{\gamma\nu}{2i}\right)^2 \tag{16}$$

and rewriting the equation in the form

$$\xi\ln\xi = \eta \tag{17}$$

where $\eta = -i \dfrac{\gamma^2}{2} \dfrac{\mu_1}{\mu_2} \dfrac{k_2{}^2 a}{k_1}$

As will be shown later in this report a good first approximation for $\ln\xi$ is $2 \ln \dfrac{a}{a+\delta_2}$, where a is the conductor radius and δ_2 is the skin depth in the surrounding dielectric.

Thus we are able to find the propagation constant h, and the final remaining problem is to determine the amplitude as a function of some applied excitation.

The Impedance Characteristics

We have determined that the form of the fields about the conducting cylinder is

$$E_z^e = a_o^e \, H_o^{(1)}(\lambda_2 r) F_o(z,t)$$

$$E_r^e = a_o^e \frac{ih}{\lambda_2} H_1^{(1)}(\lambda_2 r) F_o(z,t) \tag{18}$$

$$H_\theta^e = a_o^e \frac{ik_2{}^2}{\omega\mu_2\lambda_2} H_1^{(1)}(\lambda_2 r) F_o(z,t)$$

Knowledge of the azimuthal magnetic field at the surface of the wire immediately tells us that the current through the wire is (ref. 5)

$$I_z = a_o^e \frac{2\Pi a\sigma_1\mu_1 k_2{}^2 H_1^{(1)}(\lambda_2 a)}{\lambda_2\mu_2 k_1{}^2} \tag{19}$$

We will now define three impedances. These impedances will play an important role in studying the effect of an axially directed electric field excitation and will also be important in developing a model for the problem.

The first impedance is defined as

$$Z_s = \frac{-E_z(a)}{I_z} \tag{20}$$

Using the approximation that $\lambda_2 a << 1$ and equation (14), we find that

$$Z_s = \frac{1+i}{\sqrt{2}}\,\frac{1}{2\Pi a}\left(\frac{\omega\mu_1}{\sigma_1}\right)^{1/2} \text{ ohms/meter} \tag{21}$$

This is just the value of the "skin impedance" per unit length of the conductor, the impedance to a high-frequency current caused by the finite conductivity of the cylinder (ref. 7).

The next impedance is principally inductive. Starting with the definition of inductance L_o

$$L_o I_z = \Phi \tag{22}$$

where Φ is the flux per unit cylinder length,

$$\Phi = \frac{d}{dz}\int_z\int_a^\infty B_\theta\, dr dz = \int_a^\infty B_\theta\, dr \tag{23}$$

and by noting that

$$\int_a^\infty H_1^{(1)}(\lambda_2 r) dr = \frac{1}{\lambda_2} H_o^{(1)}(\lambda_2 a) \tag{24}$$

we find that

$$Z_L = i\omega L_o = -\frac{i\omega\mu_2}{2\Pi}\,\ell n\left(\frac{\gamma\lambda_2 a}{2i}\right) \text{ ohms/meter} \tag{25}$$

This impedance is called the longitudinal inductive impedance of the conductor.

To find the third impedance, we first note that radial current per unit length flowing out of the conductor is

$$I_r(a) = -\frac{dI_z}{dz} = ihI_z \tag{26}$$

Furthermore, a potential V_r may be defined in any plane perpendicular to the cylinder by the relation (ref. 8)

$$V_r = \int_a^\infty E_r dr \tag{27}$$

Then we shall define the transverse impedance, Z_t, by

$$Z_t = \frac{V_r}{I_r} \tag{28}$$

Calculations similar to those performed in finding Z_s and Z_L gives us

$$Z_t = -\frac{1}{2\Pi\left(\sigma_2+i\omega\varepsilon_2\right)} \ell n\left(\frac{\gamma\lambda_2 a}{2i}\right) \text{ ohm-meters} \tag{29}$$

External Excitation

To find the current induced by an external, axially directed field, we start with the integral form of one of Maxwell's equations:

$$\oint \vec{E} \cdot d\vec{\ell} = -\int \frac{\partial\vec{B}}{\partial t} \cdot d\vec{s}$$

We integrate this equation around the path and over the area shown in figure 1.

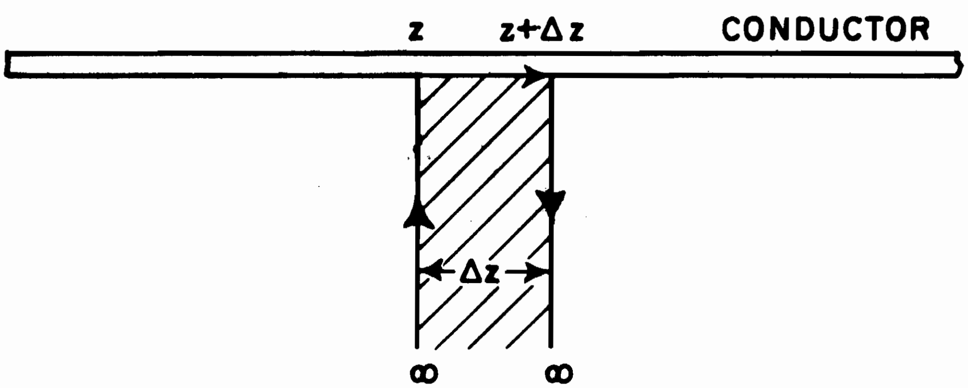

Figure 1. The Path of Integration for Determining the Effect of a Driving Field on a Bare Wire in the Earth.

The equation then is

$$\int_{\infty}^{a} E_r(z)\,dr + \int_{z}^{z+dz} E_z\,dz + \int_{a}^{\infty} E_r\ (z + dz)\ dr = -\int \frac{d\vec{B}_\theta}{dt} \cdot d\vec{s} \qquad (30)$$

If we divide this equation by Δz and take the limit as $\Delta z \to o$, the equation becomes

$$\frac{d}{dz} \int_{a}^{\infty} E_r\,dr + E_z = -\frac{d}{dt} \int_{a}^{\infty} B_\theta\,dr \qquad (31)$$

From equations (26), (27), and (28) we find that

$$\frac{d}{dz} \int_{a}^{\infty} E_r\,dr = -Z_t \frac{d^2 I_z}{dz^2} \qquad (32)$$

From (22) and (23), we find that

$$\frac{d}{dt} \int_{a}^{\infty} B_\theta\,dr = Z_L I_z \qquad (33)$$

The only E_z that can exist at the surface of the conductor is that caused by I_z, the current in the wire. If E_z were to be different from $I_z\ Z_s$, then, since E_z is continuous across the interface at the cylinder, a current different from I_z would flow in the wire, a contradiction.

Let us assume that there is an external source of axially directed electric field which would cause a field E_{zo} to exist at the location in space where the cylinder is were the cylinder not there. Furthermore, let us assume that the introduction of the cylinder does not affect the source. From superposition we can add the externally generated E_{zo} to the E_{z1} generated by the wire to obtain the total E_z. This total E_z must be just $I_z Z_s$; therefore we have

$$E_{zo} + E_{z1} = I_z\ Z_s$$

Putting this all into equation (31) we have the equation which describes the flow of current in the cylinder:

$$Z_t \frac{d^2 I_z}{dz^2} - \left(Z_L + Z_s\right) I_z = -E_{zo} \qquad (34)$$

The solutions to this equation are known, but before we examine them, we shall consider another physical situation which leads to this equation.

An Analogous Problem:

The equation which governs the flow of current in the transmission line shown in figure 2 is exactly the same as the equation which governs the flow of current in the single conductor embedded in the dielectric (ref. 9).

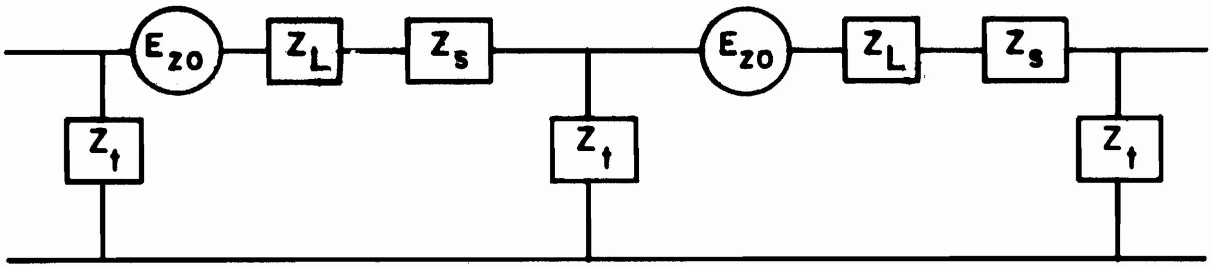

Figure 2. The Equivalent Dispersive Transmission Line.

The dielectric acts as the other conductor of the transmission line by being the return path for the current.

As a matter of fact, we can imagine a transmission line which has properties very close to those of the single cylindrical conductor, but which is much simpler to deal with, and much easier to generalize.

Since the problem we have been considering has cylindrical symmetry, the model we shall consider is a cylindrical transmission line. We are principally concerned with a poorly conducting dielectric surrounding the highly conducting cylinder, and would expect that the fields produced by the conducting cylinder would be considerably diminished a "skin depth" in the dielectric away from the cylinder. A somewhat idealized version of the field pattern around the cylinder excited by an external axially directed electric field is shown in figure 3.

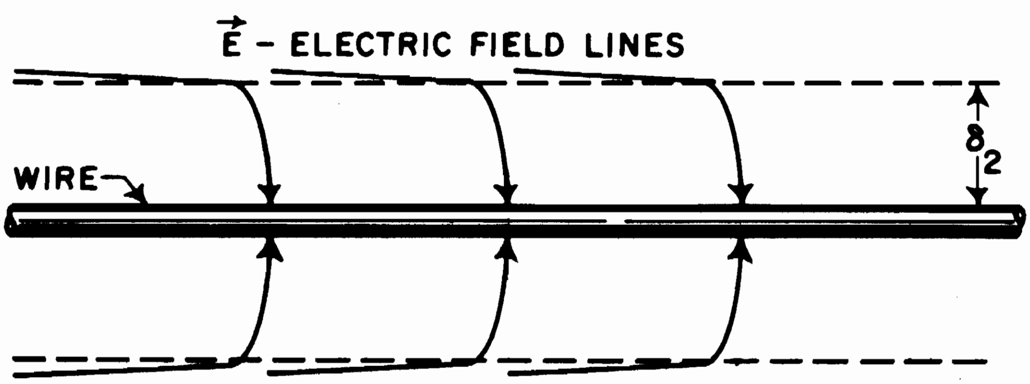

Figure 3. The Electric Field Near the Wire.

If the field lines are still nearly perpendicular to the conductor a skin depth away, then the cylinder $r = \delta_2$ must be nearly an equipotential, and we would not disturb the field distribution between the wire and $r = \delta_2$ by inserting a conducting cylinder at this radius. In doing this, we have formulated a cylindrical transmission line of inner radius a and outer radius δ_2, filled with a conducting dielectric characterized by the parameters μ_2, ε_2, and σ_2.

The impedances which characterize this coaxial transmission line are (refs. 7 and 9)

$$Z_t = -\frac{1}{2\Pi\left(\sigma_2+i\omega\varepsilon_2\right)}\ \ell n\left(\frac{a}{a+\delta_2}\right)$$

$$Z_L = -\frac{i\omega\mu_2}{2\Pi}\ \ell n\left(\frac{a}{a+\delta_2}\right) \tag{35}$$

$$Z_s = \frac{1+i}{\sqrt{2}}\ \frac{1}{2\Pi a}\left(\frac{\omega\mu_1}{\sigma_1}\right)^{1/2}$$

An inspection of equations (21), (25), and (29) shows that the impedances which characterize the cylindrical conductor imbedded in the dielectric differ from those of the cylindrical transmission line only in the logarithmic factor.

Even in this factor, the difference is not very great, as the following two examples will indicate.

Example I. Number 10 copper wire,

Wire Radius = 1.28×10^{-3}m

Wire conductivity = 5.88×10^{7} mho/m

Wire Magnetic Permeability = $4\Pi \times 10^{-7}$ henry/meter

Ground Conductivity = 2.9×10^{-2} mho/m

Ground Magnetic Permeability = $4\Pi \times 10^{-7}$ henry/meter

Even at 1 mc, the displacement current is <1% of the conduction current, $\therefore$ ε_2 was set to zero.

Frequency	$\ln \frac{a}{a+\delta_2}$	$\ln \frac{\gamma\lambda_2 a}{2i}$	
		Real	Imaginary
10^2 cps	-12.34	-12.75	-1.25
10^3 cps	-11.19	-12.15	-1.23
10^4 cps	-10.04	-11.55	-1.23
10^5 cps	- 8.89	-10.95	-1.23
10^6 cps	- 7.74	-10.34	-1.24

Example II. Lead Sheath Cable

Wire Radius = 2.07×10^{-2}m

Wire Conductivity = 4.45×10^6 mho/m

Wire Magnetic Permeability = $4\Pi \times 10^{-7}$ henry/m

Ground Conductivity = 2.9×10^{-2} mho/m

Ground Magnetic Permeability = $4\Pi \times 10^{-7}$ henry/meter

$\varepsilon_2 \cong 0$

Frequency	$\ln \frac{a}{a+\delta_2}$	$\ln \frac{\gamma\lambda_2 a}{2i}$	
		Real	Imaginary
10^2 cps	-9.56	-10.63	-1.24
10^3 cps	-8.41	-10.02	-1.24
10^4 cps	-7.26	- 9.42	-1.24
10^5 cps	-6.11	- 8.81	-1.25
10^6 cps	-4.96	- 8.20	-1.25

Thus, it is easy to see that our simple model is similar to the single conducting cylinder--conductive dielectric system, and may give a useful approximation to the more accurate, but more complicated, solutions.

Solution to the Transmission Line Equation

If the transmission line or cylindrical conductor is of length d and terminated in impedances Z_1 and Z_2*, with the definitions

---

*The nature of the termination impedance will be discussed in section III.

$$\Gamma \equiv \left(\frac{Z_L + Z_s}{Z_t}\right)^{1/2} \tag{36}$$

$$Z_o \equiv \left[Z_t \left(Z_L + Z_s\right)\right]^{1/2} \tag{37}$$

and

$$F(z) \equiv \frac{1}{2Z_o} \int_o^d E_{zo} (v) e^{-\Gamma|z-v|} \, dv \tag{38}$$

then

$$I(z) = Ke^{-\Gamma z} + Le^{\Gamma z} + F(z) \tag{39}$$

where K and L are related to the reflected currents at the respective terminations (see appendix II) (ref. 3). In general,

$$K = \frac{\left(Z_1-Z_o\right)\left(Z_2-Z_o\right) F(d) - \left(Z_2+Z_o\right)\left(Z_1-Z_o\right) e^{\Gamma d} F(o)}{\left(Z_1+Z_o\right)\left(Z_2+Z_o\right) e^{\Gamma d} - \left(Z_1-Z_o\right)\left(Z_2-Z_o\right) e^{-\Gamma d}}$$

$$L = \frac{\left(Z_1-Z_o\right)\left(Z_2-Z_o\right) e^{-\Gamma d} F(o) - \left(Z_1+Z_o\right)\left(Z_2-Z_o\right) F(d)}{\left(Z_1+Z_o\right)\left(Z_2+Z_o\right) e^{\Gamma d} - \left(Z_1-Z_o\right)\left(Z_2-Z_o\right) e^{-\Gamma d}} \tag{40}$$

Since the impedances used in quations (36) and (37) are complex, it is often easier for the purpose of calculation to split the impedances into their real and imaginary parts. The total longitudinal impedance Z and the transverse admittance Y_t are defined as follows:

$$Y_t \equiv \frac{1}{Z_t} = G' + i\omega C' \tag{41}$$

where G' is the conductive admittance per unit length, and C' is the transverse capacitance per unit length; and

$$Z \equiv \left(Z_L + Z_s\right) = R + i\omega L' \tag{42}$$

where R is the longitudinal resistance per unit length and L' is the total inductance per unit length. From equations (35), (41) and (42),

$$
\begin{aligned}
G' &= Y_t \text{ (real)} = -\frac{2\Pi\sigma_2}{\ln\left(\frac{a}{a+\delta_2}\right)} \\
C' &= \frac{Y_t\text{(imaginary)}}{i\omega} = -\frac{2\Pi\varepsilon_2}{\ln\left(\frac{a}{a+\delta_2}\right)} \\
R &= Z_s \text{ (real)} = \frac{1}{2\sqrt{2}\Pi a}\left(\frac{\omega\mu_1}{\sigma_1}\right)^{1/2} \\
L' &= \frac{Z\text{ (imaginary)}}{i\omega} = -\frac{\mu_2}{2\Pi}\ln\left(\frac{a}{a+\delta_2}\right) + \frac{|R|}{\omega}
\end{aligned}
\tag{43}
$$

Also, from equations (36), (37), (41) and (42)

$$
\Gamma = \left[(R + i\omega L')(G' + i\omega C')\right]^{1/2} \tag{44}
$$

and

$$
Z_o = \left[(R + i\omega L')\big/(G' + i\omega C')\right]^{1/2} \tag{45}
$$

From the above analysis, given the excitation field and the electrical characteristics of the wire and the dielectric, we can find the current induced in the wire by the excitation field.

Additional Properties of the Transmission Line Model

The transmission line model would be of limited value if it only allowed us to solve approximately a problem which we could also solve exactly by other similar means. But the transmission line model has the additional value of guiding us to approximate solutions of problems which are much more difficult to solve exactly.

For example, we can observe that this theory should apply to curved conductors as well as straight conductors so long as the radius of curvature is large compared with δ_2. Furthermore, if the excitation electric field is not parallel to the conductor, then only the parallel component of the field need be considered, since the normal component of the field will generate only highly damped modes.

Other special cases of the transmission line model are considered in the following sections.

SECTION III

EXTENSION OF THE TRANSMISSION LINE MODEL

The previous section considered the fields and currents in an infinitely long wire buried in a lossy dielectric of infinite extent. It was found that the relation between the impressed field and the current in the wire was equivalent to the relation for a driven coaxial transmission line.

In this section, the transmission line model will be used to determine the currents induced by a CW electric field in wires of finite length, including the effect of the termination reflections. These wires will be lying on the earth, or buried within a distance δ_2 of the surface. They may be bare wires, or they may have coverings of some homogeneous material. By considering these variations, the current relations for the ideal configuration of the previous section will be converted into current relations for practical wire configurations.

A Wire at the Earth-Air Interface

The transmission line equation, discussed in the previous section for the long underground wire, will now be further exploited as an approximation to solve some specialized wire current problems. Specialized problems may be solved in terms of the transmission-line current solution, equation (39), by determining the equivalent impedance characteristics and propagation constant for the given earth-wire configuration. In particular, the problem of a wire lying on the surface of the earth will now be studied.

This problem is very difficult to solve exactly, since there are a multiplicity of interfaces which must be considered. However, by use of the transmission-line model and several basic assumptions, the problem in the geometry of figure 4 can be solved approximately.

Assume that the wire is the inner conductor of a coaxial transmission line (outer conductor has radius b, as in figure 4) which is half-filled with earth, the remaining half being air-filled. It will be assumed that the electric field lines will maintain their radial direction, even near the earth-air interface, and not have any appreciable θ components. The general relations between the electrical characteristics of the air and the earth are:

$$\mu_2 = \mu_o$$

$$\sigma_o \cong 0$$

$$\varepsilon_2 = C\varepsilon_o \text{ where } C > 5 \text{ for most earth.}$$

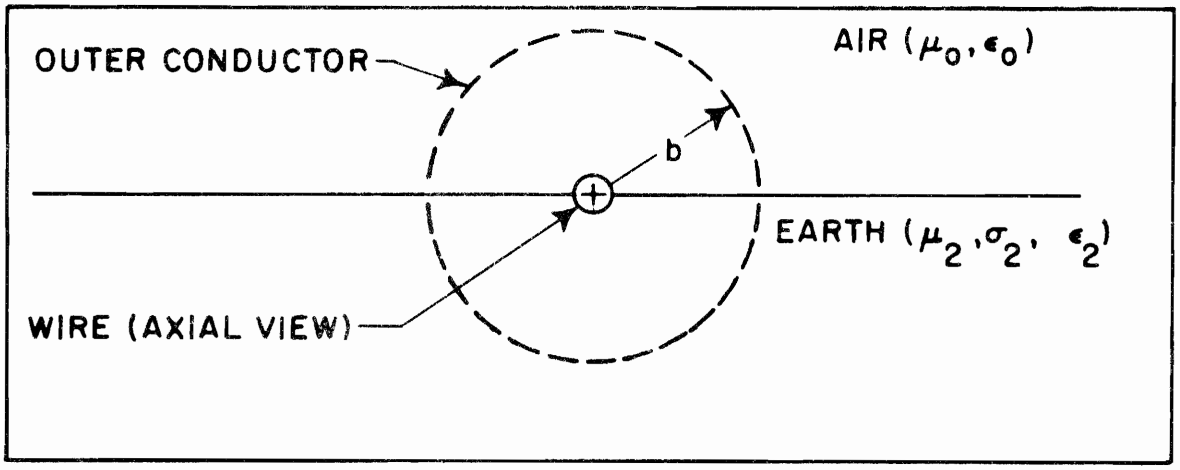

Figure 4. A Wire at the Surface of the Earth.

The transverse admittance will be the sum of the admittance through the earth and the admittance through the air as shown in figure 5.

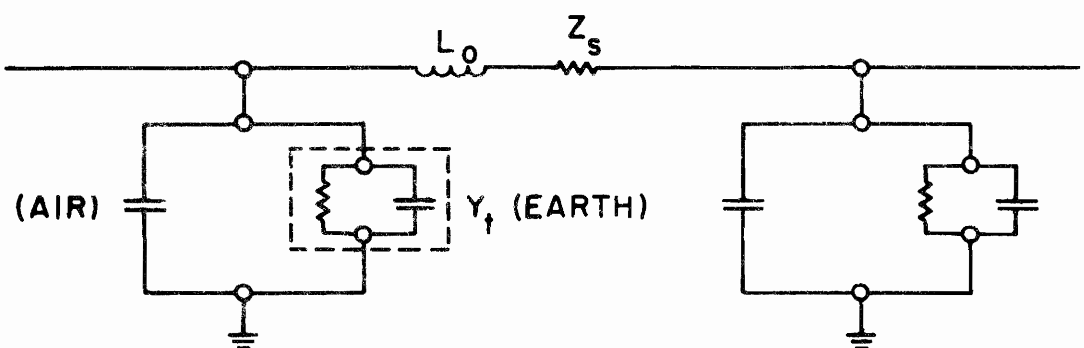

Figure 5. The Impedance of a Wire at the Surface of the Earth.

But the high conductivity of the earth produces an admittance which heavily outweighs that of the air. Therefore, the transverse admittance may be calculated as half the transverse admittance of a dirt-filled transmission line:

$$Y_t = \frac{1}{2}\left[2\Pi\left(\sigma_2 + i\omega\varepsilon_2\right)/\ell n\left(\frac{b}{a}\right)\right]$$

Since the magnetic characteristics of the air are the same as those of the earth the magnetic field lines show no appreciable deviation from those of a transmission line filled with a single medium. Therefore, we have the inductance per unit length:

$$L_o = \frac{\mu_2}{2\Pi} \ell n\left(\frac{b}{a}\right)$$

The skin impedance is the same as previously calculated for a wire in equation (21), and, for the frequency range of interest, $i\omega L_o >> Z_s$. Therefore, from equation (36), the propagation constant for the wire is given by:

$$\Gamma = \left[\left(Z_s + i\omega L_o\right) Y_t\right]^{1/2}$$

$$\cong \left[\frac{i\omega\mu_2}{2}\left(\sigma_2 + i\omega\varepsilon_2\right)\right]^{1/2} \tag{46}$$

the latter equation which is independent of the outer radius of the transmission line.

In these approximations it was assumed that, for a wire at the surface of the earth,

$$L_o \text{ (surface)} = L_o \text{ (infinite depth)}$$

$$Y_t \text{ (surface)} = 1/2\ Y_t \text{ (infinite depth)} \tag{47}$$

where the values for infinite depth are given by equations (22), (25), and (41). The values for the impedances of a wire given above will be used in theoretical current predictions for a wire that is near the surface of the earth (that is, when the depth of burial is less than δ_2).

A Covered Wire

In this section, an infinitely long wire with a concentric cylindrical covering will be studied using the transmission line approximation.

This covering will be homogeneous, constant thickness throughout, and will have a conductivity much less than that of the wire metal. Also, the attenuation of the fields through the covering will be negligible; that is, $t << \frac{1}{k_{3i}}$ where k_{3i} = imaginary part of $\left[-i\omega\mu_3\left(\sigma_3 + i\omega\varepsilon_3\right)\right]^{1/2}$.
Figure 6 illustrates the geometry of this wire.

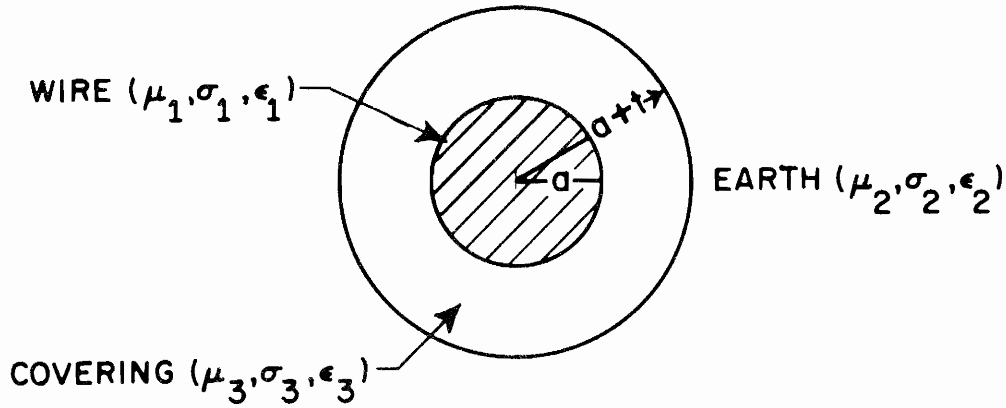

Figure 6. The Covered Wire.

With the attenuation condition imposed, the covering will have little effect on the magnetic flux generation relative to the current in the wire. That is, the inductance per unit length will remain approximately the same as given for the bare wire.

However, the covering may have a very definite effect on the transverse impedance, as shown in figure 7, since a covering of an insulating material will block the flow of conduction currents between the wire and the earth (in figure 7, $R_i \rightarrow \infty$).

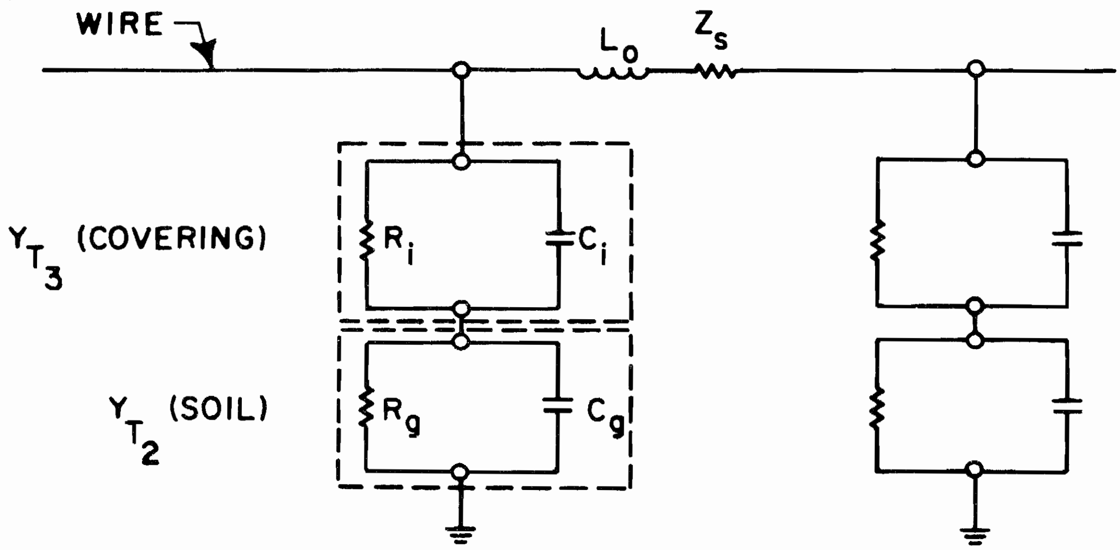

Figure 7. The Impedance of a Covered Wire.

If, as in most practical cases, the diameter of the wire-covering combination is much less than a wave length in the earth for the frequency range of interest $\left(2[a+t] < \frac{1}{|k_2|}\right)$, then the fields for the system may again be described by zero order fields with no θ dependence.

The covered wire can be approximated by a single bare wire of radius (a+t) for the purpose of determining the transverse admittance from the outer surface of the covering to the earth. To determine the transverse admittance through the covering, the wire will be approximated by a coaxial transmission line filled with the covering material. With these approximations

$$Y_{t_3}\ \text{(covering)} = \frac{2\Pi\left(\sigma_3+i\omega\varepsilon_3\right)}{\ell n\left(\frac{a+t}{a}\right)}$$

$$Y_{t_2}\ \text{(soil)} = \frac{2\Pi\left(\sigma_2+i\omega\varepsilon_2\right)}{\ell n\left[\frac{2i}{\gamma\lambda_2(a+t)}\right]} \tag{48}$$

The total transverse admittance is then given by

$$Y_t = \frac{Y_{t_3} Y_{t_2}}{Y_{t_3} + Y_{t_2}} \tag{49}$$

If the covered wire is placed at the surface of the earth, approximately half of the covering will be in contact with the air and half with the earth. It is noted in equation (49) that if the admittance of the outside medium is very low, the total admittance is low. Therefore, since the covering is of insufficient thickness to distort the fields appreciably, little current will pass through the half of the covering in contact with the air. Therefore, from the analysis performed in the previous section, and using equation (48)

$$Y_{t_3}\ \text{(surface)} \cong \frac{1}{2} Y_{t_3}\ \text{(infinite depth)}$$

$$= \frac{\Pi\left(\sigma_3+i\omega\varepsilon_3\right)}{\ell n\left(\frac{a+t}{a}\right)}$$

$$Y_{t_2} \text{ (surface)} \cong \frac{1}{2} Y_{t_2} \text{ (infinite depth)}$$

$$= \frac{\Pi\left(\sigma_2 + i\omega\varepsilon_2\right)}{\ell n \dfrac{2i}{\gamma\lambda_2(a+t)}} \tag{50}$$

The relation for Y_t (total) still holds (equation 49).

The propagation constant for the covered wire can be calculated from equations (36) and (49) using the transverse admittances calculated above. In general, this propagation constant will be given by

$$\Gamma \text{ (covered wire)} = \left[Z \left(\frac{Y_{t_3} Y_{t_2}}{Y_{t_3} + Y_{t_2}} \right) \right]^{1/2}$$

In this section the propagation and impedance factors of the covered wire have been derived in terms of the transmission line theory. These factors may now be used with equation (39) to determine the current induced in a covered wire.

Termination Impedances of Finite Wires

A practical transmission line is generally terminated by a reasonably well defined and well known impedance. However, the termination of the equivalent transmission line model, as presented in previous sections, in general is not well defined. A few possible wire termination conditions will be considered in this section, and attempts will be made to estimate the termination impedance produced for each condition.

One possible termination condition, shown in figure 8, involves a wire that is arbitrarily cut off at some point, with no further attempt made to control the termination impedance. The lines of the driving electric field in the earth are by definition parallel to the axis of the wire far beyond the end of the wire. At a distance from the wire termination of less than δ_2, the field lines are bent toward the wire. Since the diameter of the wire is much less than the wave length of the electric field, any irregularities in the end of the wire will not produce any appreciable irregularities in the field. Therefore, the field will converge approximately isotropically on a hemisphere at the end of the wire.

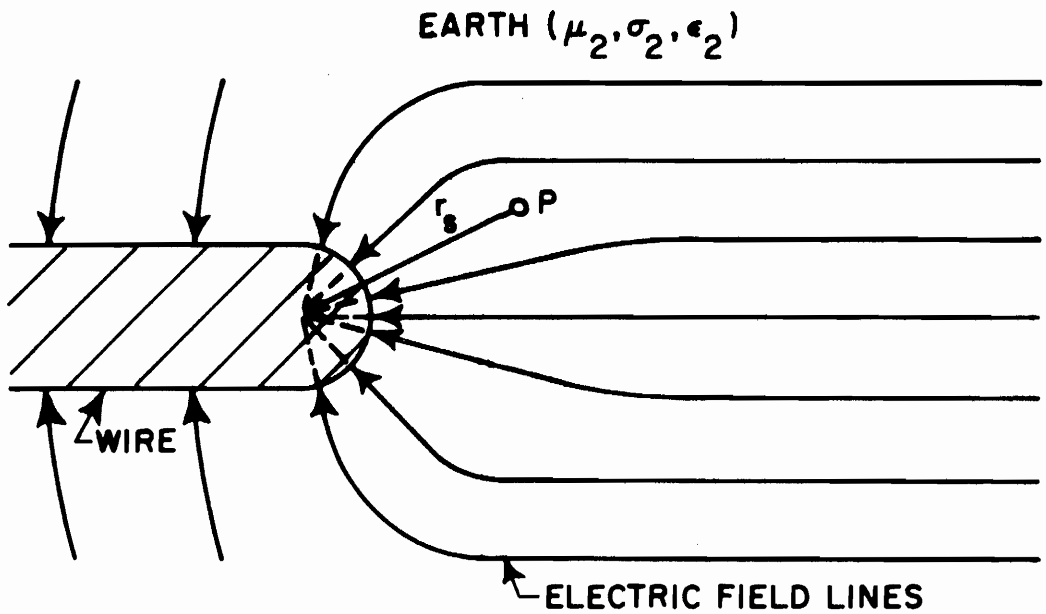

Figure 8. Electric Field Near a Wire Termination.

If the total current entering the end of the wire is I_e, then the current density in the earth near the end of the wire must be

$$J_{r_s} \cong \frac{I_e}{2\Pi r_s^{\,2}}$$

where r_s is measured from the point on the wire axis which is the apparent point of convergence of the electric field lines. The current density J_{r_s} includes both conductive currents and displacement currents. It will be assumed here that the termination of the wire is a hemispherical cap of radius a, equal to the radius of the wire. Then ignoring the driving field, the component of the electric field converging to the wire termination will be

$$E_{r_s} \cong \frac{I_e \, e^{-ik_2 r_s}}{2\Pi r_s^{\,2}\left(\sigma_2 + i\omega\varepsilon_2\right)}$$

the electric potential at the end point is

$$V_e = -\int_{\infty}^{a} E_{r_s}\, dr_s$$

$$= \frac{I_e}{2\Pi\left(\sigma_2+i\omega\varepsilon_2\right)}\left[\frac{e^{-ik_2a}}{a} - ik_2G\left(ik_2a\right)\right]$$

where $G(x) = \int_{x}^{\infty} \frac{e^{-v}}{v}\, dv$ is the exponential integral function (ref. 9).

Within the limits previously placed on ω, σ_2, ε_2, and a,

$$V_e \cong \frac{I_e}{2\Pi a\left(\sigma_2+i\omega\varepsilon_2\right)}$$

Therefore, the termination impedance, defined by

$$Z_e = \frac{V_e}{I_e}$$

$$Z_e = \frac{1}{2\Pi a\left(\sigma_2+i\omega\varepsilon_2\right)} \tag{51}$$

In the range of the earth electrical characteristics and frequencies previously mentioned, this impedance can vary from values comparable to the line impedance of an insulated wire, as defined in equation (49), to several orders of magnitude higher than the line impedance. However, a condition implied in this impedance derivation is that there must be good electrical contact between the end of the wire and the earth. This condition may not be true for a wire cut and arbitrarily placed in the earth.

When there is an insulative covering of thickness t placed uniformly over the termination, where $t \ll \frac{1}{|k_2|}$, an added impedance term is present. This term, which is the capacitative impedance through the termination covering, is

$$Z_c \cong \frac{1}{2\Pi i\omega\varepsilon_3}\left[\frac{1}{a} - \frac{1}{a+t}\right]$$

$$= \frac{1}{2\Pi i\omega\varepsilon_3}\left[\frac{t}{a(a+t)}\right]$$

where ε_3 is the dielectric permittivity of the insulation. The impedance to ground from the outside of the insulation is

$$Z_G = \frac{1}{2\Pi(a+t)\left(\sigma_2+i\omega\varepsilon_2\right)}$$

The total termination impedance to ground is

$$Z_e = \frac{1}{2\Pi(a+t)}\left[\frac{1}{\sigma_2+i\omega\varepsilon_2} + \frac{t}{i\omega\varepsilon_3 a}\right] \tag{52}$$

The added impedance, which could be caused by an air space at the end rather than specific insulation, is always orders of magnitude higher than the line impedance for the frequency range of interest.

The above determinations indicate that, unless special care is taken to ensure good electrical contact with the earth at the wire ends, a wire that is terminated only by cutting off the end will result in a termination impedance Z_e much greater than Z_o, the line impedance. This is true even for insulated wires.

One method of lowering the termination impedance is to connect the end of the wire to a vertical metal rod driven into the earth. The rods commonly used for this purpose are 1 to 2 meters long and 1 to 2 centimeters in diameter.

From these dimensions $\quad a' << \ell' << \dfrac{1}{|k_2|}$

where a' is the radius of the ground rod and ℓ' is the length.

A theoretical study was performed by Sunde on the impedance of various grounding arrangements (ref. 9). The short length of the rod, in addition to the fact that it is perpendicular to the wire in the earth, ensures that its inductance effects are small. It was found that a single grounding rod with the above characteristics has a resistance,

$$R_G \cong \frac{1}{2\Pi\ell'\sigma_2}\left[\ell n\left(\frac{4\ell'}{a'}\right) - 1\right] \tag{53}$$

For an insulated wire in extremely high-conductivity soil, the resistance will be down an order of magnitude from the line impedance. However, for average or low-conductivity soil, this grounding arrangement will not reduce the termination impedance appreciably below the line impedance. In particular for bare wires, the wire itself may be a much better grounding arrangement that the vertical ground rod.

Although there are many other methods of electrically terminating the wire in the earth, the above cases were of special interest, since these termination methods were used on the wires in which measurements of induced currents have been taken. The experimental results will be discussed later.

Up to this point the discussion has been guided toward the determination of a theoretical expression to predict the currents that will be induced in a wire in the earth by a continuous-wave electric field of arbitrary spatial dependence. It is now necessary to compare the predictions calculated by this theory with actual measured data to test the reliability of the theory.

SECTION IV

THE EXPERIMENTAL WORK

The experimental results discussed in this section were obtained by Mr. A. Whitson and his associates at the Stanford Research Institute under a research contract with the Air Force Weapons Laboratory (reference 3).

A vertical monopole ground antenna was set up by Stanford Research Institute to transmit a continuous wave signal at a series of discrete frequencies between 500 cps and 510 kcs. A number of wires were laid in and on the ground near the antenna, and the currents induced in these wires were measured at several points along each wire. The experimental results of this work will be compared with calculations from the induced current theory to test the accuracy of the theory in predicting the currents induced by a continuous wave field parallel to the wire. This section will explain the experimental work that was performed.

Work Performed by Stanford Research Institute

A large percentage of the present data on currents induced in wires in the earth by continuous wave electromagnetic fields was collected by Stanford Research Institute in extensive experiments performed with a vertical monopole antenna field source (reference 3). The height of the antenna was 30.5 meters over a counterpoise which was constructed of 19 radial wires, each 30 meters long. The ground plane was suspended 3 meters above the earth and was terminated in the ground with 2-meter-long metal ground stakes. The antenna itself was placed atop an instrumentation van containing the devices for measuring the input to the antenna. The antenna complex is shown in figure 9.

The transmission system was designed to operate at the fixed frequencies of 0.5, 1, 2, 5, 10, 21, 62, 100, 200, 450, and 510 kc with antenna voltages varying from 18 KV at 0.5 kc to 0.5 KV at 510 kc. These particular frequencies were transmitted by resonating the specially designed loading coils with the measured antenna capacitance of 426 pf. A variable capacitor in parallel with the antenna was used for fine adjustment of the resonant frequency.

Measurement of the antenna impedance indicated that it was essentially a pure capacitance. Therefore, the base current of the antenna could be

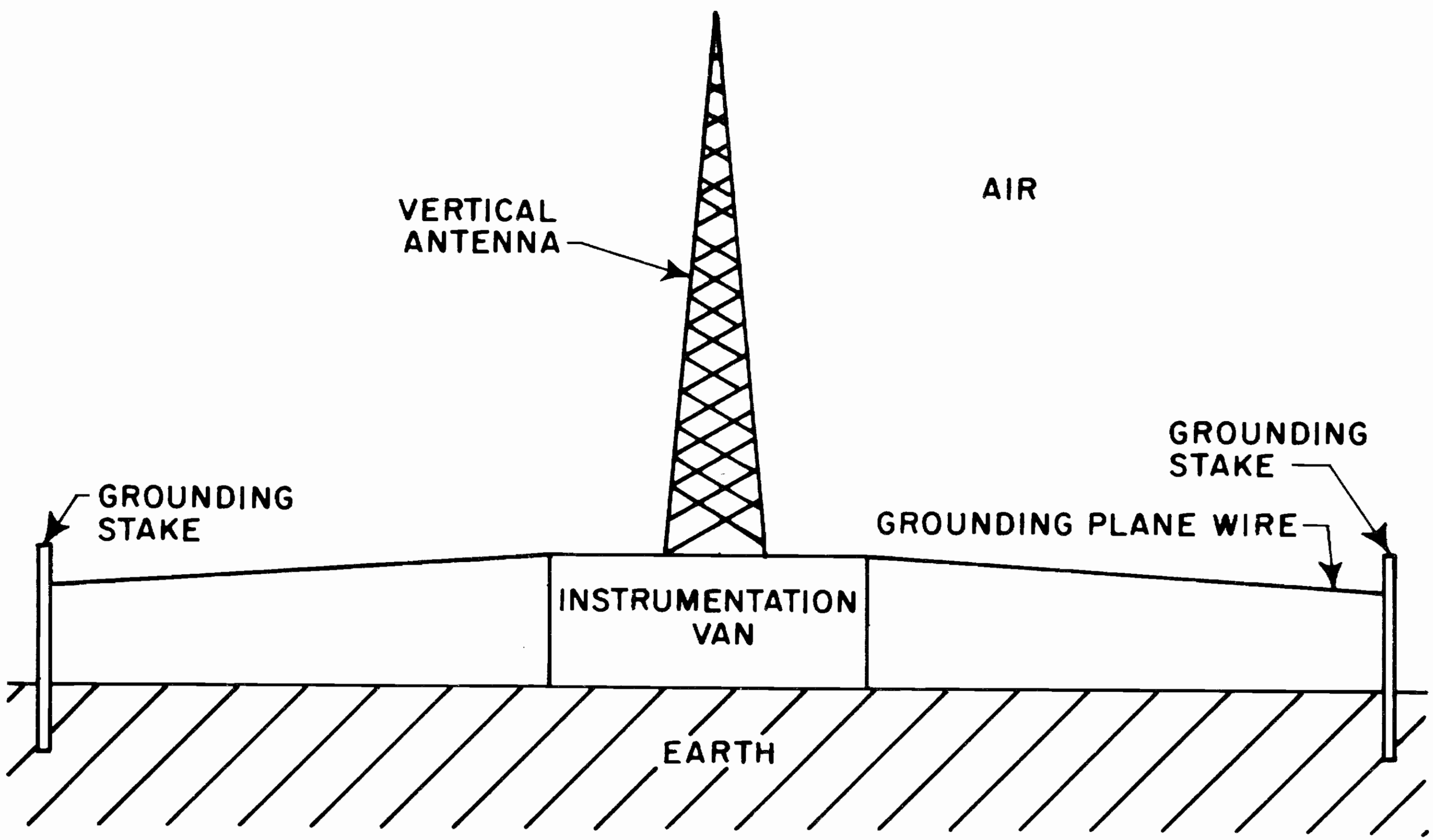

Figure 9. The Stanford Research Institute Vertical Monopole Antenna.

determined from the antenna capacitance (C_A), the frequency (ω) and the antenna voltage (V_A) by the relation

$$I_o = i\omega C_A V_A \tag{54}$$

From equations (54) and (71), predictions of the transmitted azimuthal magnetic fields were calculated by Stanford Research Institute and were later confirmed by measurements made of the fields.

Predictions of the radial electric field were also made. However, the radial electric-field measurements were unreliable, because the electric-field sensor could not be entirely decoupled from the much larger vertical electric field.

The transmitting monopole antenna was set up in two separate test areas. These regions are called Area 1 and Area 5. Area 1 earth had an average measured conductivity of approximately 4.4×10^{-3} mhos/m. Area 5 earth had an average measured conductivity of approximately 2.9×10^{-2} mhos/m.

In other ways, the two areas were quite similar. Both areas were flat beds of alluvial soil, which had a hard, dry surface crust. Laboratory measurements indicated that the dielectric constant of the soil was approximately 40 for a alluvium at a frequency of 1 Mcs and had a tendency to increase with an inverse frequency dependence at lower frequencies (reference 10).

The wires and cables used for the induced-current measurements were laid parallel to the surface of the earth in these two areas, in a radial orientation from the base of the antenna. These wires were buried at depths from zero to one meter, zero depth corresponding to wires laid on the surface of the earth. In cases where more than one wire was present, the individual wires were sufficiently far apart to prevent any appreciable interaction.

A variety of bare wires, insulation-covered wires, and armor-sheathed cables were used. One cable had a covering with conductivity comparable to the conductivity of the surrounding earth. Some of the particular conductors used will be detailed in a later section.

The currents in the wires were detected by circling the wire at the desired point with a toroidal solenoid. The solenoid was constructed of 260 turns of #22 enameled copper wire wound around a composite core with a relative permeability of 125. The winding was cast in epoxy resin and the unit was then split into halves to facilitate installation onto the wire. The coil picked up the magnetic field produced by the current in the wire, and transformed the field into a measured voltage signal.

A capacitor was placed in series with the coil to produce resonance at 0.5 kc. By using only a part of the toroidal solenoid in the sensor, it was possible to produce resonance in the pickup circuit at frequencies as high as 21 kc. For higher frequencies, it was unnecessary to use resonance in the circuit, since the signal was sufficiently large to measure without tuning the circuit to the transmitted frequency.

The phase of the current at each point on the wire was measured relative to the phase of the vertical electric field at the point of measurement. This was done by receiving the electric field on a small vertical antenna and comparing the phase of the signal from the antenna to the phase of the signal from the current sensor. The induced currents were measured at several points along the length of each wire for each frequency transmitted by the antenna.

The specific details of some of the wires used and the results of the currents measured on these wires will be presented in the next section.

SECTION V

RESULTS

In this section, the currents calculated from the transmission-line differential equations are compared with the Stanford Research Institute experimental measurements of these currents (reference 3). The calculations were programmed for an IBM 7044 computer. The essential features of this program are discussed in Appendix V. Discrepancies between the data and the theoretical calculations are analyzed in an attempt to specify the practical limitations of this method of predicting the induced currents.

The accuracy of the Stanford Research Institute measurements was determined in private communications with Mr. Whitson, the principal investigator (reference 3). The magnitudes of the currents measured are accurate within a factor of 2, while phase measurements are within ± 30 degrees of the actual value of all frequencies. However, since the polarity of the current sensor was not kept the same for all measurements, the phase measurements were in many cases 180 degrees from the true values. This latter point must be remembered when analyzing the forthcoming data-theory comparisons.

When calculating the theoretical currents for the wires, it was recognized that all wires were buried at a depth small compared with δ_2 which necessitated the use of the impedance relations for a wire at the surface of the earth.

The Bare Wire

This wire was a 10-gauge copper wire buried approximately one-third of a meter under the surface of the earth in Area 5 (see section IV). The wire extended from 213.5 meters to 1128.5 meters radially from the base of an antenna. The terminations were formed by arbitrarily cutting off the wire, with no special grounding method used. Figures 10 to 17 show the current magnitudes and phases for this wire, both measured and theoretically predicted, for frequencies of 0.5, 10, 62, and 510 kc. The values of the current are given in amperes of current per kilovolt of antenna voltage. The logarithm of the current is plotted.

The tendency of the current to fall off at the ends indicates that termination impedances at both ends were much greater than the effective line impedance of the wire. The relatively high termination impedances are anticipated by the analysis given in the termination impedance discussion.

The agreement between experimental and theoretical calculations is good for the three highest frequencies. It must be kept in mind that, since the polarity of the sensor was not specified in the experimental data, it may be necessary to adjust the experimental phase values by 180 degrees. This appears to be the case in figures 13 and 15.

At the lowest frequency, predicted currents are high by an order of magnitude, and the predicted phases are off by 90 degrees. The most likely reason for the discrepancy relates to the assumption in the theoretical treatment that the bare wire had good electrical contact with the earth. Simply burying a wire in the earth does not ensure good electrical contact, since a rough textured soil permits air spaces between the wire and the length of the wire. Also, a metal oxide coating the bare wire could produce an effective insulation. In case of copper wire, copper oxide may even act as a rectifying layer, an effect that cannot be easily considered in the present linear analysis.

Any insulation, such as air spaces and oxide coatings, produces a high capacitance in the transverse admittance. At high frequencies, this capacitance appears as a low impedance and therefore is inconsequential. At lower frequencies, however, the impedance caused by this capacitance reduces the observed currents induced in the wires and shifts their phase by 90 degrees.

The Insulated-Wire, High-Impedance Terminations

The first insulated wire was an insulated 10-gauge wire placed on the surface of the earth in area 1 (see section IV). The thickness of the insulation was approximately 1.2 mm, and its measured dielectric constant for this frequency range was approximately 2.7. The wire extended from 91.5 meters to 1220.5 meters radially from the base of the antenna. The terminations were formed by arbitrarily cutting off the wire, making no attempt to ground the cut ends of the wire. Figures 18 to 25 show the theoretical and experimental current magnitude and phases for this wire for frequencies of 2, 10, 62, and 510 kcs.

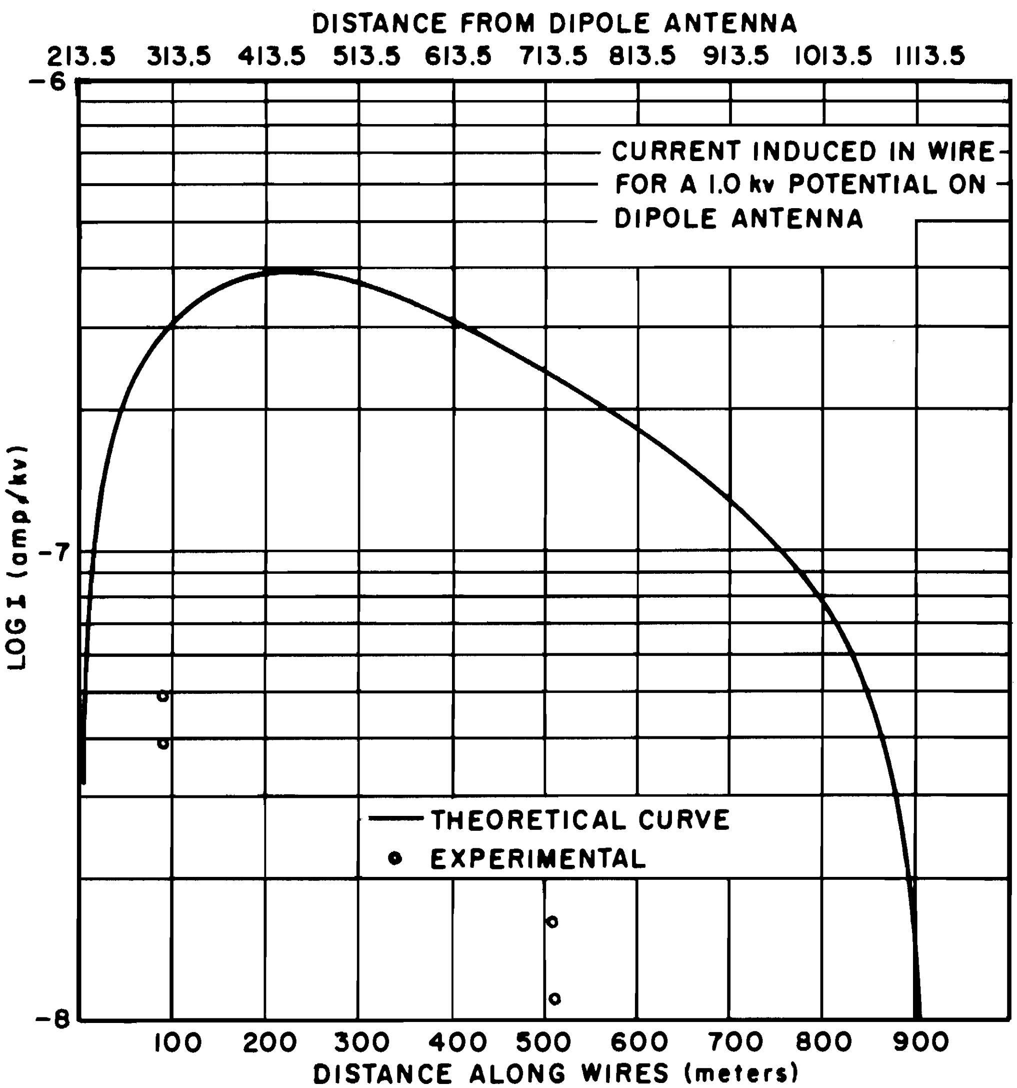

Figure 10. Bare Wire Current Magnitude at 0.5 kcs.

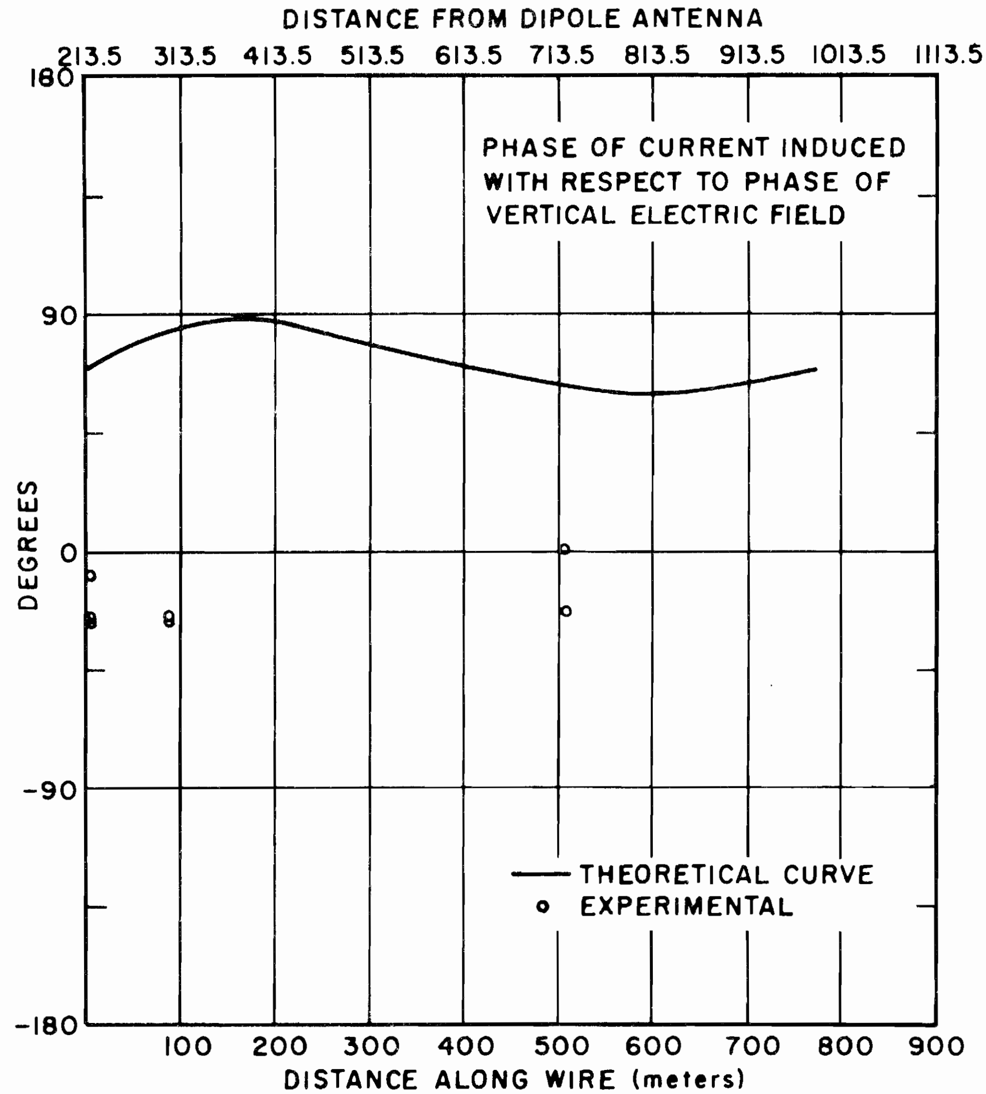

Figure 11. Bare Wire Current Phase at 0.5 kcs.

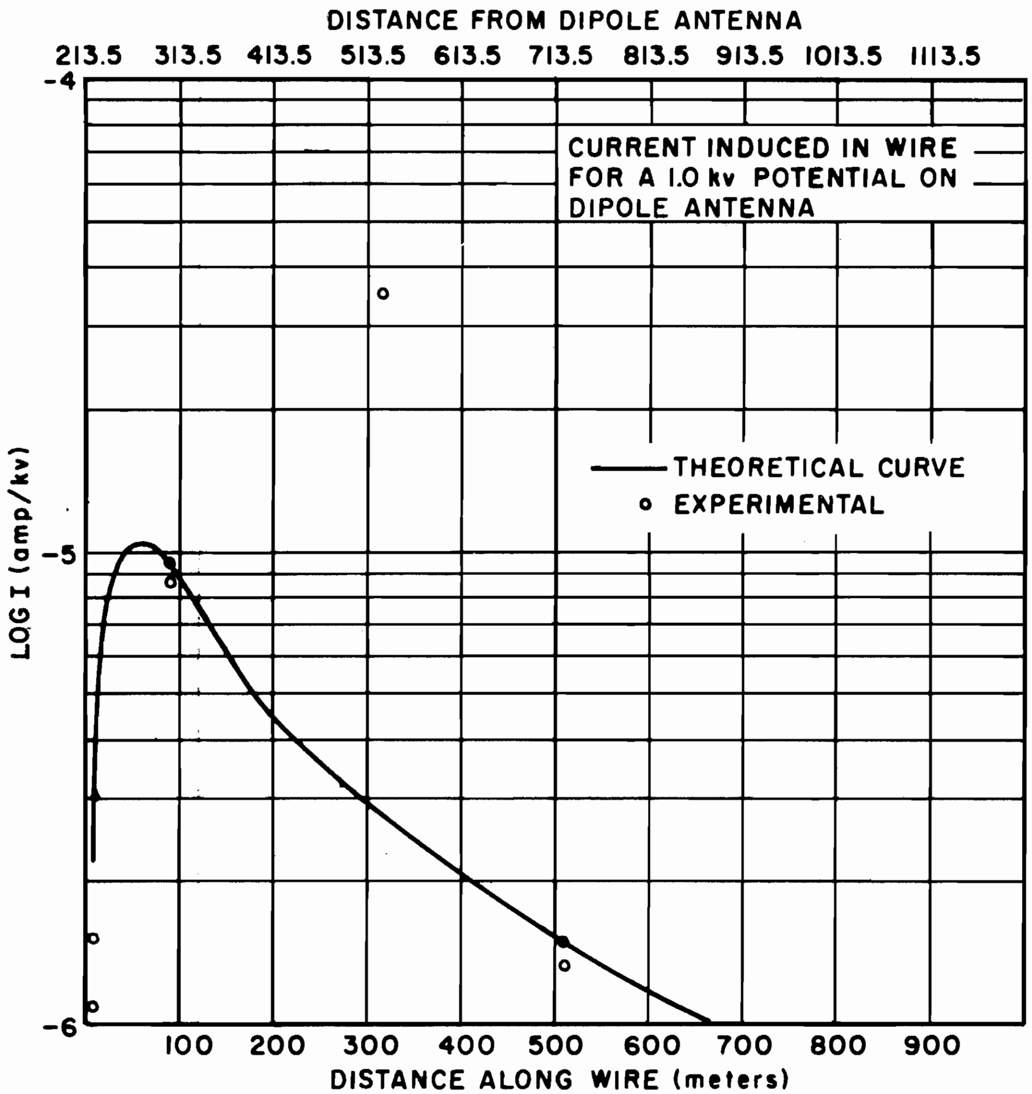

Figure 12. Bare Wire Current Magnitude at 10 kcs.

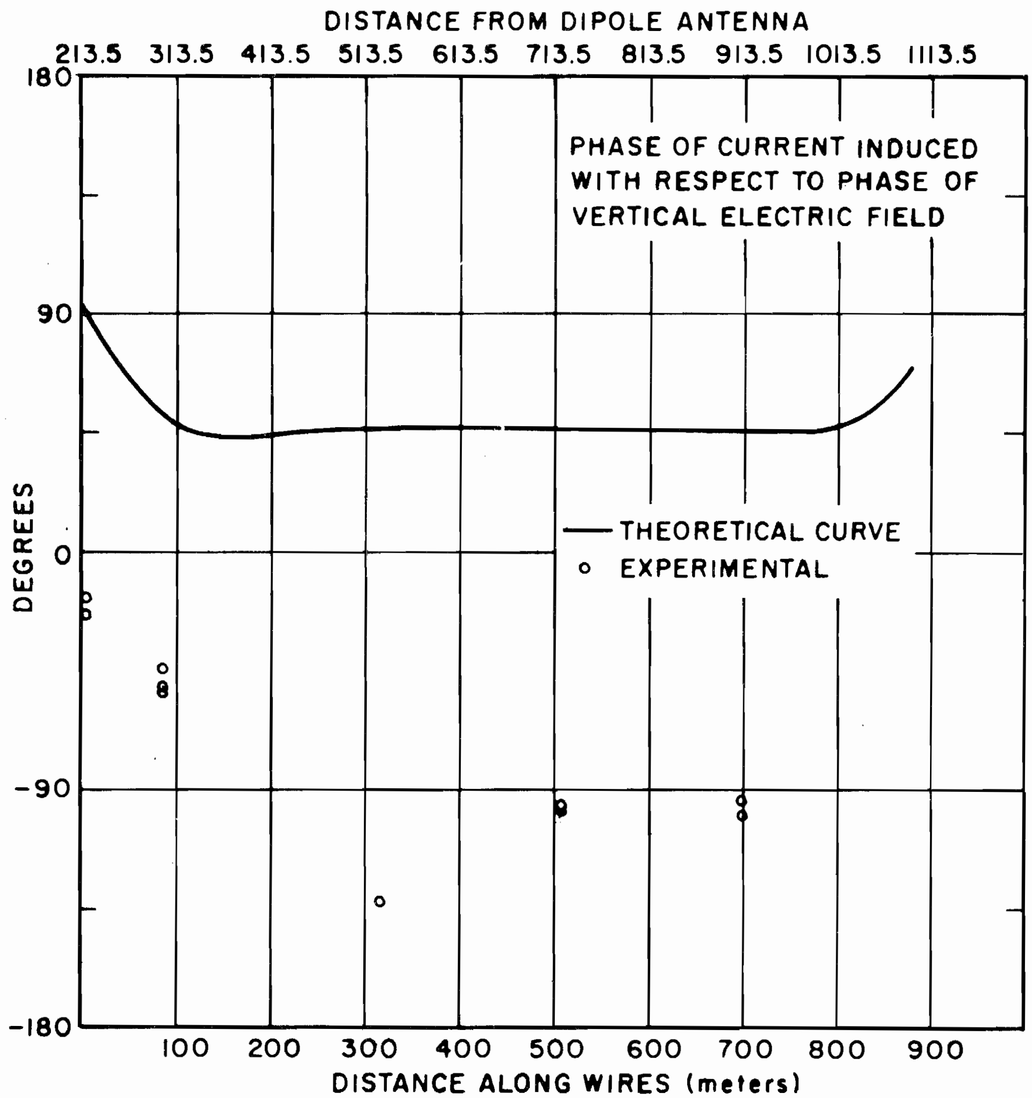

Figure 13. Bare Wire Current Phase at 10 kcs.

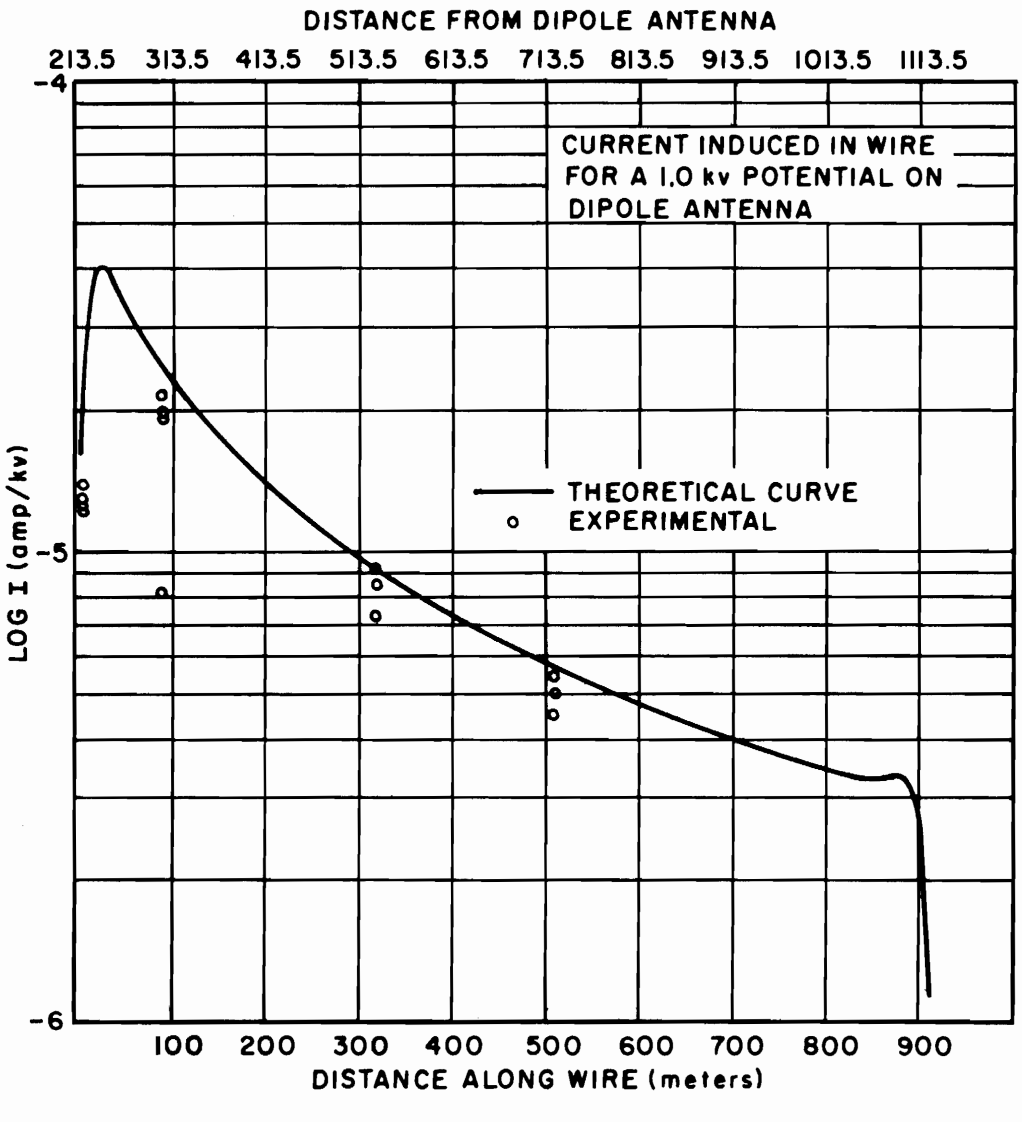

Figure 14. Bare Wire Current Magnitude at 62 kcs.

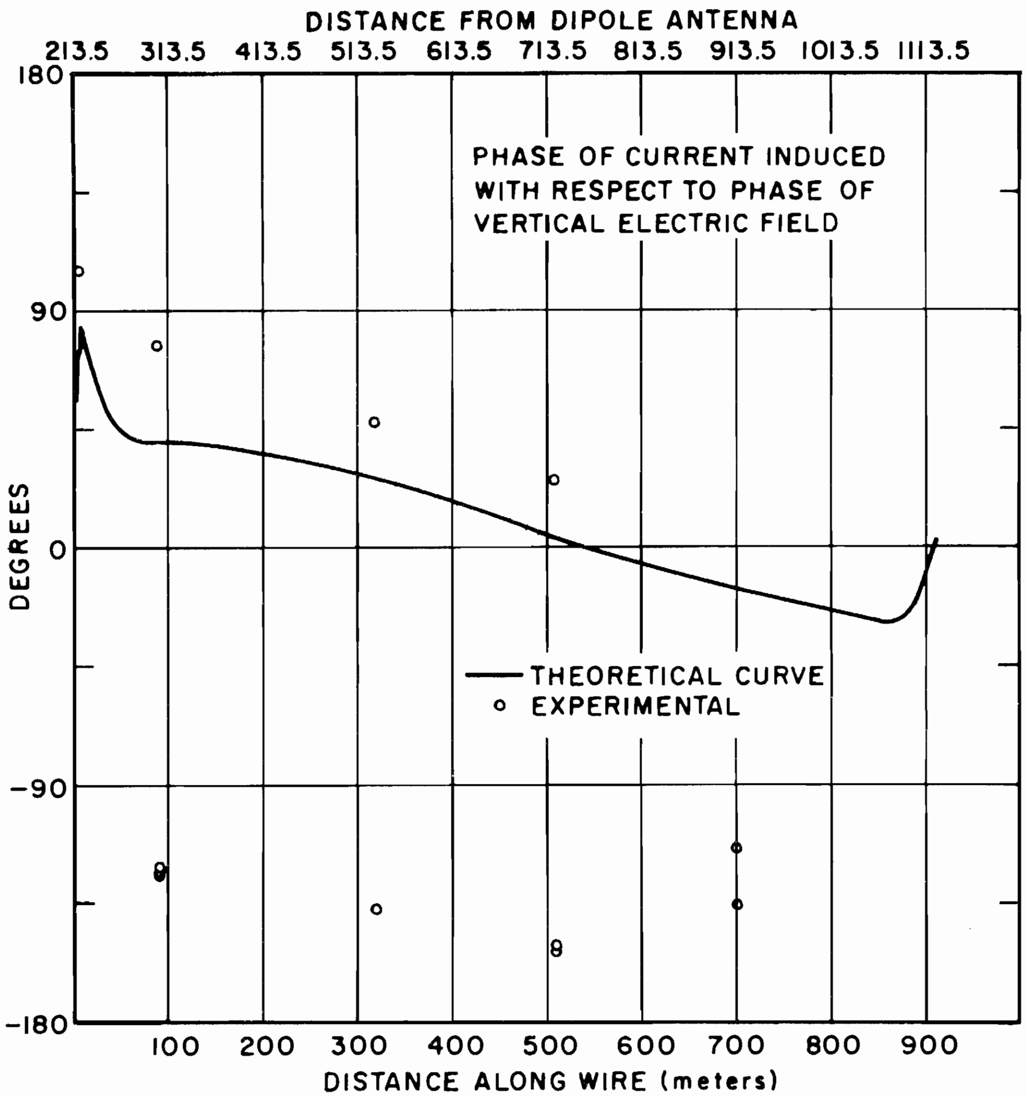

Figure 15. Bare Wire Current Phase at 62 kcs.

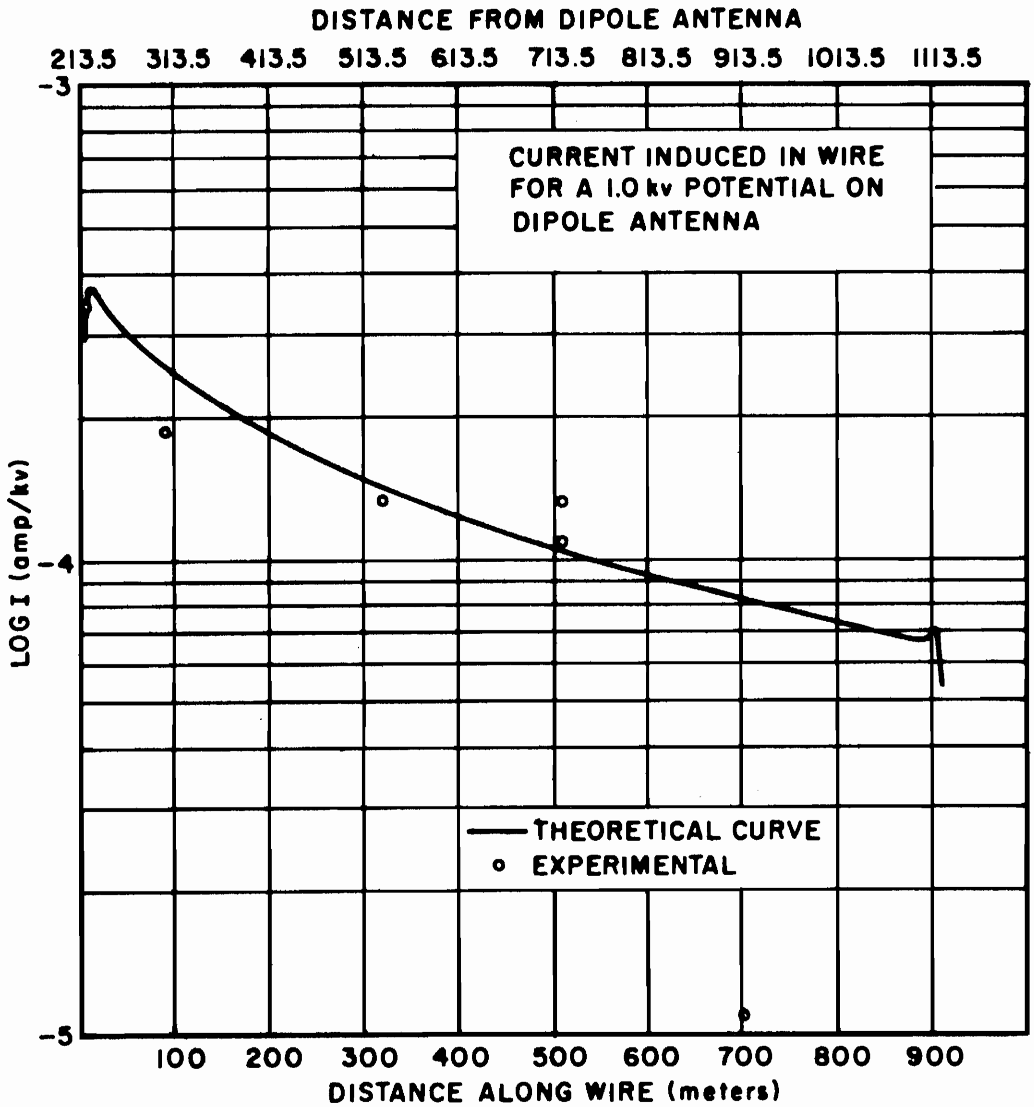

Figure 16. Bare Wire Current Magnitude at 510 kcs.

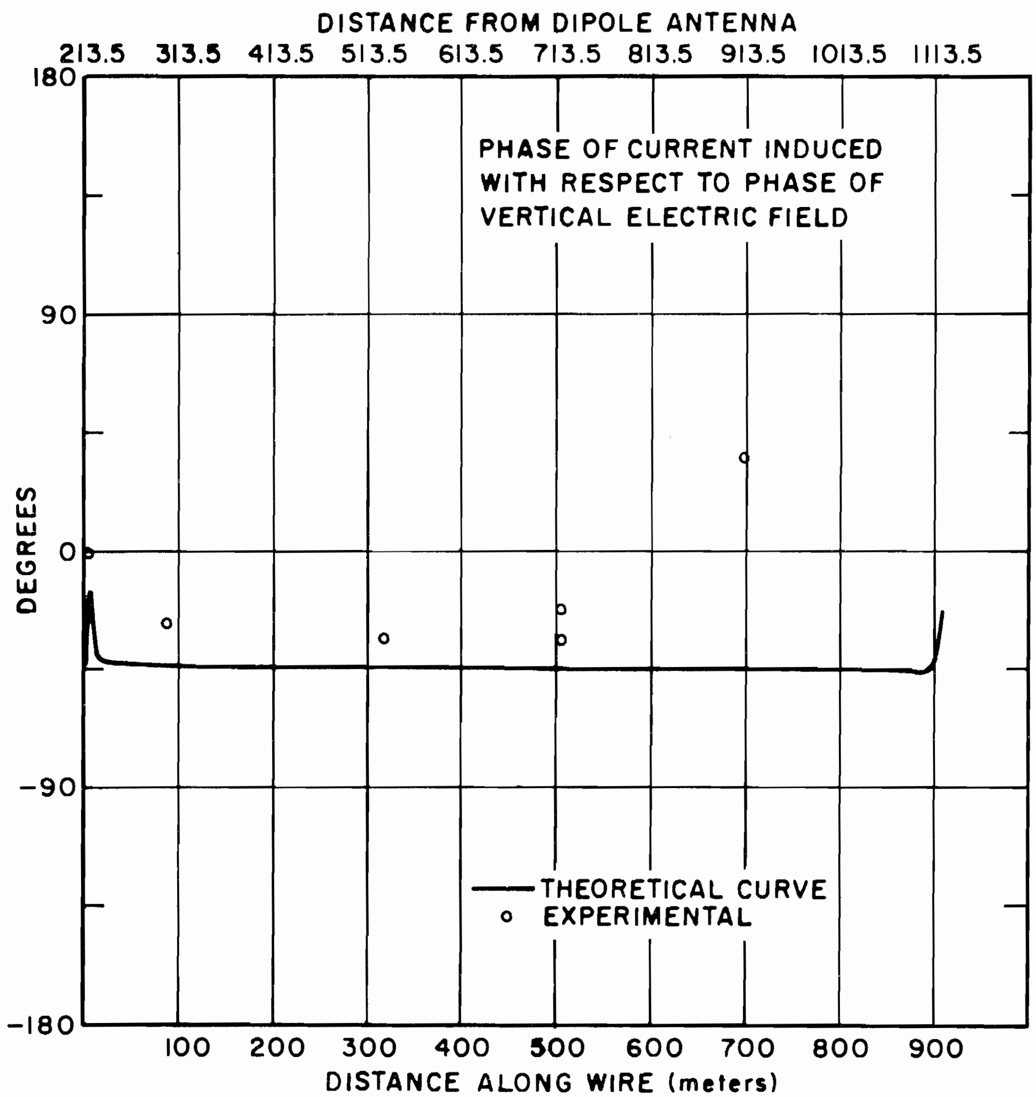

Figure 17. Bare Wire Current Phase at 510 kcs.

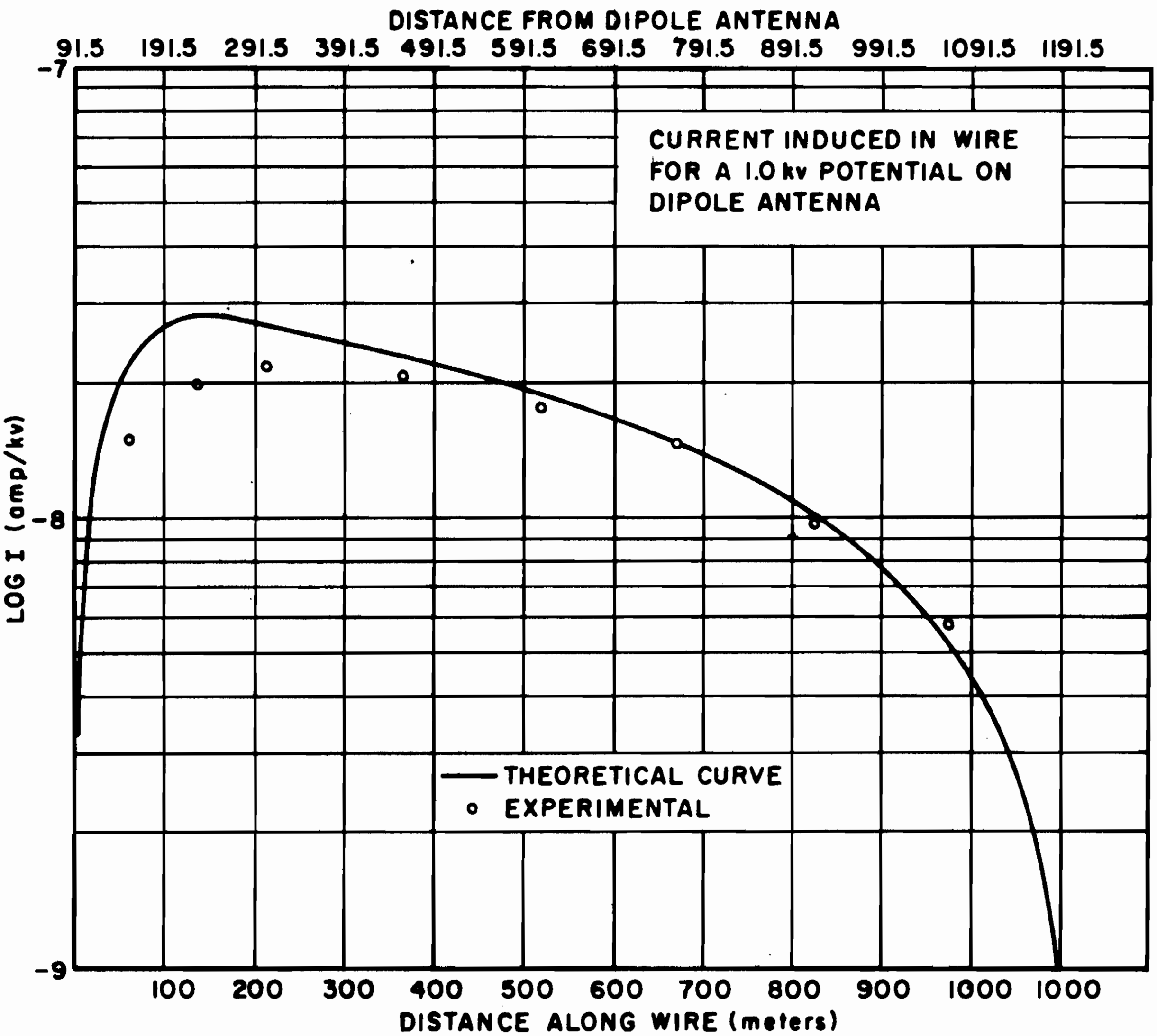

Figure 18. Current Magnitude, Insulated Wire, High-Impedance Terminations, 2 kcs.

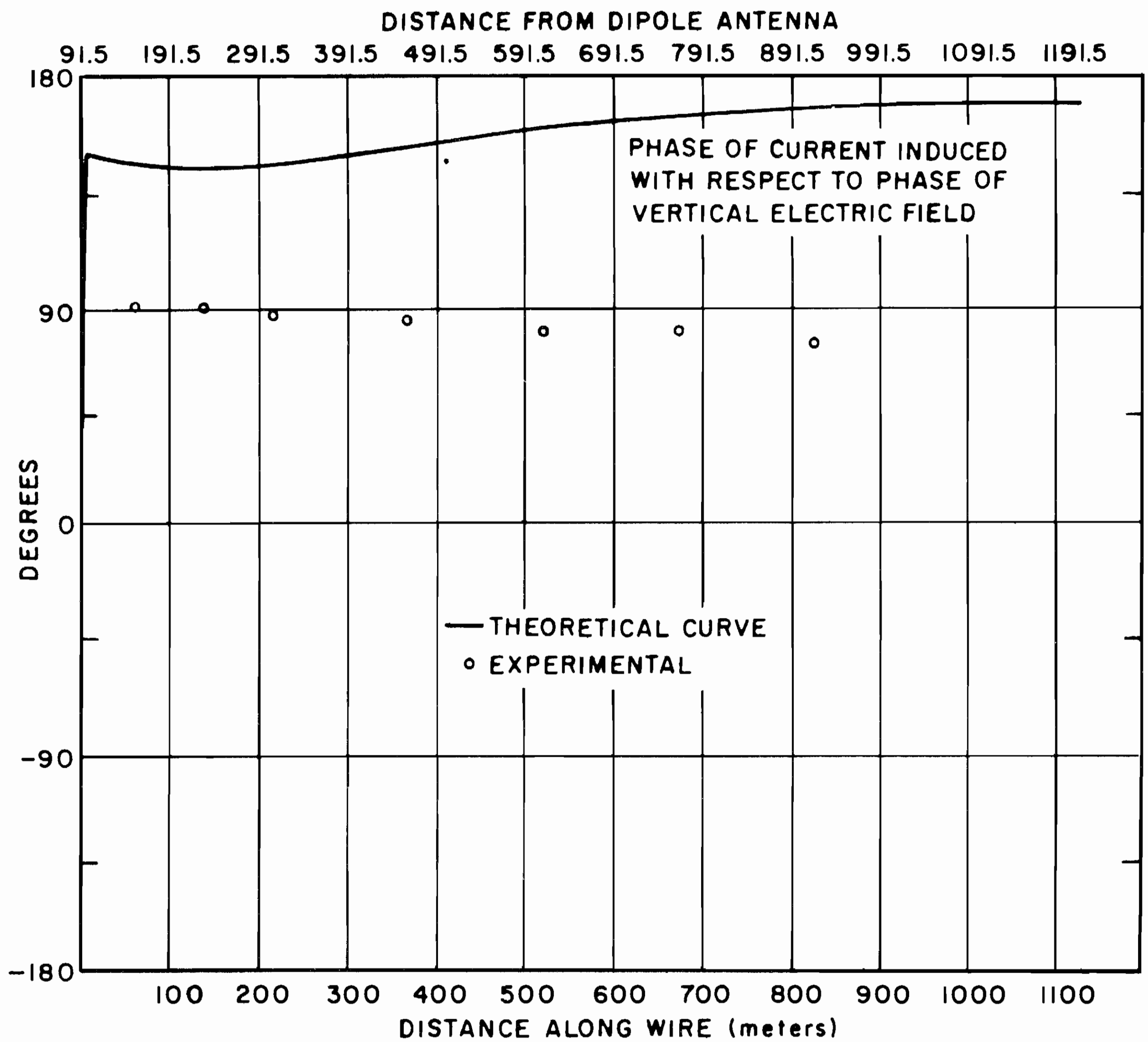

Figure 19. Current Phase, Insulated Wire, High-Impedance Terminations, 2 kcs.

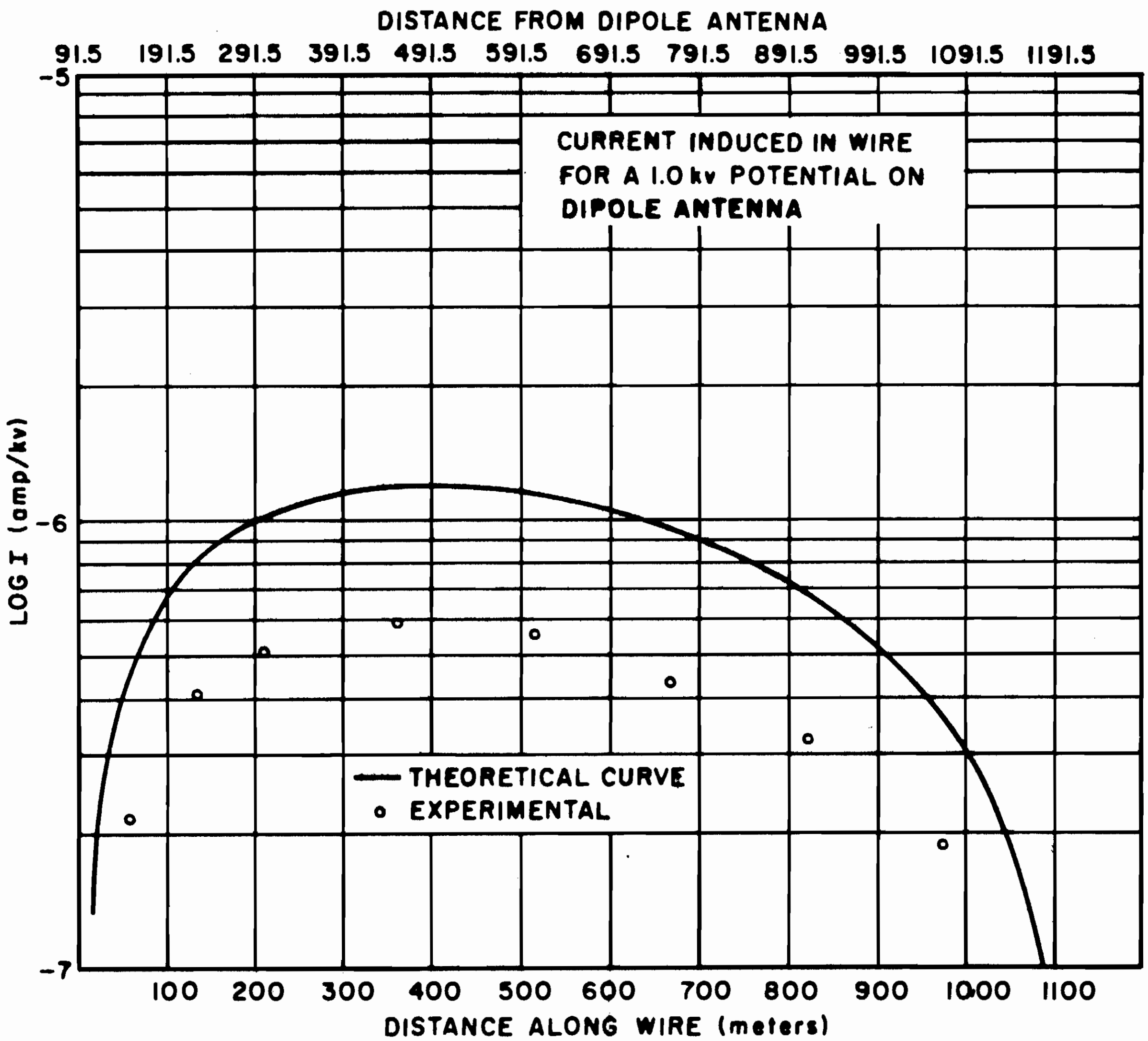

Figure 20. Current Magnitude, Insulated Wire, High-Impedance Terminations, 10 kcs.

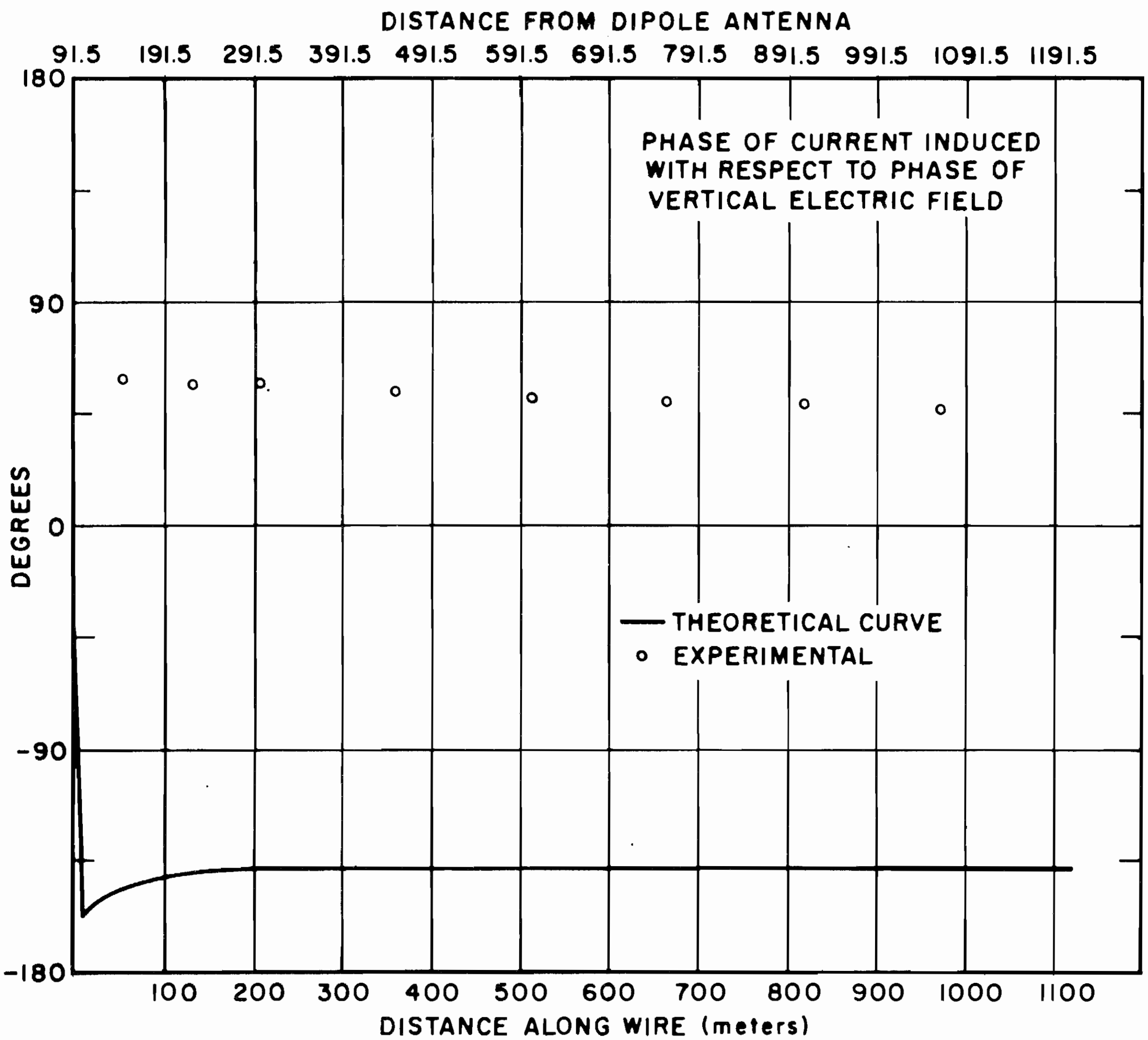

Figure 21. Current Phase, Insulated Wire, High-Impedance Terminations, 10 kcs.

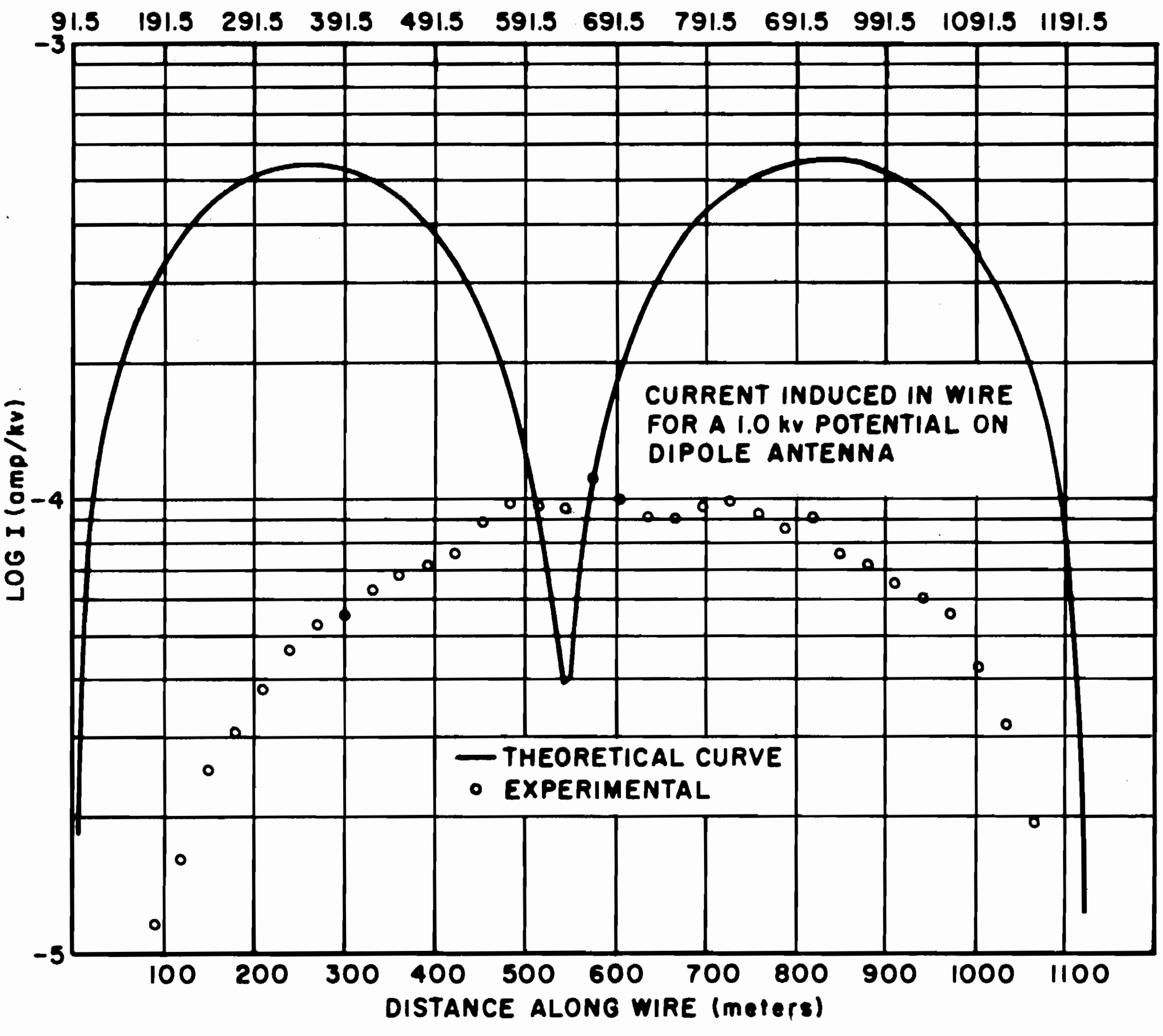

Figure 22. Current Magnitude, Insulated Wire, High-Impedance Terminations, 62 kcs.

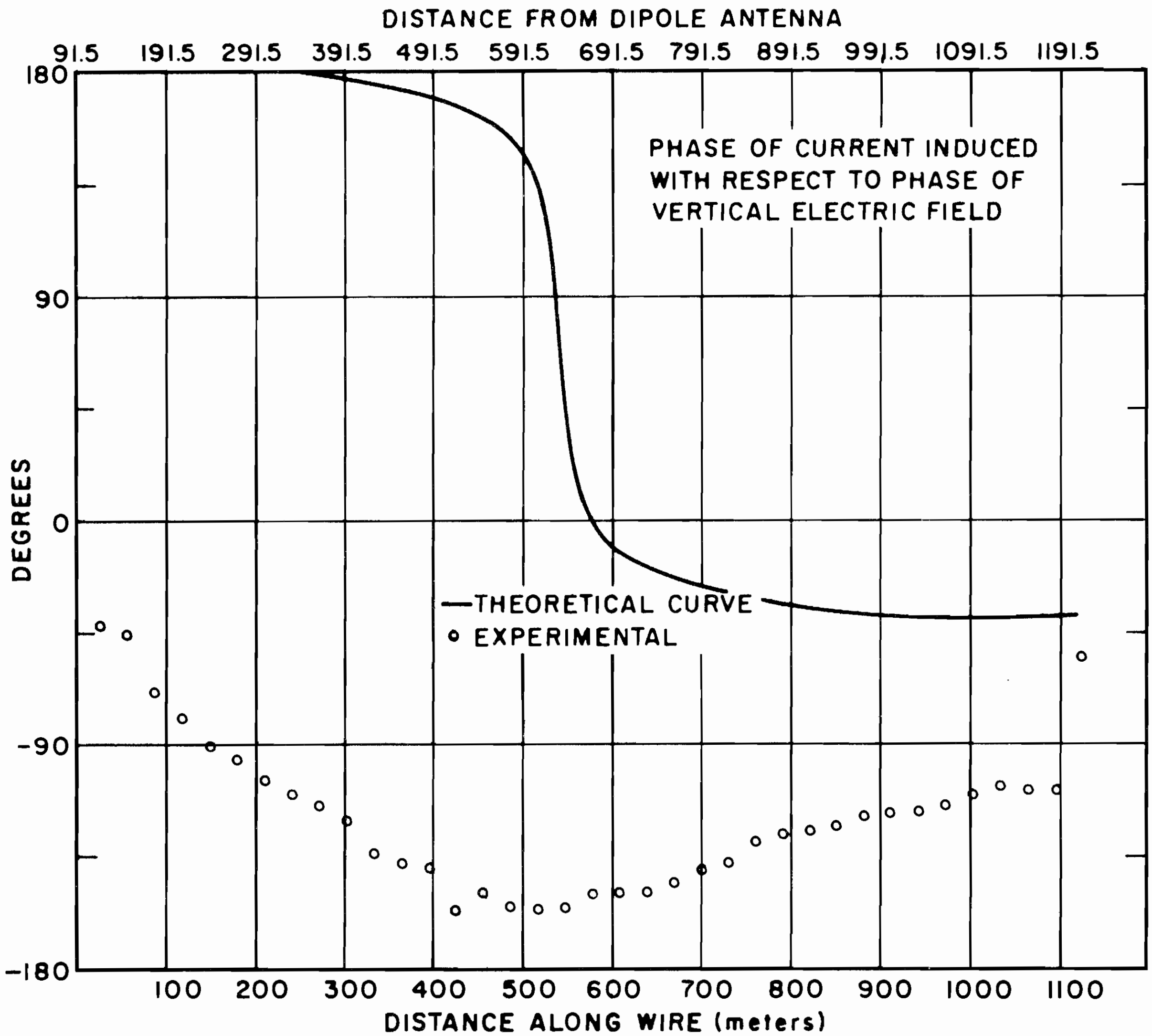

Figure 23. Current Phase, Insulated Wire, High-Impedance Terminations, 62 kcs.

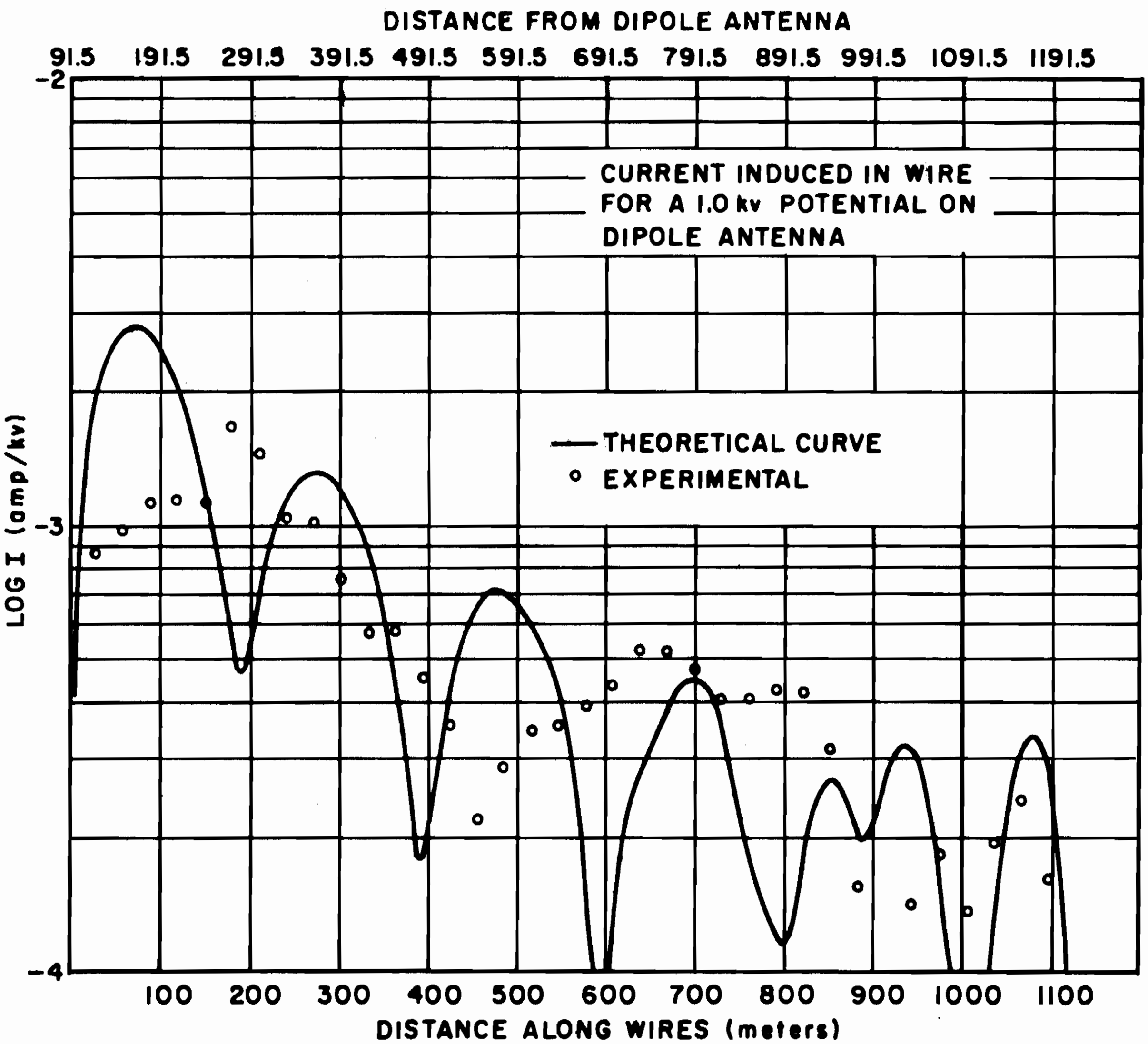

Figure 24. Current Magnitude, Insulated Wire, High-Impedance Terminations, 510 kcs.

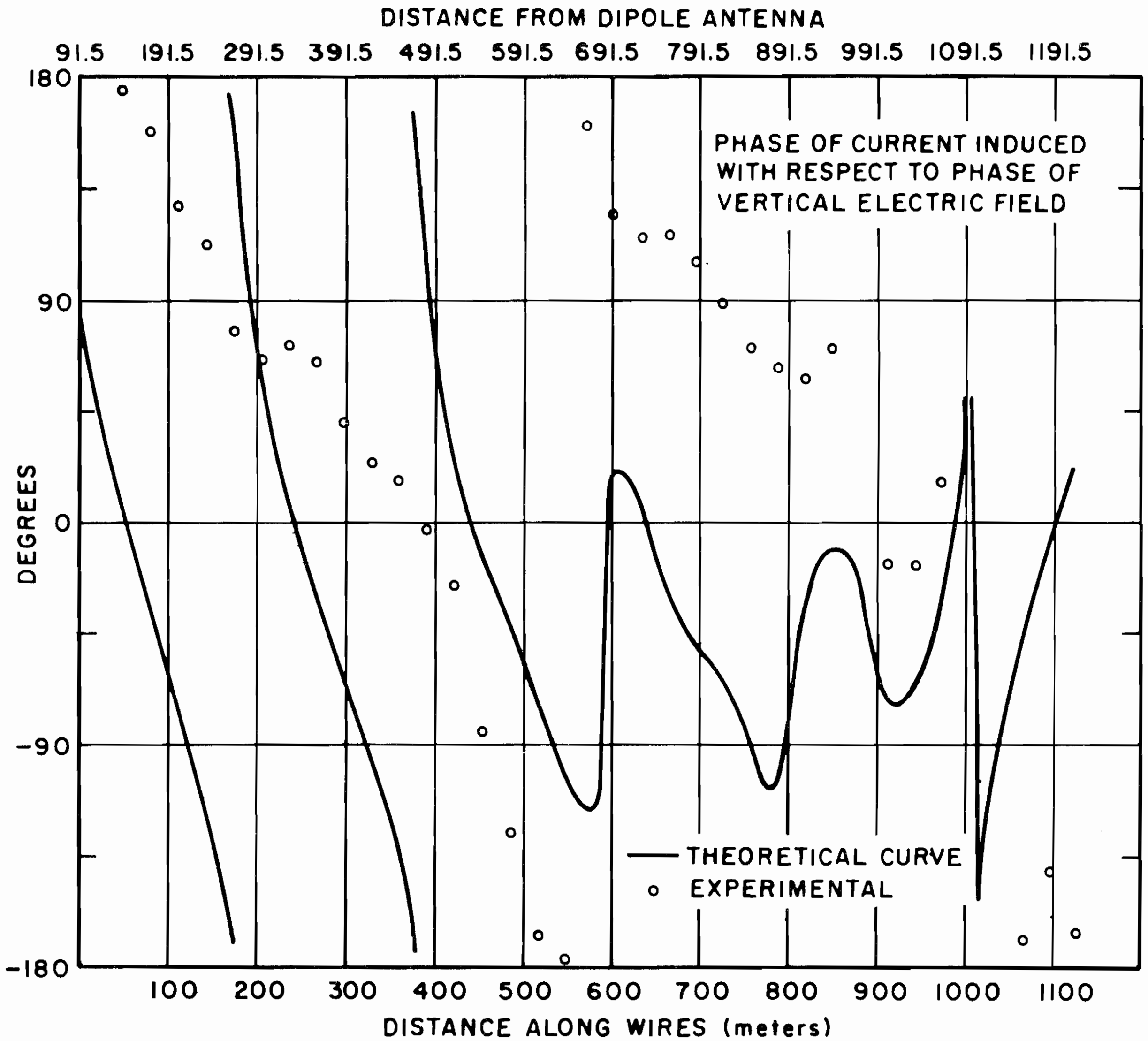

Figure 25. Current Phase, Insulated Wire, High-Impedance Terminations, 510 kcs.

Again, the drop in current near the terminations indicates that the impedances at the ends were higher than the line impedance of the wire. Since no attempt is made to ensure good electrical contact with the earth at the terminations, it is to be expected that these impedances were much higher than the impedance at any other point along the wire.

A noticeable characteristic of the insulated wire is the standing wave structure at frequencies at which the wave length of the current wave is comparable to or less than the length of the wire. In the bare wire, the reflected waves are so strongly attenuated that they do not produce a prominent standing wave structure.

The magnitude of the currents shows a good comparison between experiment and theory, except at 62 kcs. Only the phase at 10 kcs shows good comparison between experiment and theory in the phase comparisons.

The agreement between the experimental and theoretical values of phase cannot be quantitatively discussed at this point. Both theoretical and experimental programs investigating this question should be carried out to determine the real reasons for the present lack of quantitative agreement.

The magnitude discrepancy at 62 kcs is explained by the fact that the electrical characteristics used for the theoretical calculations give a current distribution at or near the second current resonance of the wire. Near resonance, a small error in the electrical characteristics of the wire or in the frequency of the input wave can result in a large error in the predicted current value. Figure 26 illustrates how the maximum wire current varies rapidly near resonance.

However, the fact remains that the theoretical predictions are near the second resonance while the data appeared to be closer to the primary resonance, both in magnitude and phase. This discrepancy is also noted in the fine structure of the 510 kcs magnitude and phase comparisons. Since the wave length of the current wave is inversely proportional to the transverse capacitance of the insulation, the comparisons indicate that the calculated transverse capacitances are too high.

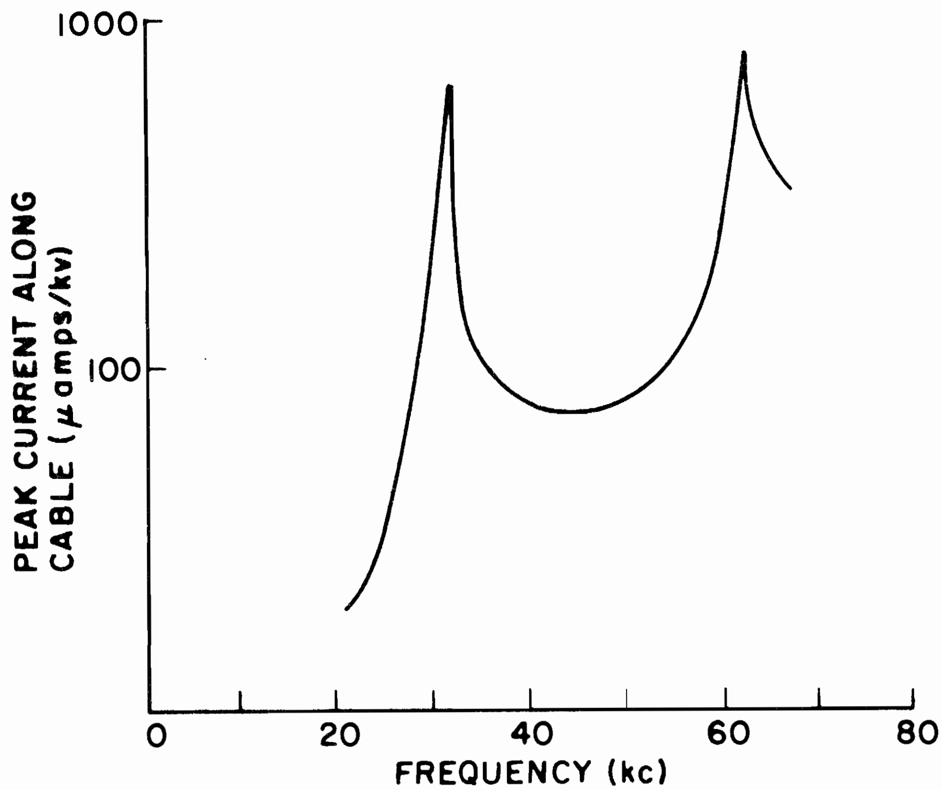

Figure 26. Theoretical Peak Current Versus Frequency Near Primary And Secondary Resonance for the First Insulated Wire.

The reason for this is again the basic assumption that there must be good electrical contact between the outside of the wire covering and the earth. In the actual case, the wire was laid on the surface of the earth with no provision made to ensure good electrical contact. The contact is more realistically depicted by figure 27.

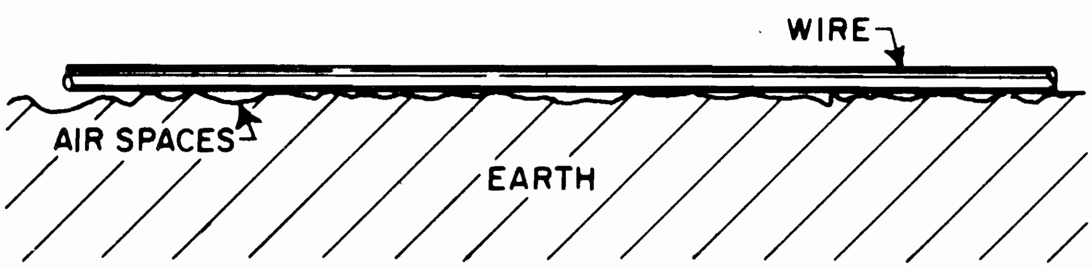

Figure 27. Wire Lying on the Surface of the Earth.

The air spaces between the wire and the earth produced a capacitance in series with the insulation capacitance, thereby reducing the total capacitance of the system. An accurate theoretical analysis of this effect is very difficult, but the effect is approximated by assuming that the wire had an insulating covering of air of some appropriate thickness.

However, if the interest of the problem lies in estimating the peak currents induced in the wire, the only difficulty presented here is the problem of resonance at high frequencies. Except for the 62 kcs theoretical resonance, all magnitude comparisons are good.

The Insulated Wire, Grounded Terminations

The second insulated wire was identical with the first except for the wire terminations. In this case, each end was terminated by connecting the end of the wire to a one-meter-long metal stake driven vertically into the earth in an attempt to reduce the termination impedance to a minimum. The actual termination impedance was measured to be 1900 ohms, which was comparable to the equivalent line impedance of the insulated wire. In the theoretical calculations, the terminations are assumed to be zero at each end. Indicative of the lower termination impedance, the current at the ends is comparable with the current elsewhere in the wire.

Comparison of the theoretical and experimental current magnitude and phases is found in figures 28 to 31 for frequencies of 10 and 510 kcs. The theoretical calculation of the magnitude at 10 kcs is 3 to 4 times higher than the current actually measured. This is due to misjudging the termination impedances in the calculations. Calculations indicate that at 0.5 kc, the peak current can vary by 4 orders of magnitude if the termination impedances vary from zero ohms to infinity. There are large variations of this nature for all frequencies below the primary resonant frequency, which explains the discrepancy at 10 kcs.

The high-frequency phase discrepancy was produced by the added capacitance caused by poor electrical contact, as in the previous insulated wire test. Unfortunately, there are insufficient data to make a detailed analysis at either frequency or at any of the other frequencies at which data were taken.

The High-Conductivity Covering

The conductor used in this experiment was a double-sheath armored communications cable buried at a depth of approximately one meter. The outside metal sheath, made of 0.7-mm-thick copper, was covered with a 0.55-mm-thick covering of a material which had a conductivity of approximately 1 mho/meter; comparable conductivity to that of earth, but much less than that of the metal. It is assumed, for the sake of simplicity, that the thickness of the outer copper sheath is greater than the thickness of copper necessary to produce an

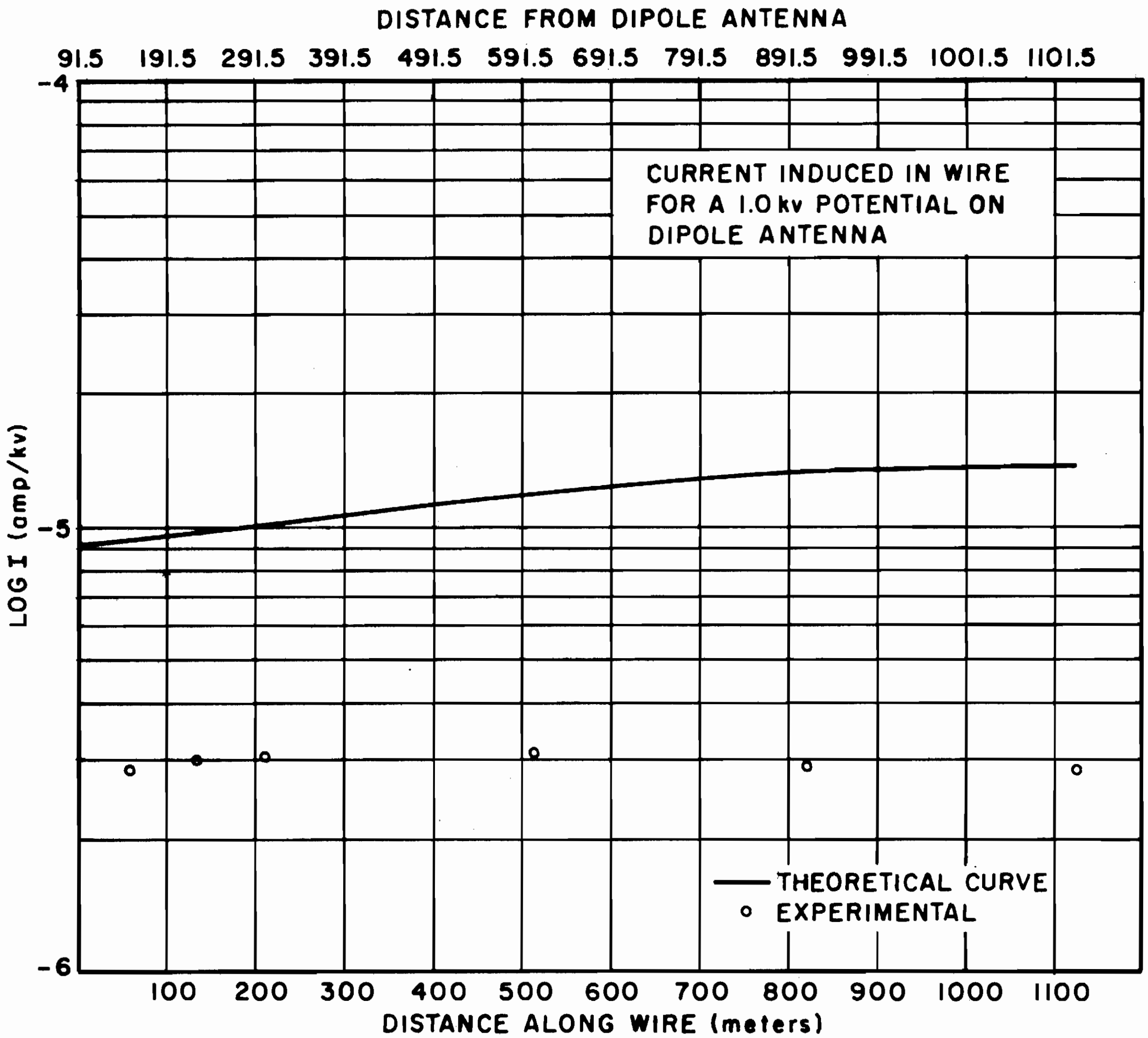

Figure 28. Current Magnitude, Insulated Wire, Grounded Terminations, 10 kcs.

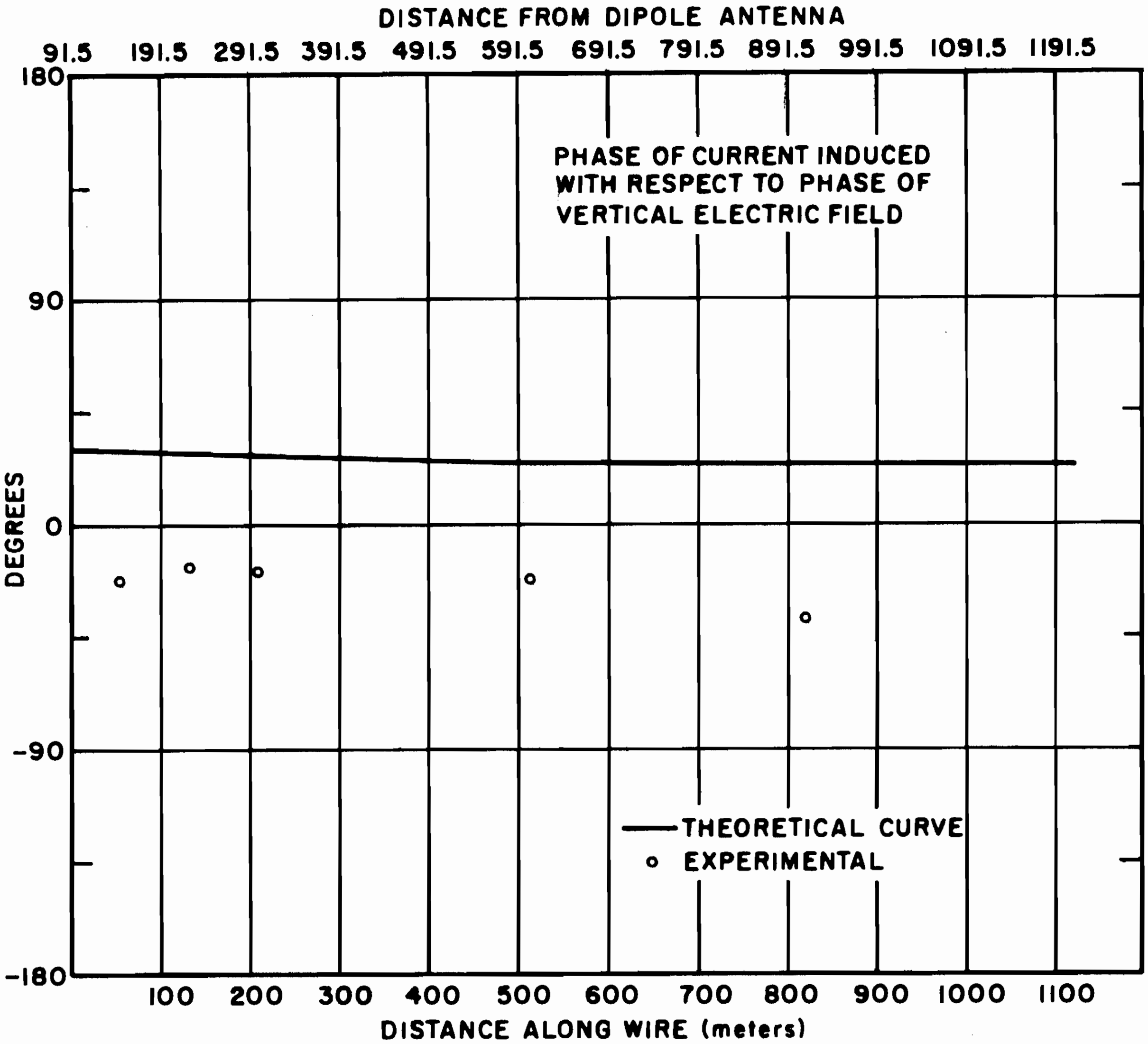

Figure 29. Current Phase, Insulated Wire, Grounded Terminations, 10 kcs.

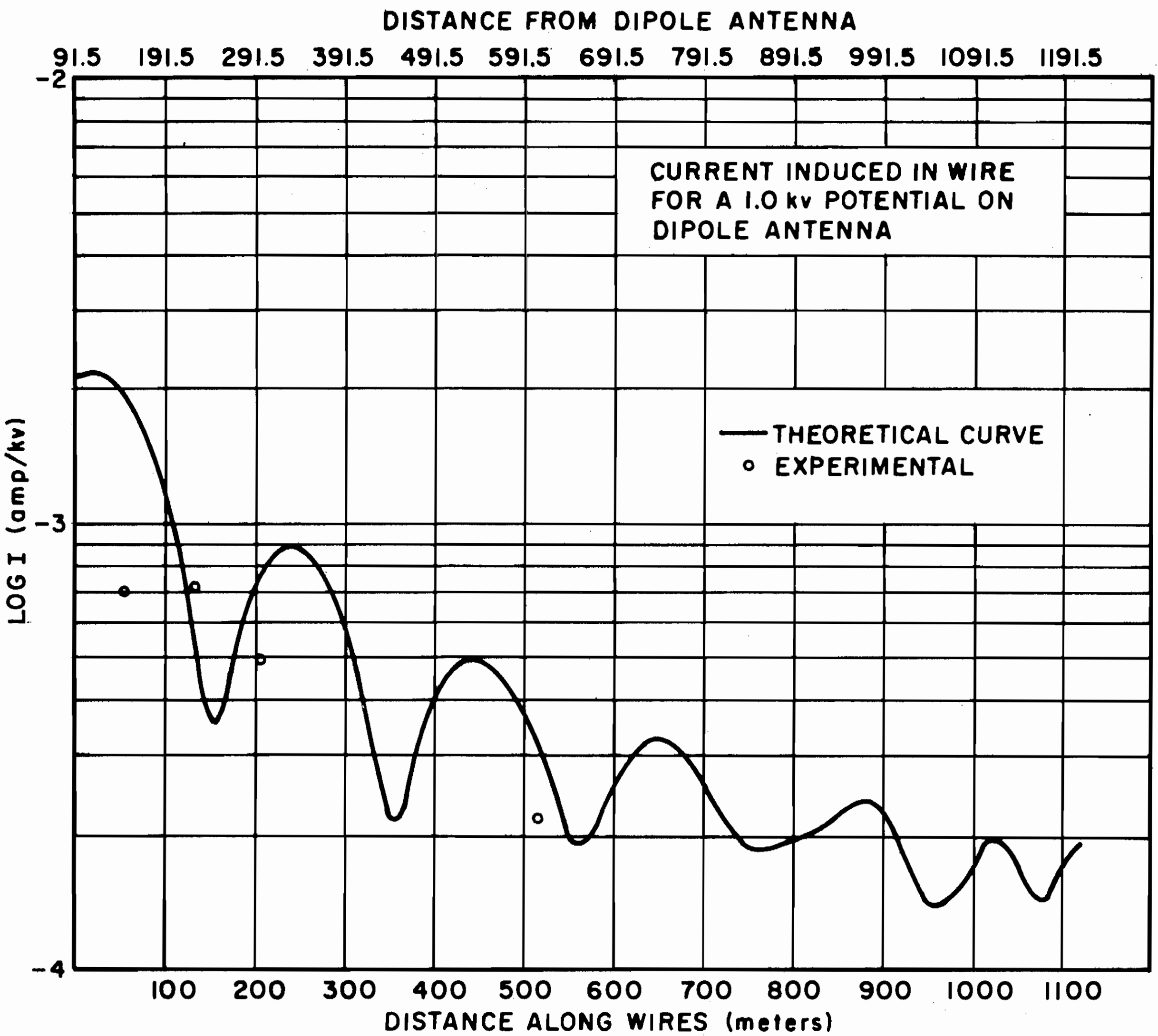

Figure 30. Current Magnitude, Insulated Wire, Grounded Terminations, 510 kcs.

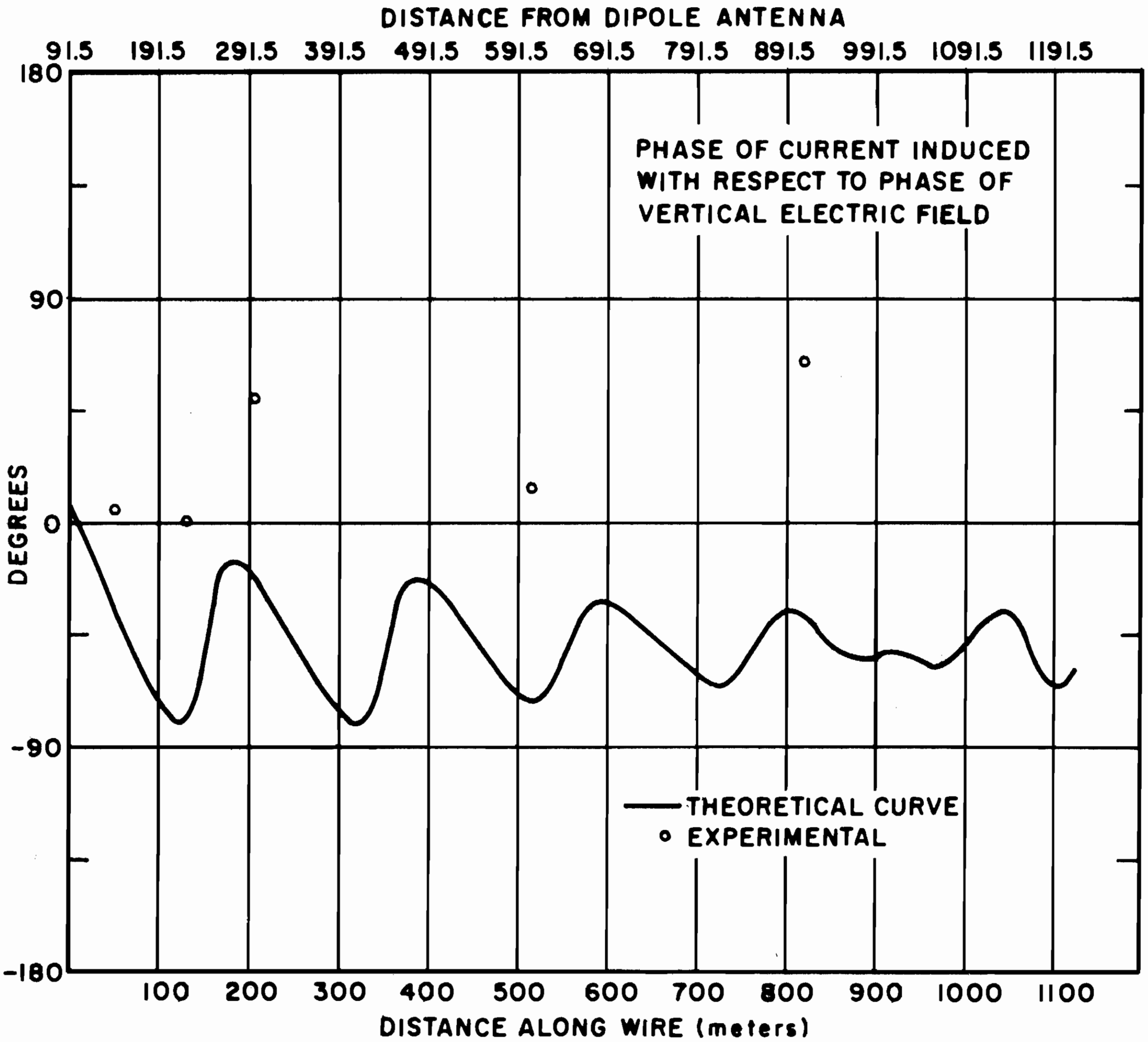

Figure 31. Current Phase, Insulated Wire, Grounded Terminations, 510 kcs.

attenuation of $\frac{1}{e}$ in the outside tangential electric field. This is a good approximation for all frequencies above 10 kcs. When the approximation holds, the hollow metal sheath appears as a solid conductor to outside fields. Therefore, the relations that are used for the solid wire can be used, independent of the structure inside the external metal sheath.

The terminations of the cable were cut off, with no special grounding arrangement used. The data confirm the current magnitude decrease at each end associated with this method of terminating a wire. These experimental data for the current magnitudes in the neighborhood of the ends of the cable are so small that they do not appear on the graphs. In some cases, these currents could not be measured due to their small magnitudes.

Figures 32 to 39 show the comparison of the experimental current magnitude and phase data with the corresponding theoretical calculations for 0.5, 10, 62, and 510 kcs. There is excellent agreement in magnitude and phase for all frequencies except for the apparent discrepancy in phase at 0.5 kc.

The high-conductivity covering, together with burying the cable, appears to provide a much better electrical contact with the earth than a surface cable or a noncovered cable. The covering also prevents oxidation of the outer surface of the metal. Therefore, the electrical characteristics of this cable are known more precisely than the characteristics of the other cables studied.

Conclusions

Several limitations on the transmission line model are obvious at the start. The local electrical characteristics of the earth, such as the conductivity and the dielectric constant, may vary rapidly over the lengths of the wires. These variations may produce error in both the wire impedance characteristics and the postulated impressed electric field. Lacking convincing experimental evidence, it is difficult to give a quantitative measure of this limitation. It would seem to be a reasonable first approximation, however, to assume that the ground has its average electrical properties everywhere.

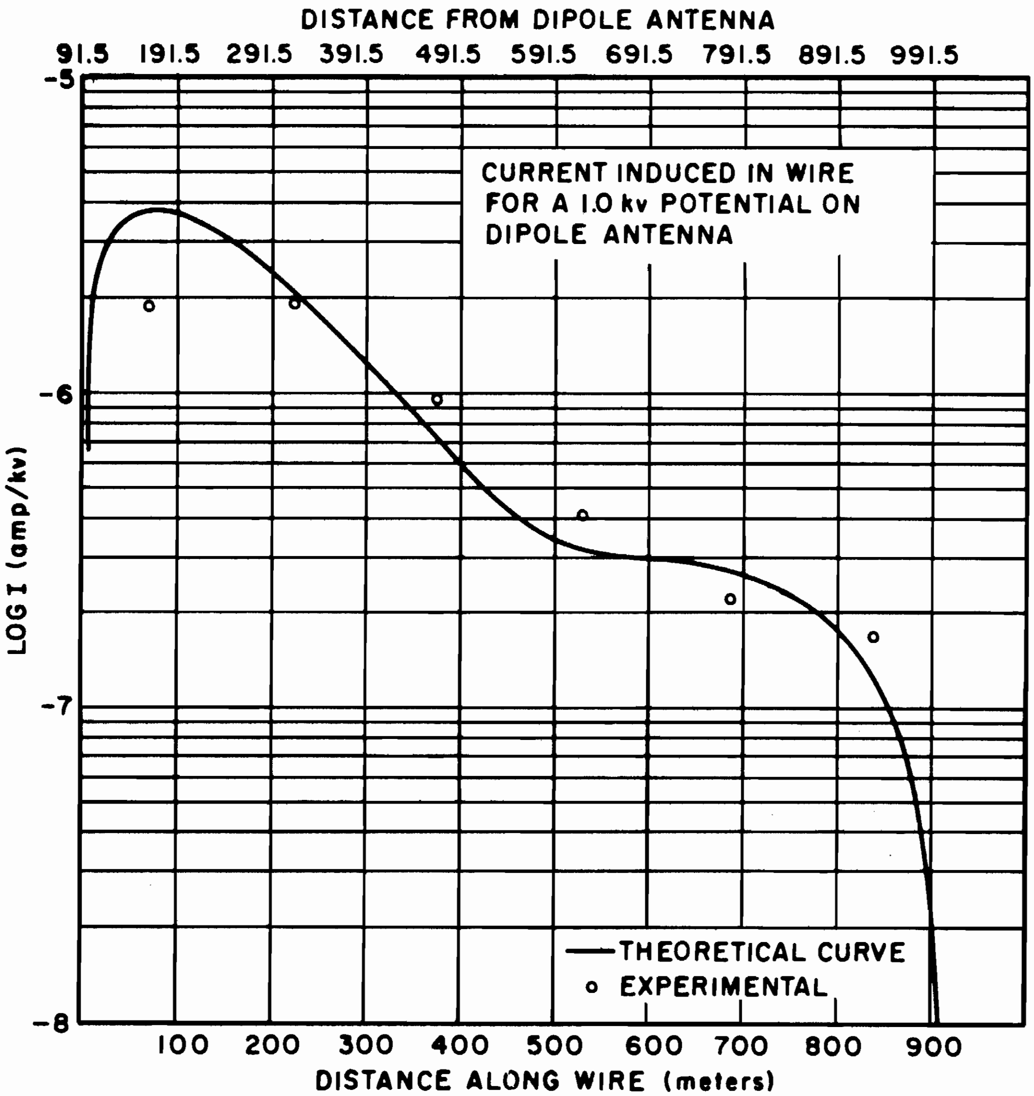

Figure 32. Current Magnitude in Wire with High Conductivity Covering at 0.5 kcs.

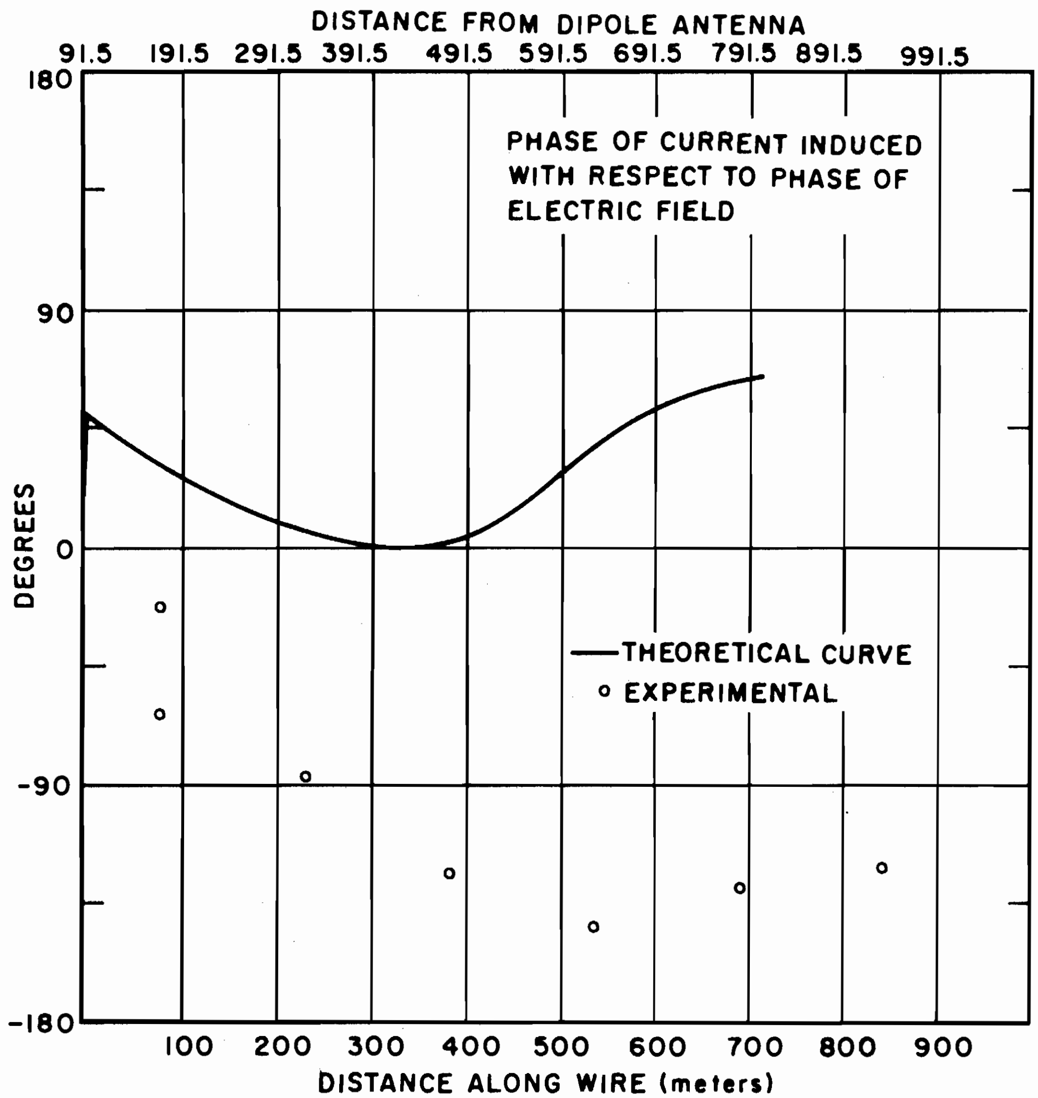

Figure 33. Current Phase in Wire with High Conductivity Covering at 0.5 kcs.

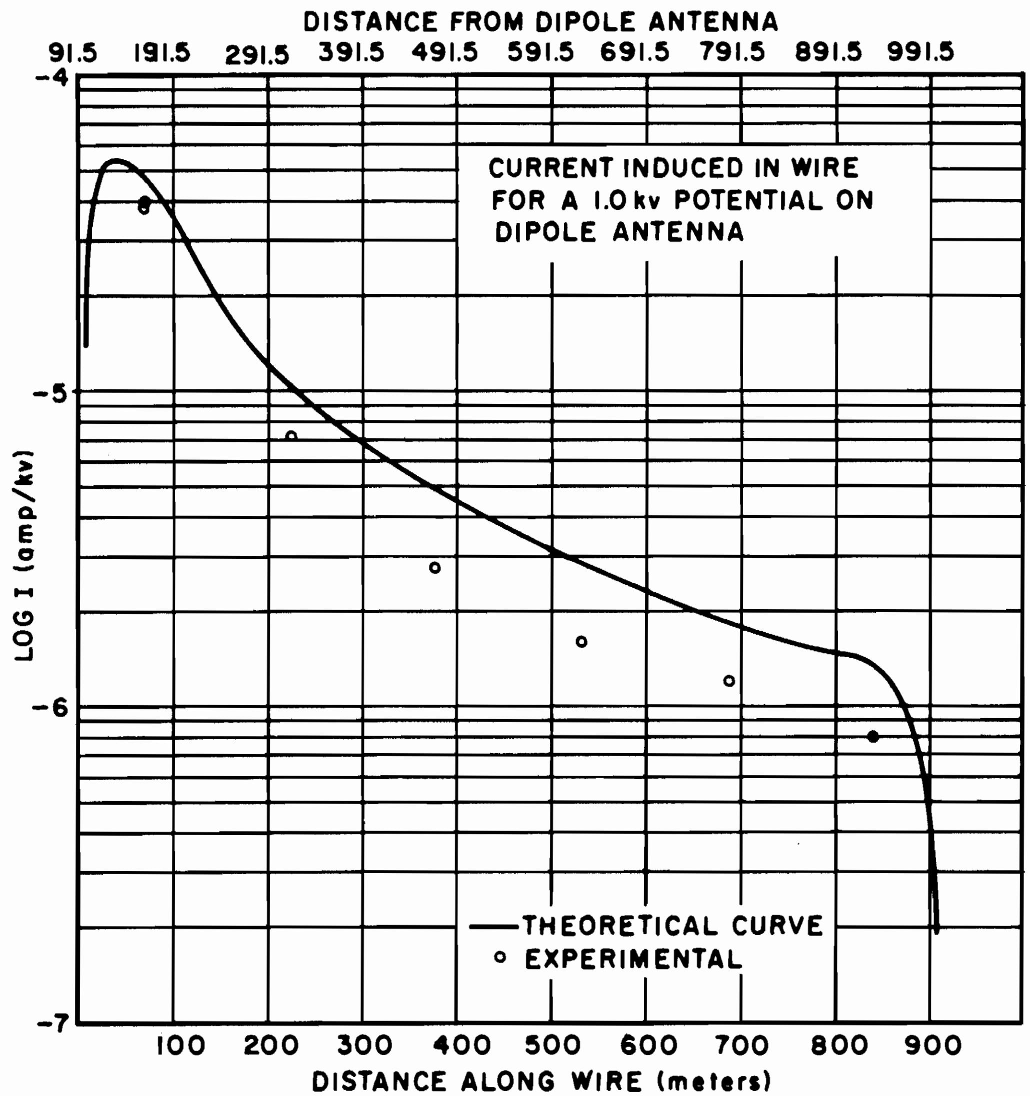

Figure 34. Current Magnitude in Wire with High Conductivity Covering at 10 kcs.

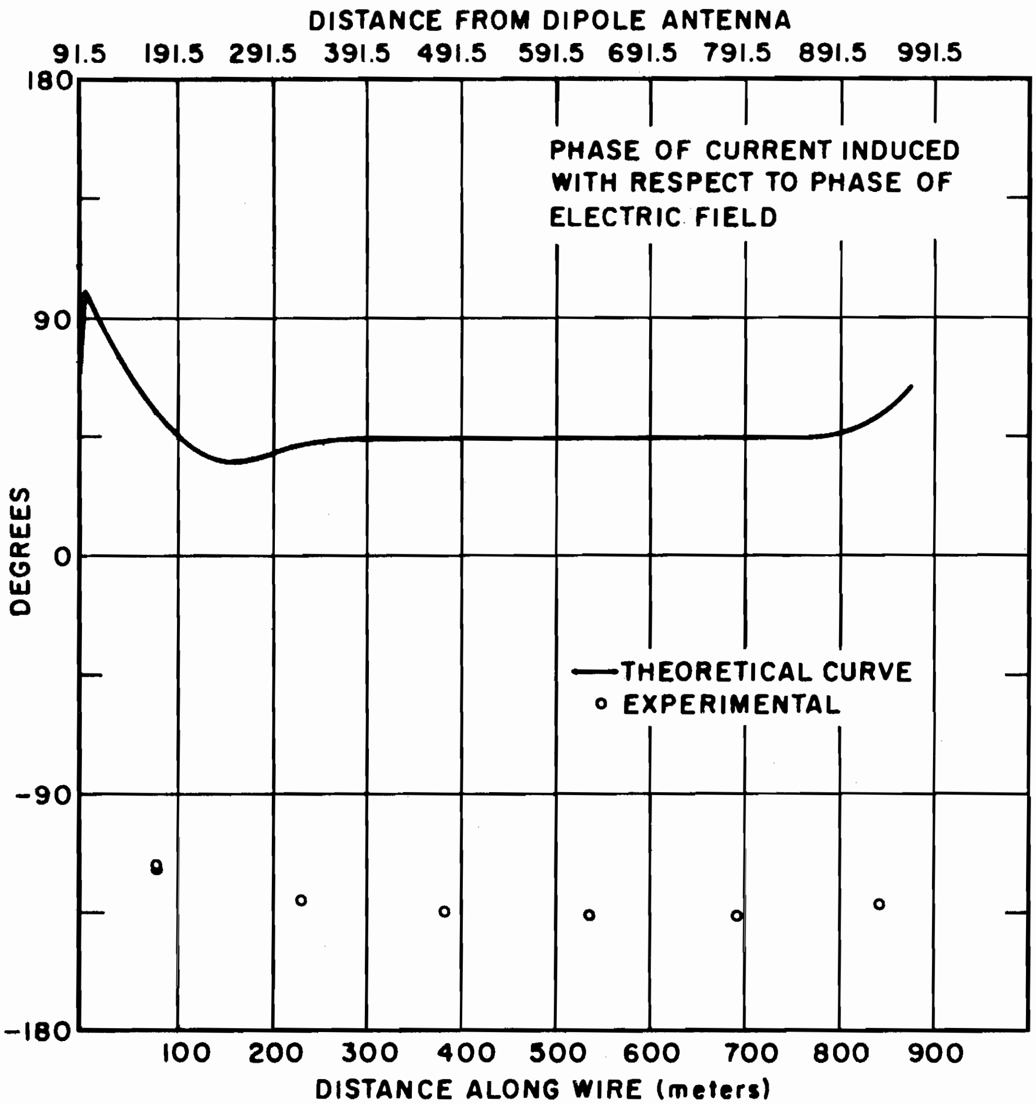

Figure 35. Current Phase in Wire with High Conductivity Covering at 10 kcs.

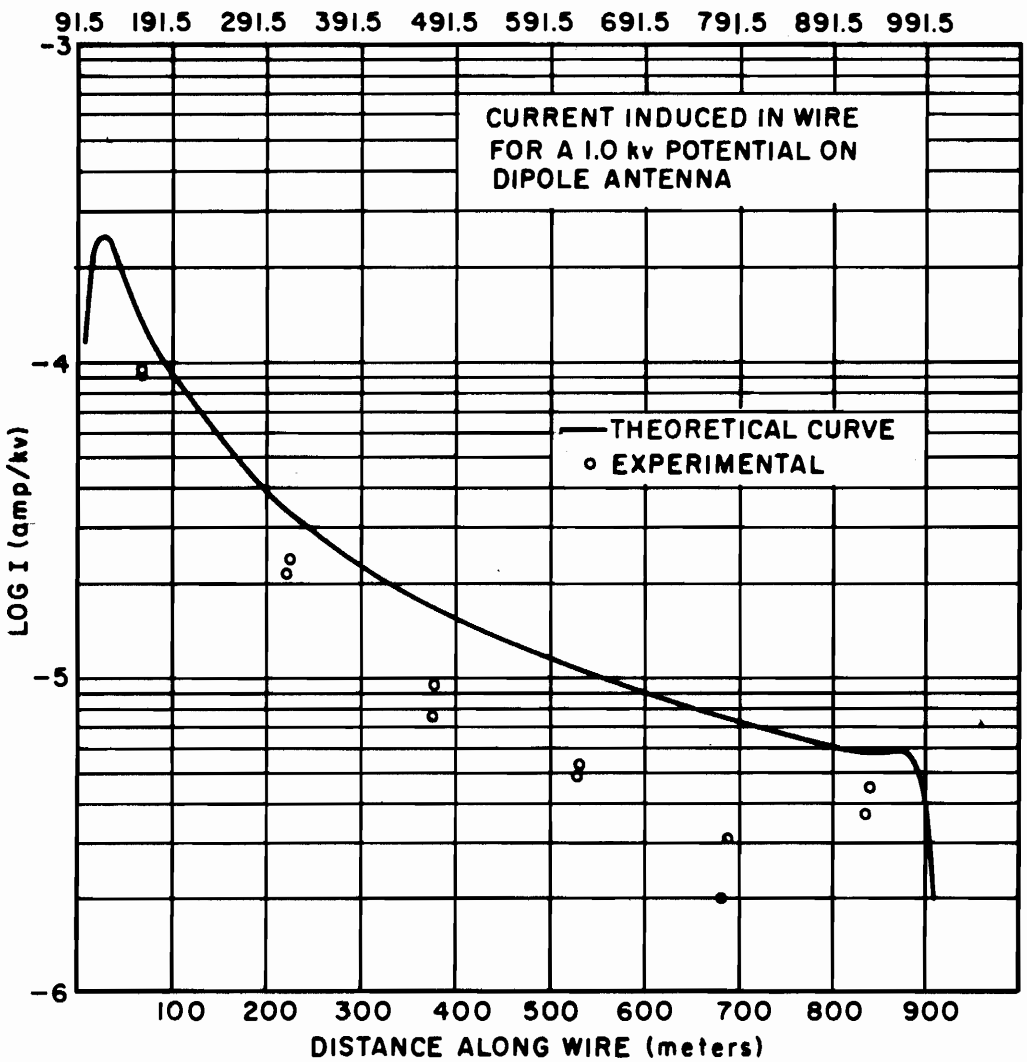

Figure 36. Current Magnitude in Wire with High Conductivity Covering at 62 kcs.

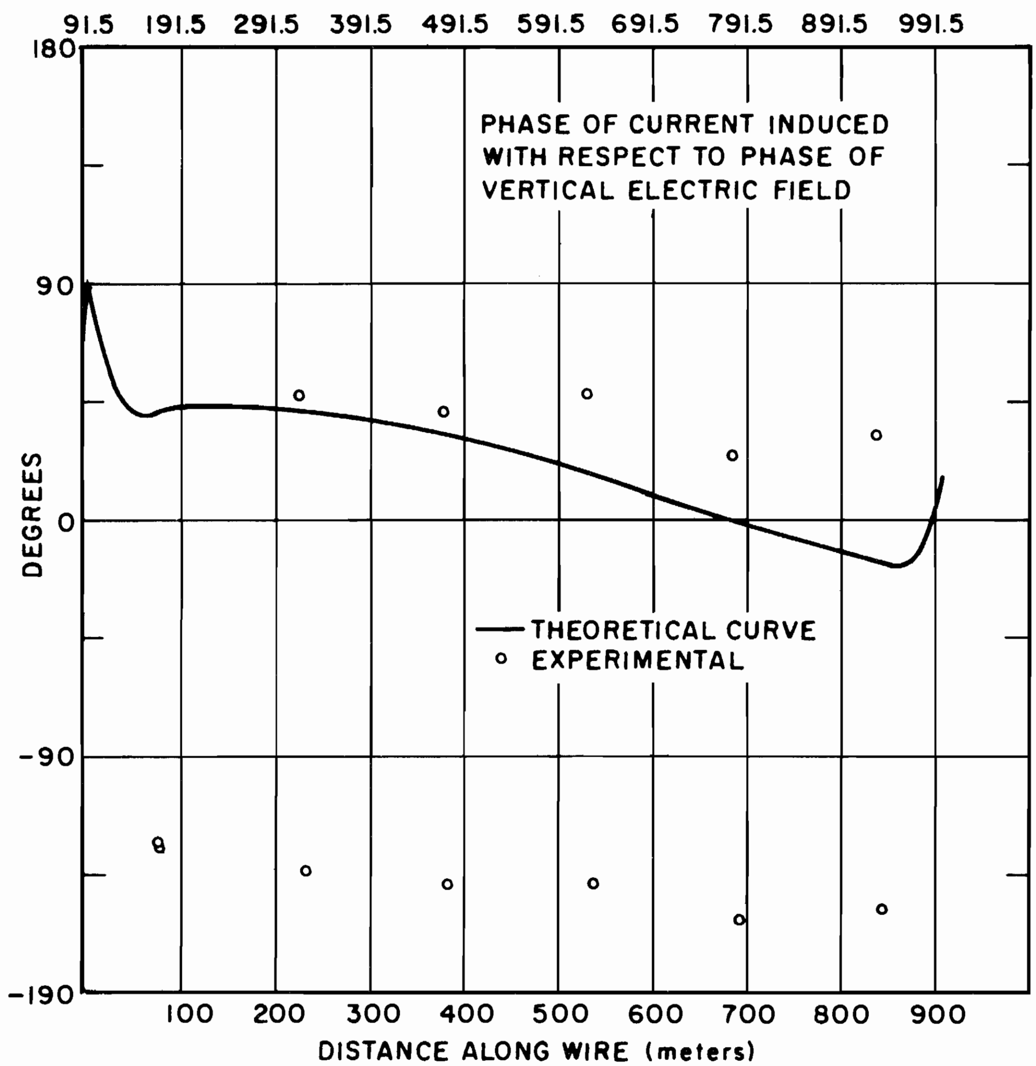

Figure 37. Current Phase in Wire with High Conductivity Covering at 62 kcs.

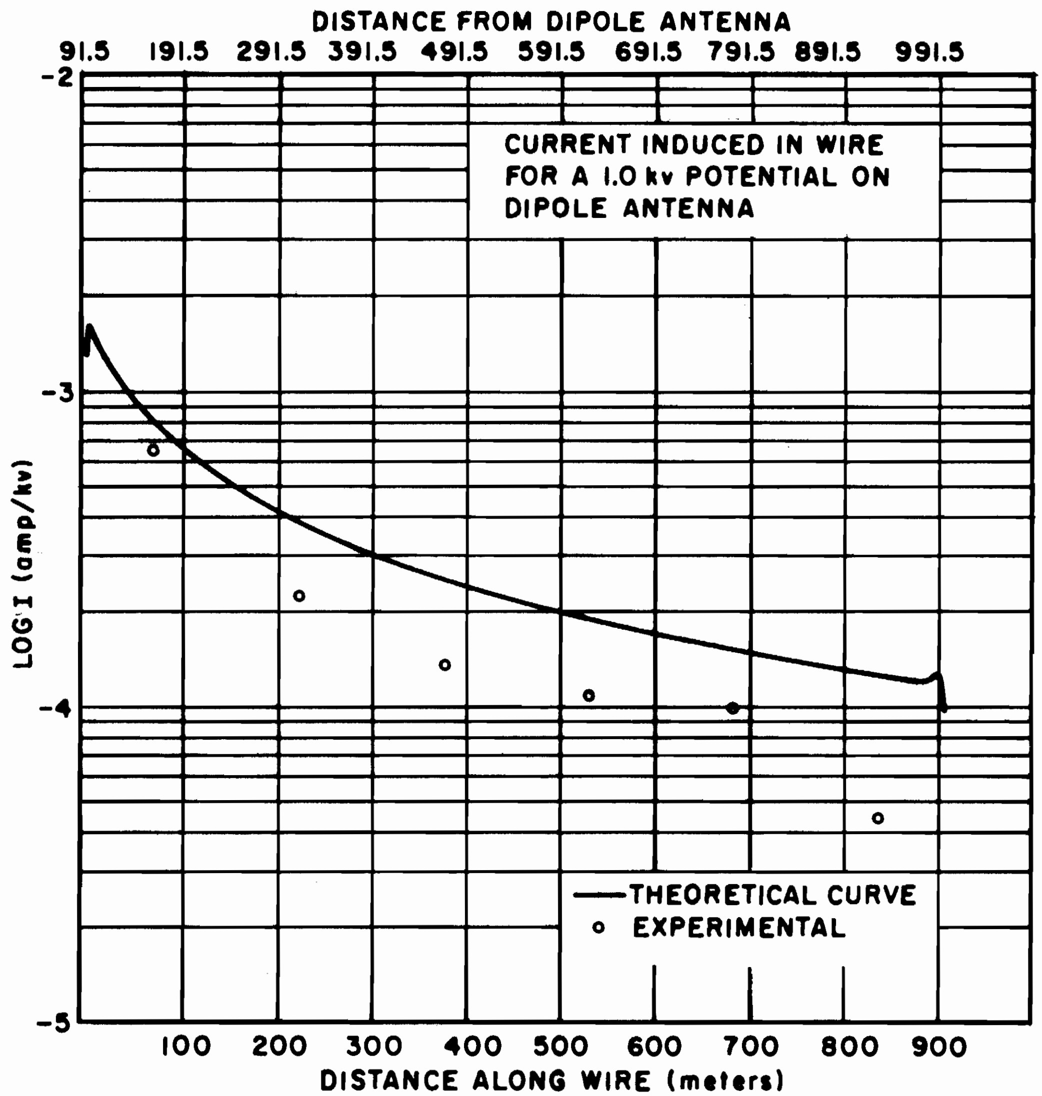

Figure 38. Current Magnitude in Wire with High Conductivity Covering at 510 kcs.

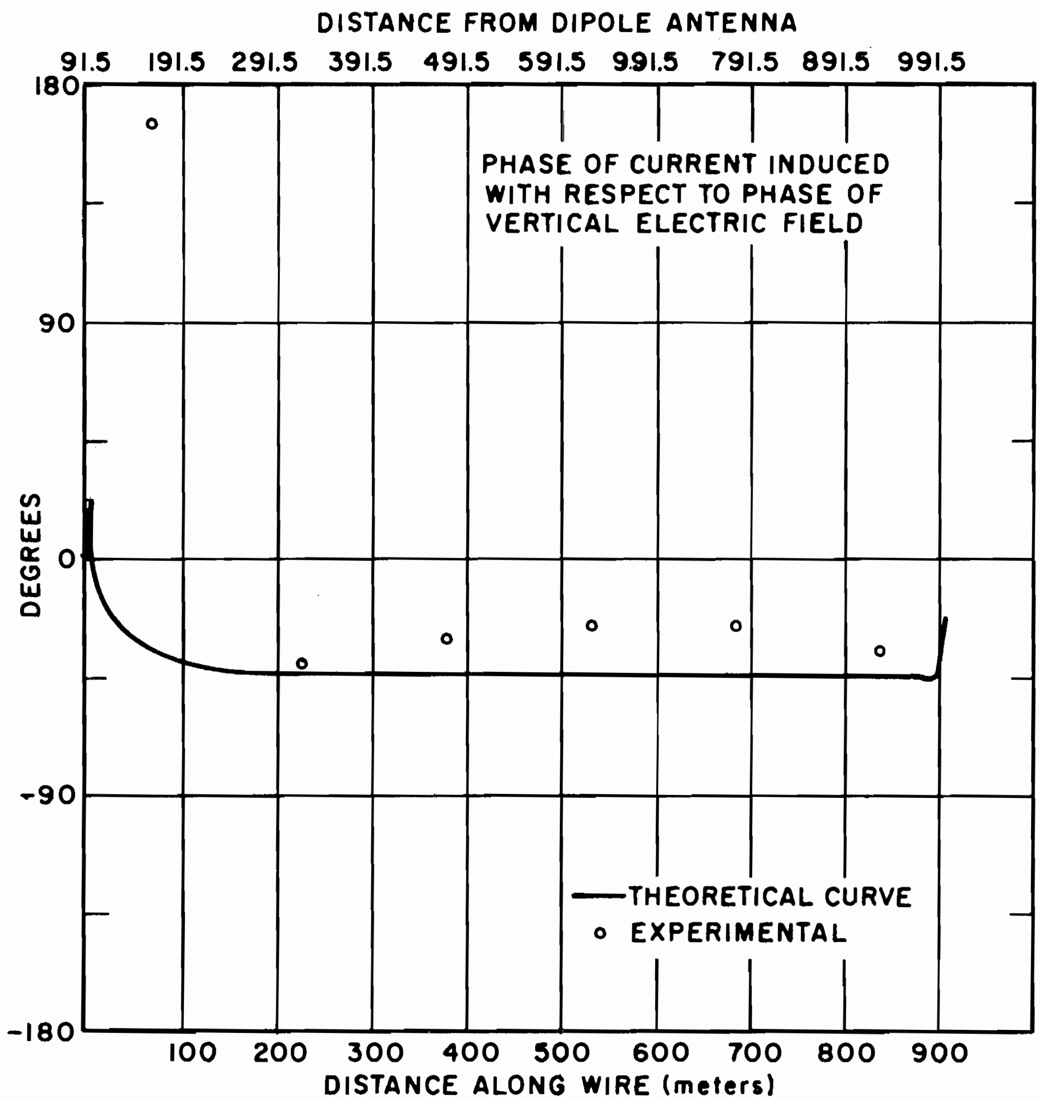

Figure 39. Current Phase in Wire with High Conductivity Covering at 510 kcs.

The major source of error in high-frequency current calculations in insulated wires of finite length appears to be associated with current resonance. Near resonance, a relatively small error in calculating a wire impedance factor can produce as much as an order of magnitude error in the magnitude of the peak current over the length of the wire. The most critical situation occurs when there is an actual current resonance; this can mean that the actual current induced is much greater than the predicted current.

It is often difficult to determine exactly the transverse impedance characteristics of a given wire because of unpredictable electrical contact with the earth. Effects such as air spaces and oxide coatings on the metal surfaces can produce additional capacitances. At low frequencies, these capacitances modify both the phase and amplitude characteristics. At the higher frequencies, the predominant effect of the capacitances is a modification of the phase function.

Other low-frequency current errors in insulated wires are termination impedances which are not precisely known. At extremely low frequencies, the peak current can vary by several orders of magnitude due to this uncertainty in termination impedance. However, with proper precautions, the termination impedances can be controlled within practical limits.

The present study appears to satisfactorily answer the engineering problem of determining peak currents produced by a given impressed continuous wave field in those cases considered. The largest discrepancies occur for the insulated wire with floating terminations. For these reasons, it would seem desirable to make a more detailed theoretical and experimental investigation of this case. Such a detailed study would be absolutely essential for the determination of currents induced by pulsed impressed fields.

Although an extended general study of this nature would be valuable in further defining the essentials of the problem, the present study has, from a practical point of view, provided a means for conservatively estimating the peak currents to be expected in a typical cable installation.

SECTION VI

CONCLUSIONS AND SUMMARY

The purpose of this paper has been to illustrate a method for determining the currents induced in a long wire or cable in or on the ground by a distributed continuous-wave electric field parallel to the wire or cable. The method used is to approximate the wire as a transmission line to determine the impedance factors and propagation constant for the currents in the wire.

To test this theory, a variety of cables in the ground were exposed to the surface radial electric field from a grounded vertical monopole antenna, and the current magnitudes and phases produced in the wires were measured. These currents and phases were compared with those predicted from the postulated theory and the known radial electric field distribution of the antenna.

The theory as postulated usually made current predictions within the confidence limits of the data obtained by Stanford Research Institute (as explained in the results), especially at higher frequencies and for the covered wires. The theoretical peak magnitudes were consistently within a factor of two of the peak magnitudes of the data for corresponding conductors and frequencies. The corresponding phases consistently matched within the 20 to 30 degree accuracy limit imposed by experimental considerations.

The problem in predicting the currents for practical wires in and on the ground lies in the examination of the electrical contact with the earth along the full length of the wire. Air spaces, oxide coatings, and varying electrical 'constants' in the earth produce the deviations between the data and the theory. The air spaces and oxide coatings produced added transverse capacitances which cause deviations in current phases and magnitudes at low frequencies. The variation of the electrical properties of the earth can produce large deviations between theory and measured results primarily at high frequencies, when the earth-wire system is near a resonant frequency.

The next step in the study of cable currents is to further refine the theory of currents from continuous-wave fields. The ultimate goal will be to extend this CW theory to determine the currents induced by fields arbitrary in space and in time. With this goal reached, the vulnerability of cables to lightning and to the electromagnetic pulse from a nuclear detonation can be studied in detail.

This page intentionally left blank.

Appendix I

THE DERIVATION OF THE REAL AND IMAGINARY PARTS OF THE TRANSVERSE ADMITTANCE Y_t

The purpose of this derivation is to determine the real (G') and imaginary ($\omega C'$) components of the transverse admittance for a wire in terms of the admittance characteristics of the wire covering and the admittance to ground.

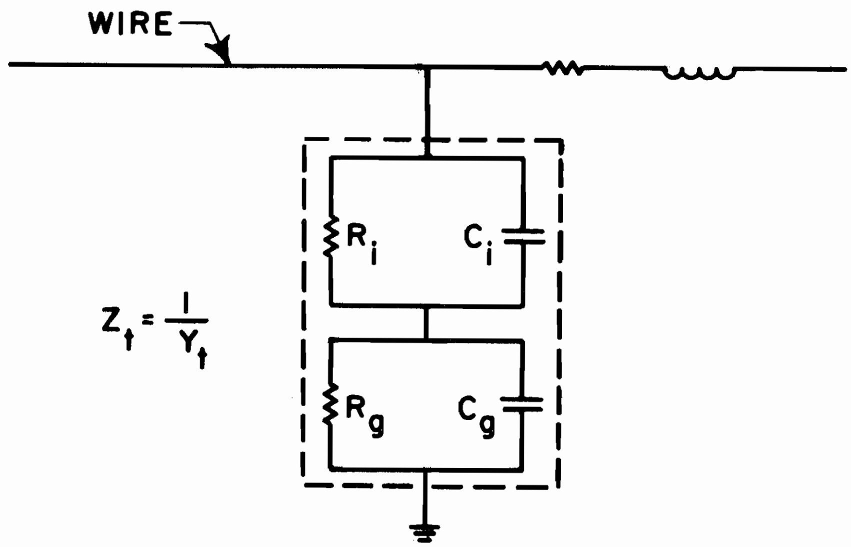

Figure 40. The Transverse Impedance $Z_t = 1/Y_t$.

The transverse impedance, as shown in figure 40, is

$$Z_t = \frac{1}{G_i + i\omega C_i} + \frac{1}{G_g + i\omega C_g} \tag{55}$$

where

$G_i = 1/R_i$ = the conductive admittance of the wire covering

$G_g = 1/R_g$ = the conductive admittance to ground

ωC_i = the capacitive admittance of the wire covering

ωC_g = the capacitive admittance to ground

This gives for the transverse admittance

$$Y_t = 1/Z_t$$

$$= \frac{\left(G_i + i\omega C_i\right)\left(G_g + i\omega C_g\right)}{\left(G_i + G_g\right) + i\omega\left(C_i + C_g\right)} \tag{56}$$

From this, upon expansion of the numerator and eliminating the imaginary terms in the denominator, the expressions for G' and C' are obtained.

$$G' = Y_t \text{ (real)} = \frac{(G_i+G_g)(G_iG_g-\omega^2C_iC_g) + \omega^2(C_i+C_g)(G_iC_g+G_gC_i)}{(G_i+G_g)^2 + \omega^2(C_i+C_g)^2}$$

$$C' = \frac{Y_t \text{ (imaginary)}}{\omega} = \frac{(G_i+G_g)(G_iC_g+G_gC_i) - (C_i+C_g)(G_iG_g-\omega^2C_iC_g)}{(G_i+G_g)^2 + \omega^2(C_i+C_g)^2} \tag{57}$$

The conductive admittance G_i of a good insulator is, by definition of an insulator, negligible compared to the other admittance term. Other than the DC case for a very long cable or a cable which has a covering which is not an insulator, G_i may be omitted, giving the simplified relations below

$$G' = \frac{\omega^2 C_i^2 G_g}{G_g^2 + \omega^2(C_i+C_g)^2}$$

$$C' = \frac{C_iG_g{}^2 + \omega^2(C_i+C_g)\ C_iC_g}{G_g^2 + \omega^2(C_i+C_g)^2} \tag{58}$$

The general equations, equations (57), were used in the computer program (appendix V) for the calculation of the cable currents in a given wire.

Appendix II

THE DETERMINATION OF THE REAL AND IMAGINARY PARTS OF THE PROPAGATION CONSTANT OF THE CONDUCTOR

The propagation constant of a given cable for a given set of conditions is (reference 9)

$$\Gamma = \left(ZY_t\right)^{1/2} = [(R + i\omega L')(G' + i\omega C')]^{1/2}$$

where Γ is the propagation constant,

Z is the longitudinal impedance per unit length of the cable,

Y_t is the transverse admittance per unit length of the cable,

R is the resistance per unit length of the cable,

L' is the inductance per unit length of the cable,

G' is the transverse conductive admittance per unit length of the cable,

C' is the effective capacitance per unit length of the cable, and

ω is the radian frequency of the CW current.

To separate Γ into its real part, the attenuation coefficient, and its imaginary part, the phase factor, the general expression for the square root of a complex number must be found. This is determined as follows

Let $z = x + iy$ and $w = u + iv$ be complex numbers such that $z = \sqrt{w}$

Squaring both sides, we have $z^2 = w$, or

$$x^2 - y^2 + 2ixy = u + iv$$

This gives

$$u = x^2 - y^2$$

$$v = 2xy$$

Therefore

$$u = x^2 - \frac{v^2}{4x^2}$$

or

$$x^4 - ux^2 - \frac{v^2}{4} = 0$$

By the binomial theorum

$$x^2 = \frac{u \pm \sqrt{u^2 + v^2}}{2}$$

and, by letting $x = \frac{v}{2y}$ and repeating the above arguments for y, we get

$$y^2 = \frac{-u \pm \sqrt{u^2 + v^2}}{2}$$

For our specific case, consider the expression for Γ

$$u = RG' - \omega^2 L'C'$$

$$v = \omega(L'G' + RC')$$

so

$$x = \left[\frac{RG' - \omega^2 L'C' \pm \sqrt{[RG' - \omega^2 L'C']^2 + \omega^2 [L'G' + RC']^2}}{2}\right]^{1/2}$$

Note, as $R \to 0$ and $G' \to 0$ (very high conductivity wire in a high impedance medium), we have the known conditions

$$\Gamma \text{ (real)} \to 0$$

$$\Gamma \text{ (imaginary)} \to \omega\sqrt{L'C'}$$

which sets the signs in front of square root as positive.

Therefore

$$\Gamma \text{ (real)} = \left[\frac{RG' - \omega^2 L'C' + \sqrt{[RG' - \omega^2 L'C']^2 + \omega^2 [L'G' + RC']^2}}{2}\right]^{1/2} \tag{59}$$

Similarly

$$\Gamma \text{ (imaginary)} = \left[\frac{\omega^2 L'C' - RG' + \sqrt{[RG' - \omega^2 L'C']^2 + \omega^2 [L'G' + RC']^2}}{2}\right]^{1/2} \tag{60}$$

For the case of a cable in good electrical contact with the ground, the following special cases are most applicable in the frequency range of interest (500 cps to 500 kcs). It is assumed in these situations that the wire resistance $R \ll \omega L'$, the inductive impedance.

For an insulated wire, the capacitance of the insulation rules over any conductive effects. Therefore, G' is small compared with C', which gives

$$\Gamma \text{ (real)} \cong \left[\frac{L'^2 G'^2 + R^2 C'^2}{4L'C'}\right]^{1/2}$$

$$\Gamma \text{ (imaginary)} \cong \omega\sqrt{L'C'} \tag{61}$$

For a bare wire, the transverse conductive admittance outweighs the capacitive admittance, or $G' > \omega C'$. This results in the propagation constant components

$$\Gamma \text{ (real)} \cong \Gamma \text{ (imaginary)} \cong \left[\frac{\omega L'G'}{2}\right]^{1/2} \tag{62}$$

Appendix III

THE DERIVATION OF THE REFLECTION CONSTANTS K AND L

The solution to the current induced in a finite single wire of length d by a distributed sinusoidal current along the wire, as given by equation (39) is

$$I(z) = Ke^{-\Gamma z} + Le^{\Gamma z} + F(z)$$

where K and L are the end reflection coefficients and

$$F(z) = \frac{Y_t}{2\Gamma} \int_o^d E_o(v)e^{-\Gamma|z-v|}dv$$

is the integral term. Also from section III, we note that

$$\frac{dI(z)}{dz} = - Y_t V(z)$$

where V (z) is the voltage with respect to the earth at a point z on the conductor. This gives, for the voltage along the conductor

$$V(z) = - \frac{1}{Y_t}\left[-\Gamma Ke^{-\Gamma z} + \Gamma Le^{\Gamma z}\right] - \frac{1}{Y_t}\frac{dF(z)}{dz}$$

or

$$V(z) = - Z_o\left[-Ke^{-\Gamma z} + Le^{\Gamma z}\right] - F_v(z) \tag{63}$$

where $Z_o = \frac{\Gamma}{Y_t}$

and $F_v(z) = \frac{1}{Y_t}\frac{dF(z)}{dz}$

At the termination z = 0, the wire is terminated with impedance Z_1 and at termination z = d, the wire is terminated with impedance Z_2 (see figure 41).

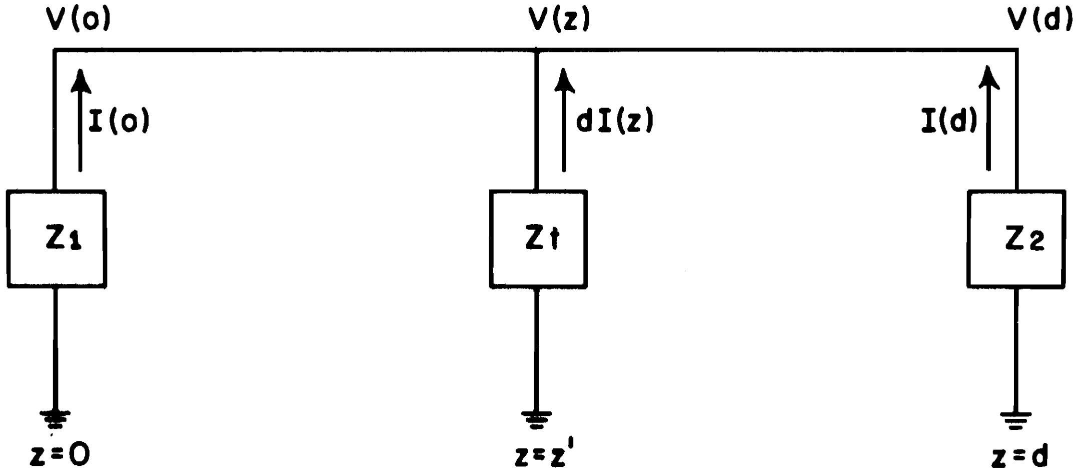

Figure 41. The Currents and Voltages in the Wire and Its Terminations.

This gives the two boundary condition equations at the terminations

$$Z_1 I(o) = -V(o)$$
$$Z_2 I(d) = V(d)$$

Setting these expressions for the voltage at points z' = 0 and z' = d separately equal to the voltage expression, equation (63), with z = 0 and z = d, respectively

$$Z_1\left[K + L + F(o)\right] = Z_o\left[-K + L\right] + F_v(o)$$
$$Z_2\left[Ke^{-\Gamma d} + Le^{\Gamma d} + F(d)\right] = -Z_o\left[-Ke^{-\Gamma d} + Le^{\Gamma d}\right] - F_v(d)$$

Rewriting these equations, we get

$$\begin{aligned}(Z_1 + Z_o)\,K + (Z_1 - Z_o)\,L &= F_v(o) - Z_1 F(o)\\ (Z_2 - Z_o)\,Ke^{-\Gamma d} + (Z_2 + Z_o)\,Le^{\Gamma d} &= -\left[F_v(d) + Z_2 F(d)\right]\end{aligned} \tag{64}$$

Note that

$$F_v(z) = \frac{1}{Y_t}\frac{dF(z)}{dz} = -\frac{1}{2}\left\{e^{-\Gamma z}\int_o^z E_o(v)e^{\Gamma v}dv - e^{\Gamma z}\int_z^d E_o(v)e^{-\Gamma v}dv\right\}$$

therefore, since

$$F(z) = \frac{1}{2Z_o}\left\{e^{-\Gamma z}\int_o^z E_o(v)e^{\Gamma v}dv + e^{\Gamma z}\int_z^d E_o(v)e^{-\Gamma v}dv\right\}$$

then

$$\begin{aligned} F_v(o) &= Z_o F(o) \\ F_v(d) &= -Z_o F(d) \end{aligned} \tag{65}$$

Solving equation (64) simultaneously using equation (65), we obtain for the reflection constants

$$\begin{aligned} K &= \frac{(Z_1-Z_o)(Z_2-Z_o)\ F(d) - (Z_2+Z_o)(Z_1-Z_o)\ e^{\Gamma d}F(o)}{(Z_1+Z_o)(Z_2+Z_o)\ e^{\Gamma d} - (Z_1-Z_o)(Z_2-Z_o)\ e^{-\Gamma d}} \\ L &= \frac{(Z_1-Z_o)(Z_2-Z_o)\ e^{-\Gamma d}\ F(o) - (Z_1+Z_o)(Z_2-Z_o)\ F(d)}{(Z_1+Z_o)(Z_2+Z_o)\ e^{\Gamma d} - (Z_1-Z_o)(Z_2-Z_o)\ e^{-\Gamma d}} \end{aligned} \tag{66}$$

For the case of high impedance ends, where Z_1 and $Z_2 >> Z_0$ the reflection terms are approximated by

$$K \cong \frac{F(d) - F(o)e^{\Gamma d}}{2\ \mathrm{Sin\ h}\ \Gamma d}$$

$$L \cong \frac{F(o)e^{-\Gamma d} - F(d)}{2\ \mathrm{Sin\ h}\ \Gamma d}$$

This same approximation may be found by setting the current equal to zero at the terminations, which implies an infinite termination impedance.

When matched impedances are placed at the ends; that is, $Z_1 = Z_0$ and $Z_2 = Z_0$, the respective terminations will no longer reflect the transmitted current. This is seen from equation (66)

$$\text{as } Z_1 \longrightarrow Z_0, \quad K \longrightarrow 0$$

$$\text{as } Z_2 \longrightarrow Z_0, \quad L \longrightarrow 0$$

With both terminations completely 'shorted out'; that is, $Z_1 = Z_2 = 0$, the reflection terms become

$$K \cong \frac{F(o)e^{\Gamma d} + F(d)}{2 \sinh \Gamma d}$$

$$L \cong \frac{F(o)e^{-\Gamma d} + F(d)}{2 \sinh \Gamma d}$$

This result may also be found by setting the termination voltages equal to 0, as would be required at a short.

Now we will note the effect of the propagation constant Γ. If the real part of Γ, representing the exponential decrease in magnitude of a propagating current with distance, is very large, such that

$$e^{\Gamma d} >> 1 >> e^{-\Gamma d}$$

then

$$K \cong \frac{(Z_o - Z_1)}{(Z_1 + Z_o)} F(o) = -\mu_1' F(o)$$

$$L \cong \frac{(Z_o - Z_2)}{(Z_2 + Z_o)} \frac{F(d)}{e^{\Gamma d}} = -\mu_2' \frac{F(d)}{e^{\Gamma d}}$$

where μ_1' and μ_2' are the respective single reflection constants for each terminal. In this approximation, the reflected wave length is very short compared to the length of the conductor, and the coefficients are dependent only on the impedance and induced current at their respective terminations. These same results are obtained for L by letting $Z_1 \rightarrow Z_0$ and for K by letting $Z_2 \rightarrow Z_0$, therefore eliminating the effect of reflection from the opposing terminal in each case.

Appendix IV

FIELDS PRODUCED BY A VERTICAL MONOPOLE ANTENNA

Starting from the general electromagnetic field equations the following expressions were developed for the fields produced by a filament sinusoidal current dipole of infinitesimal length in free space. As shown in figure 42 these fields were derived in spherical coordinates.

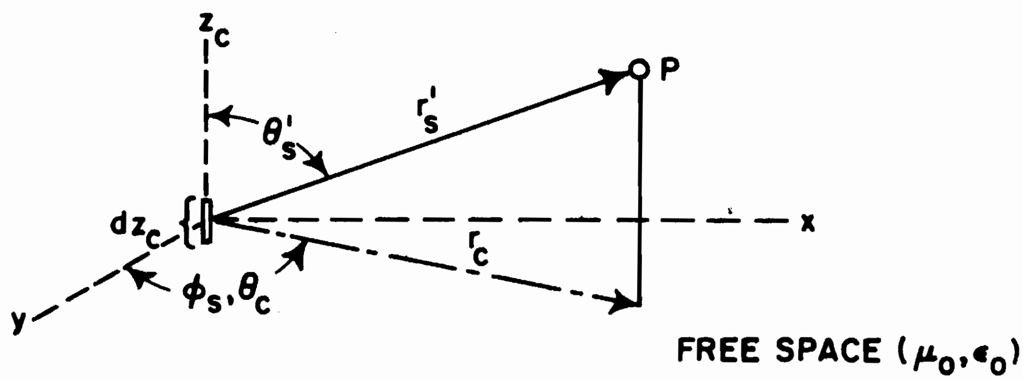

Figure 42. The Filament Current Dipole, Comparing Rectangular, Spherical and Cylindrical Coordinates.

The fields at the point P from the current dipole are (reference 7)

$$E_{\theta'_s} = \frac{Idz_c}{4\Pi}\left[\frac{i\omega\mu_o}{r'_s} + \frac{1}{i\omega\varepsilon_o r'^3_s} + \frac{\eta_o}{r'^2_s}\right]e^{-ik_o r'_s} \operatorname{Sin} \theta'_s$$

$$E_{r'_s} = \frac{Idz_c}{4\Pi}\left[\frac{2\eta_o}{r'^2_s} + \frac{2}{i\omega\varepsilon_o r'^3_s}\right]e^{-ik_o r'_s} \operatorname{Cos} \theta'_s \qquad (67)$$

$$H_{\phi_s} = \frac{Idz_c}{4\Pi}\left[\frac{ik_o}{r'_s} + \frac{1}{r'^2_s}\right]e^{-ik_o r'_s} \operatorname{Sin} \theta'_s$$

where $\eta_o = \left(\frac{\mu_o}{\varepsilon_o}\right)^{1/2}$

and $k_o = \omega(\mu_o\varepsilon_o)^{1/2}$, the propagation constant in free space.

From these field relations it was necessary to find the field transmitted by a vertical monopole antenna seated on the earth and grounded as shown in figure 43.

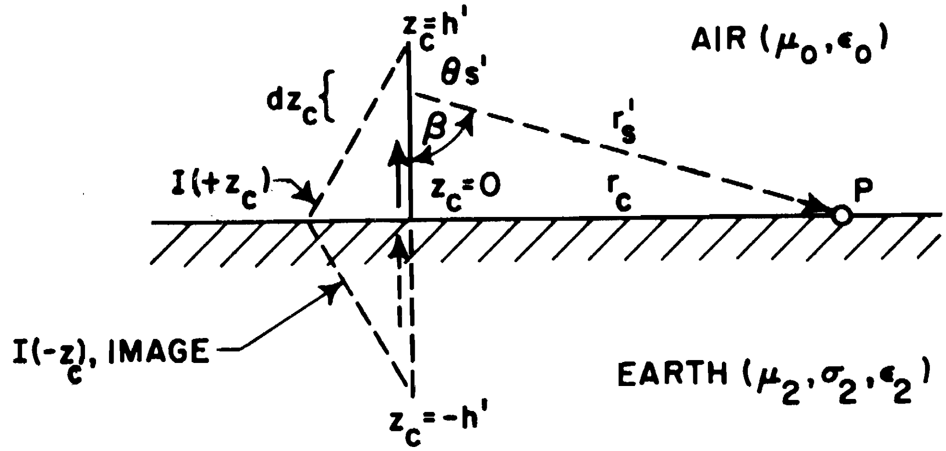

Figure 43. Vertical Monopole Antenna, With Its Electrical Image in the Earth.

For this derivation the assumption was made that the antenna is one dimensional, in the z_c dimension only. This is justifiable if the thickness of the antenna $a \ll h'$, the height of the antenna, and also $a \ll \frac{2\Pi}{k_o}$, the wave length of the transmitted signals in the air.

Also, the assumption was made that $h' \ll \frac{2\Pi}{k_o}$ for the frequency range of interest, which was $10^2 - 10^6$ cps. Since the current on the antenna will disappear at $z_c = h'$ (except for a small displacement current of negligible magnitude), the above assumption insured a roughly linear current distribution of the form (ref. 11)

$$I\left(z_c\right) = I(o)\left[\frac{h'-|z_c|}{h}\right] \tag{68}$$

where I_o is the current at the base of the antenna. This current distribution is illustrated in figure 43.

In the earth, in general the conductive currents outweigh the displacement currents for the frequency range of interest and for all but the very low-conductivity rocks and soils. If $\sigma_2 \doteqdot 10^{-4}$ or less and the frequency is on the order of 10^6 cps or higher, this assumption does not hold. However, in general, the earth may be considered a good conductor.

If the earth had infinite conductivity, the fields transmitted into the air by the antenna-earth system could be calculated by replacing the earth with a mirror image of the vertical antenna. This "image" would have a mirror-image current distribution, about the horizontal plane, with its current flowing toward the base of the real antenna when the current distribution in the real antenna is flowing away from the base. This situation is illustrated in figure 43.

The objective is to determine the fields from this antenna at the surface of the earth ($z_c = 0$) as a function of horizontal range from the base of the antenna (r_c), the base current of the antenna (I_o), the height of the antenna, and the electrical characteristics of the two media. This is done by integrating the fields from the infinitesimal dipole components of the antenna over the full length of the antenna and its image.

From figure 43, the following relations are found

$$\begin{aligned} \text{Cos } \beta &= - \text{Cos } \theta'_s \\ \text{Sin } \beta &= \text{Sin } \theta'_s \\ r'_s &= \frac{r_c}{\text{Sin } \beta} \\ z_c &= \frac{r_c}{\text{Tan } \beta} \end{aligned} \tag{69}$$

Upon close examination of figure 44

$$\begin{aligned} dz_c &= r'_s \text{ Cos } \alpha \, d\alpha \\ &= \frac{r_c}{\text{Sin } \beta} \text{ Sin } \beta \, d\alpha \end{aligned} \tag{70}$$

Since $\alpha = 90° - \beta$

then $d\alpha = - d\beta$

Therefore $dz_c = - r_c d\beta$

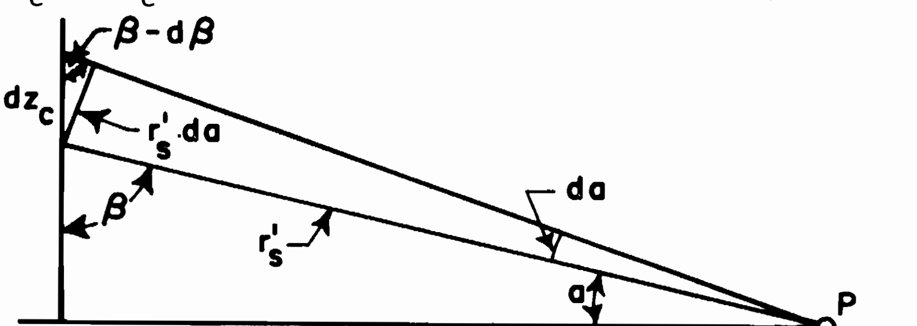

Figure 44. Exaggerated View of the Monopole Antenna.

From equation (67) we integrate over the length of the wire and its image.

$$H_{\theta_c}(z_c=0) = \int_{-h'}^{h'} \frac{I_o}{4\Pi}\left[\frac{h'-|z_c|}{h'}\right]\left[\frac{ik_o}{r'_s} + \frac{1}{r_s'^2}\right] e^{-ik_o r'_s} \operatorname{Sin}\theta'_s \, dz_c$$

The contributions from $z_c > 0$ and $z_c < 0$ are additive and equal, and

$$H_{\theta_c}(z_c=0) = 2\int_0^{h'} f(z_c)\, dz_c$$

Also, $e^{-ik_o h'} \cong 1$ since h' is much less than the wave length of the transmitted wave. Then $e^{-ik_o r'_s} \cong e^{-ik_o r_c}$ over the range of integration.

Therefore

$$H_{\theta_c}(z_c=0) = -\frac{I_o}{2\Pi} e^{-ik_o r_c} \int_{\frac{\Pi}{2}}^{\operatorname{Tan}^{-1}\frac{r_c}{h'}} \left(1 - \frac{r_c}{h'\operatorname{Tan}\beta}\right)\left[\frac{ik_o \operatorname{Sin}\beta}{r_c} + \frac{\operatorname{Sin}^2\beta}{r_c^2}\right] r_c \operatorname{Sin}\beta \, d\beta$$

$$= \frac{I_o}{2\Pi} e^{ik_o r_c}\left\{ ik_o\left[\frac{\Pi}{2} - \operatorname{Tan}^{-1}\frac{r_c}{h'} + \frac{r_c}{h'}\left(\ell n\left[\operatorname{Sin}\left(\operatorname{Tan}^{-1}\frac{r_c}{h'}\right)\right]\right)\right]\right. \tag{71}$$

$$\left. + \frac{1}{r_c}\left[\operatorname{Cos}\left(\operatorname{Tan}^{-1}\frac{r_c}{h'}\right) + \frac{r_c}{h'}\left(\operatorname{Sin}\left[\operatorname{Tan}^{-1}\frac{r_c}{h'}\right] - 1\right)\right]\right\}$$

By the geometry of the problem

$$d\,E_{r_c} = -d\,E_{\theta'_s}\operatorname{Cos}\beta + d\,E_{r'_s}\operatorname{Sin}\beta$$

The contributions from $d\,E_{r'_s}\operatorname{Sin}\beta$ and $d\,E_{\theta'_s}\operatorname{Cos}\beta$ are antisymmetric about $\beta = 90°$. Therefore,

$$E_{r_c}(z_c=0) = 0$$

The vertical electric field components, which is not of interest in this paper, may be derived by similar means.

It is of interest to note that

$$\underset{r_c \to \infty}{\text{limit}}\, H_{\theta_c}(z_c=0) = \frac{I_o h'}{4\Pi}\left[\frac{ik_o}{r_c} + \frac{1}{r_c^2}\right] e^{-ik_o r_c} \tag{72}$$

which is, in effect, the field transmitted by a small dipole of length 2h' and total dipole current magnitude of $\frac{I_o}{2}$, the average current over the length of the antenna and its image.

As previously done in the field determinations, the concept of infinite conductivity was used to simplify the problem. It is a good first approximation for the antenna fields because, in most cases, the conductivity of the earth is sufficiently high that the tangential electric field is only a nominal percentage of the transmitted vertical electric field. However, it is this tangential field that interacts with the long wires in the earth, and this field must be determined.

When the magnetic field produced by the antenna propagates along the surface of the earth, it also propagates down into the earth with a magnitude defined by

$$H_{\theta_c}\left(z_c\right) = H_{\theta_c}\left(z_c=0\right) e^{-ik_2|z_c|} \tag{73}$$

where $\left(z_c\right)$ is the depth of penetration of the field into the earth. From the general field equation

$$\vec{\nabla} \times \vec{H} = \left(\sigma_2 + i\omega\varepsilon_2\right) \vec{E}$$

it is seen that the attenuation of the magnetic field in the earth produces an electric field in the earth. Using Stoke's Theorum,

$$\underset{\text{Area of closed loop}}{\int \vec{\nabla} \times \vec{H} \cdot \vec{ds} = \int \left(\sigma_2 + i\omega\varepsilon_2\right) \vec{E} \cdot \vec{ds}} = \underset{\text{Circumference of closed loop}}{\oint \vec{H} \cdot \vec{d\ell}}$$

The closed loop chosen is shown in figure 45.

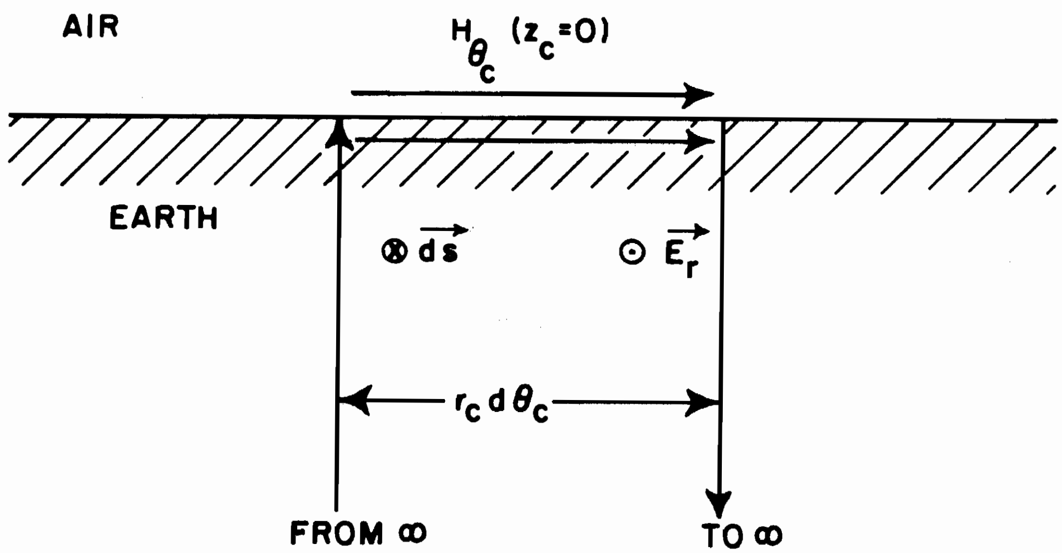

Figure 45. Path of the Line Integral in the Earth to Determine E_r.

From equation (73) and figure 45, we see that

$$\oint \vec{H} \cdot \vec{d\ell} = H_{\theta_c} \left(z_c = 0\right) \cdot r_c \, d\theta_c \tag{74}$$

The electric field produced by the attenuation of the magnetic field will also have the form

$$E_{r_c} \left(z_c\right) = E_{r_c} \left(z_c = 0\right) e^{-ik_2 |z_c|}$$

Therefore, from figure 45, we see that

$$\int \vec{E} \cdot \vec{ds} = - E_{r_c} \left(z_c = 0\right) r_c \, d\theta_c \int_{-\infty}^{0} e^{-ik_2 z_c} dz_c$$

Therefore

$$H_{\theta_c} \left(z_c = 0\right) r_c \, d\theta_c = - E_{r_c} \left(z_c = 0\right) \frac{r_c \, d\theta_c}{ik_2} \left(\sigma_2 + i\omega\varepsilon_2\right)$$

or

$$E_{r_c} \left(z_c = 0\right) = - \frac{ik_2}{\left(\sigma_2 + i\omega\varepsilon_2\right)} H_{\theta_c} \left(z_c = 0\right) \tag{75}$$

where

$$k_2 = \left[- i\omega\mu_2 \left(\sigma_2 + i\omega\varepsilon_2\right)\right]^{1/2}$$

This gives

$$E_{r_c} \left(z_c = 0\right) = - \eta_G H_{\theta_c} \left(z_c = 0\right)$$

where

$$\eta_G = \left[\frac{i\omega\mu_2}{\sigma_2 + i\omega\varepsilon_2}\right]^{1/2}$$

is the characteristic impedance to an electromagnetic wave in the earth.

At distances closer than $\frac{1}{|k_2|}$ from the base of the antenna, the earth currents will no longer have the appearance of a sheet of current near the surface of the earth. Instead, they converge to a single point at the base of the antenna, as shown in figure 46. In this close-in region, the earth currents approach an isotropic hemispherical distribution as they approach the antenna base.

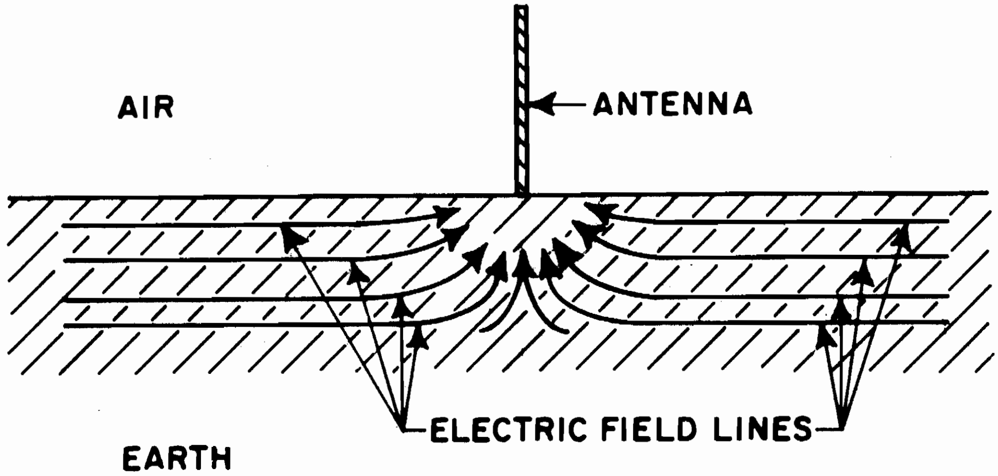

Figure 46. Earth Currents Near a Monopole Antenna.

That is

$$\lim_{r_s \to o} J_{r_s} = \frac{I_o}{2\Pi r_s^2}$$

where J_{r_s} includes both conductive and displacement currents. The electrical field produced by this current convergence is

$$E'_{r_s} = \frac{J_{r_s}}{(\sigma_2+i\omega\varepsilon_2)} = -\frac{I_o\, e^{-ik_2 r_s}}{2\Pi r_s^2(\sigma_2+i\omega\varepsilon_2)}$$

where the exponential term is added to account for the attenuation of this field distribution in the earth. The component of this field at the surface of the earth was added to that created by the magnetic field attenuation to give the total radial electric field from a vertical monopole antenna:

$$E_{r_c}\,(z_c=0) = -\,\eta_G\, H_{\theta_c}\,(z_c=0) - \frac{I_o\, e^{-ik_2 r_c}}{2\Pi r_c^2(\sigma_2+i\omega\varepsilon_2)} \tag{76}$$

At $r_c >> a$, the actual thickness of the antenna, these relations should give accurate predictions for the fields if the antenna is on homogenous earth. Inhomogenieties in the earth, such as wires, metal objects or just earth of different electrical characteristics, can not only alter these fields, but can also create new field components. These anomalous components are generally very small compared to the strength of the primary fields, when they are produced by inhomogenieties in the earth's electrical characteristics.

Appendix V

THE COMPUTER PROGRAM FOR THE CALCULATION OF THE CURRENTS INDUCED IN A LONG BURIED CABLE BY A DISTRIBUTED CW ELECTRIC FIELD

The computer program given in this section is written in FORTRAN IV for an IBM 7044 computer. Its purpose is to compute the magnitude and the phase of the current induced in a wire in the ground, as a function of distance along the wire, from a set of known electrical impedance parameters and from a known distributed continuous-wave electric field. The results of this program were compared with wire current measurements made in dipole antenna distributed fields.

The exact equation which the program will utilize is the theoretical current relation, equation (39) in Section II (using x instead of z)

$$I(x) = Ke^{-\Gamma x} + Le^{\Gamma x} + \frac{1}{2Z_o} \int_o^d E_o(v)\ e^{-\Gamma |x-v|}\ dv$$

The length d and the frequency are known, and the propagation constant Γ is calculated, using the known electrical parameters, from the relations derived in in section III and appendix II. Then the integral is solved by the computer for each desired value of x by breaking the integral down to a summation over finite intervals. This approximation equates the integral with the total area under the curve of its function in the interval of interest, the length of the cable.

$$\int_o^d E_o(v)\ e^{-\Gamma |x_1-v|}\ dv = e^{-\Gamma x_1}\int_o^{x_1} E_o(v)\ e^{\Gamma v}\ dv + e^{\Gamma x_1}\int_{x_1}^{d} E_o(v)\ e^{-\Gamma v}\ dv$$

$$\cong e^{-\Gamma x_1} \sum_{n=1}^{I_1} E_o(v_n)\ e^{\Gamma v_n}\ \Delta v + e^{\Gamma x_1}\sum_{m=1}^{I_2} E_o(v_m) e^{-\Gamma v_m}\ \Delta v$$

where x_1 is a particular point on the cable at which the solution of the current is of interest,

Δv is one of the small finite sub-intervals on which the summations are carried out (1 meter intervals were used in the program),

$I_1 = \frac{x_1}{\Delta v}$, the total number of sub-intervals in the interval of the first integral,

$I_2 = \frac{d-x_1}{\Delta v}$, the total number of sub-intervals in the interval of the first integral.

v_n is the value of v in the range of the first integral at which the function $E_o(v)e^{\Gamma v}$ is equal to its average value over the nth interval in this range (this will be taken, to a very good approximation for small Δv, at the midpoint of the nth interval; $v_n = \frac{n\Delta v + (n-1)\Delta v}{2}$), and v_m is the value of v in the range of the second integral at which the function $E_o(v)e^{-\Gamma v}$ is equal to its average value over the mth interval in this range (by the same reasoning as above, $v_m = \frac{m\Delta v + (m-1)\Delta v}{2} + x_1$).

The electric field used in the integration was the radial surface dipole electric field as theoretically determined in appendix IV, equation (76), using the soil and antenna parameters supplied by the Stanford Research Institute measurements (reference 3).

When the integral term of the solution was calculated for all desired x_1, the integral terms for $x_1 = 0$ and $x_1 = d$ were used along with the postulated termination impedances of the given wire at each frequency to determine the reflection constants K and L from the relations derived in appendix III, equation (66).

Note that practically all parameters necessary for the calculation of the currents are complex quantities. The compiler used had no way of handling complex quantities. Therefore, the calculations of these parameters, including the calculation of the propagation constant, the calculation of the reflection terms and the integration method itself has to be performed in two parts; one for the real output and one for the imaginary output.

Once the reflection terms are known, the integral term having been calculated beforehand, the real and imaginary components of the current are calculated. From these components, both the magnitude and phase of the current can be found by:

$$\text{Magnitude } [I(x)] = [I(x)^2 \text{ (real)} + I(x)^2 \text{ (imaginary)}]^{1/2}$$

$$\text{Phase } [I(x)] = \text{Tan}^{-1} \left[\frac{I(x) \text{ (Imaginary)}}{I(x) \text{ (real)}}\right] \frac{360°}{2\Pi \text{ radians}}$$

The result of these calculations, along with several of the parameters involved in the calculation, are printed out on paper and written on magnetic tape, the latter for the purpose of plotting the results by machine later.

The running time for the program, using six separate frequencies and approximately 250 values of x_1 per frequency, is close to 3 minutes. The running time goes as high as 5 minutes when the output is for 11 frequencies. The use of a binary deck instead of a FORTRAN read-in could save some time.

Table I

THE COMPUTER PROGRAM

```
C     CURRENT INDUCED IN A GROUND CABLE BY FIELD FROM A DIPOLEANTENNA
      COMMON RE1(1000),COM1(1000),RE2(1000),COM2(1000),AR,AI
      COMMON OM,GAMR,GAMI,RA,D,CMU,EG,EO,PI,SIG,I,DX,DV,CL
      COMMON GP,CP,R,DELTA2,KFR,N,GAMGR,GAMGI,W(8),CK,H
      DIMENSION AF(1000),BF(1000)
      PRINT 36
      CMU=1.27E-6
      EO=8.85E-12
      ETAA=SQRT(CMU/EO)
      PI=3.14159265
      READ 29,SIG,AA,AB,AC
      READ 30,D,RA,RAA
      READ 31,CMUW,SIGW,DECON,CT,SIGI
      EI=DECON*EO
      READ 32,DX,DV
      READ 33,AZ1,BZ1,AZ2,BZ2
      READ 34,ALTC,SCAFAC
      I=D/DX+1.
      DI=I-1
      DJ=D-DI*DX
      IF (DJ) 2,2,1
1     I=I+1
2     IF (CT) 3,3,4
3     C=1.E10
      GO TO 5
4     C=PI*EI/ALOG((RAA+CT)/RAA)/ALTC
5     WRITE (4,27) RA,I
      DO 25 KFR=1,1000
      READ 35,(W(N),N=1,8)
      WRITE (4,28) (W(N),N=1,8)
      DO 24 N=1,8
      FREQ=W(N)
      IF (FREQ-9.E19) 6,42,42
6     PRINT 37,FREQ
      PRINT 38
      EG=((AA/FREQ)**AB+1.)*AC*EO
      OM=2.*PI*FREQ
      DELTA2=(1./(PI*FREQ*CMU*SIG))**0.5
      DELTA=(1./(PI*FREQ*CMUW*SIGW))**0.5
      IF (RAA-DELTA) 7,8,8
7     DELTA=RAA
8     R=1./(SIGW*PI*(RAA**2-(RAA-DELTA)**2))
      CL=CMU/(2.*PI)*ALOG((RAA+CT+DELTA2)/RAA)+R/(2.*PI*FREQ)
      CG=PI*EG/ALOG((RAA+CT+DELTA2)/(RAA+CT))
      GG=PI*SIG/ALOG((RAA+CT+DELTA2)/(RAA+CT))
      RG=1./GG
      GI=C*SIGI/EI*ALTC
      DENO=(GI+GG)**2+OM*OM*(C+CG)**2
      ANUM1=(GI+GG)*(GI*GG-OM*OM*C*CG)+OM*OM*(C+CG)*(GI*CG+GG*C)
      ANUM2=(GI+GG)*(GI*CG+GG*C)-(C+CG)*(GI*GG-OM*OM*C*CG)
```

```
      GP=ANUM1/DENO
      CP=ANUM2/DENO
      GAMR=((R*GP-(2.*PI*FREQ)**2*CL*CP+(((2.*PI*FREQ*CL)**2+R**2)*((2.*
     1PI*FREQ*CP)**2+GP**2))**0.5)/2.)**0.5
      GAMI=OM*(CL*GP+R*CP)/(2.*GAMR)
      AZ0=(GAMR*GP+GAMI*OM*CP)/(GP*GP+OM*CP*OM*CP)
      BZ0=(GAMI*GP-GAMR*OM*CP)/(GP*GP+OM*CP*OM*CP)
      IF (AZ1) 9,10,10
9     AZ1=AZ0
10    IF (BZ1) 11,12,12
11    BZ1=BZ0
12    IF (AZ2) 13,14,14
13    AZ2=AZ0
14    IF (BZ2) 15,16,16
15    BZ2=BZ0
16    CALL ARGH (FREQ)
      U=0.
      CDEN=2.*(AZ0*AZ0+BZ0*BZ0)
      BR=(AR*AZ0+AI*BZ0)/CDEN
      BI=(AI*AZ0-AR*BZ0)/CDEN
      DO 19 L=1,I
      SI3=SIN(GAMI*U)
      CO3=COS(GAMI*U)
      AFS=CO3*(RE1(L)+RE2(L))+SI3*(COM1(L)-COM2(L))
      BFS=CO3*(COM1(L)+COM2(L))+SI3*(RE2(L)-RE1(L))
      AF(L)=BR*AFS-BI*BFS
      BF(L)=BR*BFS+BI*AFS
      IF (D-U) 20,20,17
17    U=U+DX
      IF (D-U) 18,19,19
18    U=D
19    CONTINUE
20    A1=(AZ1+AZ0)*SCAFAC
      B1=(BZ1+BZ0)*SCAFAC
      A2=(AZ2+AZ0)*SCAFAC
      B2=(BZ2+BZ0)*SCAFAC
      S1=(AZ1-AZ0)*SCAFAC
      T1=(BZ1-BZ0)*SCAFAC
      S2=(AZ2-AZ0)*SCAFAC
      T2=(BZ2-BZ0)*SCAFAC
      BDEXP=EXP(-GAMR*D)
      BDEXP2=BDEXP**2
      SI=SIN(GAMI*D)
      CO=COS(GAMI*D)
      ADEN=((A2*A1-B2*B1)*CO-(A2*B1+B2*A1)*SI)-((S2*S1-T2*T1)*CO+(S2*T1+
     1T2*S1)*SI)*BDEXP2
      BDEN=((A2*A1-B2*B1)*SI+(A2*B1+B2*A1)*CO)+((S2*S1-T2*T1)*SI-(S2*T1+
     1T2*S1)*CO)*BDEXP2
      AKN=((S1*S2-T1*T2)*AF(I)-(S1*T2+T1*S2)*BF(I))*BDEXP-((S1*A2-T1*B2)
     1*(AF(1)*CO-BF(1)*SI)-(S1*B2+T1*A2)*(AF(1)*SI+BF(1)*CO))
```

```
      BKN=((S1*S2-T1*T2)*BF(I)+(S1*T2+T1*S2)*AF(I))*BDEXP-((S1*A2-T1*B2)
     1*(AF(1)*SI+BF(1)*CO)+(S1*B2+T1*A2)*(AF(1)*CO-BF(1)*SI))
      ALN=((S1*S2-T1*T2)*(AF(1)*CO+BF(1)*SI)+(S1*T2+T1*S2)*(AF(1)*SI-BF(
     11)*CO))*BDEXP-(S2*A1-T2*B1)*AF(I)+(S2*B1+T2*A1)*BF(I)
      BLN=((S1*T2+T1*S2)*(AF(1)*CO+BF(1)*SI)-(S1*S2-T1*T2)*(AF(1)*SI-BF(
     11)*CO))*BDEXP-(S2*A1-T2*B1)*BF(I)-(S2*B1+T2*A1)*AF(I)
      AK=(AKN*ADEN+BKN*BDEN)/(ADEN**2+BDEN**2)
      BK=(-AKN*BDEN+BKN*ADEN)/(ADEN**2+BDEN**2)
      AL=(ALN*ADEN+BLN*BDEN)/(ADEN**2+BDEN**2)
      BL=(-ALN*BDEN+BLN*ADEN)/(ADEN**2+BDEN**2)
      Y=0.
      DO 23 K=1,I
      IF (Y-D) 22,22,21
21    Y=D
22    SI2=SIN(GAMI*Y)
      CO2=COS(GAMI*Y)
      BDEXP3=EXP(-GAMR*Y)
      BDEXP4=EXP(-GAMR*(D-Y))
      CIA=(AK*CO2+BK*SI2)*BDEXP3+(AL*CO2-BL*SI2)*BDEXP4+AF(K)
      CIB=(BK*CO2-AK*SI2)*BDEXP3+(AL*SI2+BL*CO2)*BDEXP4+BF(K)
      AMAG=SQRT(CIA*CIA+CIB*CIB)
50    PHASE=ATAN2(CIB,CIA)*360./(2.*PI)
54    BMAG=SQRT(AF(K)*AF(K)+BF(K)*BF(K))
      BPHASE=ATAN2(BF(K),AF(K))*360./(2.*PI)
      PRINT 39,Y,CIA,CIB,AMAG,PHASE,AF(K),BF(K),BMAG,EZ1
      WRITE (4,26) Y,AMAG,PHASE
      Y=Y+DX
23    CONTINUE
      PRINT 40,GAMR,GAMI
      PRINT 43,EI,GI,C,RG,CG
      PRINT 41,CK,AZO,BZO,GP,CP,EG,CL,R
24    CONTINUE
25    CONTINUE
26    FORMAT (3E15.5)
27    FORMAT (E15.5,I5)
28    FORMAT (8E15.5)
29    FORMAT (2E10.3,2F10.1)
30    FORMAT (3E10.3)
31    FORMAT (2E10.3,F10.2,2E10.3)
32    FORMAT (2F10.2)
33    FORMAT (4E10.2)
34    FORMAT (F10.3,E10.1)
35    FORMAT (8E10.3)
36    FORMAT (1H1,43X,32HGROUND CURRENT FROM DIPOLE FIELD/1H-/)
37    FORMAT (1H-/1H ,60X,5HFREQ=,E9.3/1H )
38    FORMAT (1HO,8X,1HY,13X,3HCIA,10X,3HCIB,10X,4HAMAG,9X,5HPHASE,8X,2H
     1AF,12X,2HBF,12X,4HBMAG,10X,6HBPHASE/1H )
39    FORMAT (9E14.4)
40    FORMAT (2E14.4)
43    FORMAT(5E14.4)
41    FORMAT (8E14.4/1H1)
42    END FILE 4
      REWIND 4
      END
```

```
      SUBROUTINE ARGH (FREQ)
      COMMON RE1(1000),COM1(1000),RE2(1000),COM2(1000),AR,AI
      COMMON OM,GAMR,GAMI,RA,D,CMU,EG,EO,PI,SIG,I,DX,DV,CL
      COMMON GP,CP,R,DELTA2,KFR,N,GAMGR,GAMGI,W(8),CK,H
      GAM1=OM*OM*CMU*EG
      GAM2=OM*CMU*SIG
      GAMGR=SQRT((SQRT(GAM1*GAM1+GAM2*GAM2)-GAM1)/2.)
      GAMGI=SQRT((GAM1+SQRT(GAM1*GAM1+GAM2*GAM2))/2.)
      COETA=SQRT(SIG*SIG+OM*EG*OM*EG)
      ETAR=SQRT((GAM1+SQRT(GAM1*GAM1+GAM2*GAM2))/2.)/COETA
      ETAI=SQRT((-GAM1+SQRT(GAM1*GAM1+GAM2*GAM2))/2.)/COETA
      CK=OM*(CMU*EO)**0.5
      QID=I-2
      X=0.
      EX=QID*DX
      QUO=D-EX
      QUK=EXP(-GAMR*QUO)
      QUJ=EXP(-GAMR*DX)
      QUI=QUJ
      IF (KFR-1) 1,1,3
1     IF (N-1) 2,2,3
2     READ 17,H,CA,VA
      RE1(1)=0.
      COM1(1)=0.
      RE2(I)=0.
      COM2(I)=0.
      M=DX/DV
3     AR=0.
      AI=FREQ*CA*VA
      DO 15 J=1,I
      Z=0.
      Q=0.
      IF (X) 12,12,4
4     NBB=I-J+1
      NCB=I-J+2
      NAB=J-1
      QWQ=J-2
      RE2(NBB)=RE2(NCB)*QUI
      COM2(NBB)=COM2(NCB)*QUI
      IF (D-X) 5,5,6
5     QUI=QUK
6     RE1(J)=RE1(NAB)*QUI
      COM1(J)=COM1(NAB)*QUI
      Z=Z+QWQ*DX+DV/2.
      Q=Q+EX+DV/2.
      DO 11 II=1,M
      IF (D-Z) 8,8,7
7     R1=RA+Z
      COEF1=CK*(PI/2.-ATAN2(R1,H)+R1/H*ALOG(R1/SQRT(R1*R1+H*H)))
      COEF2=(H/R1+R1/H)/SQRT(R1*R1+H*H)-1./H
```

```
      COEF3=1./(SIG*R1*R1)*EXP(-GAMGR*R1)
      ERR=(ETAR*COS(CK*R1)+ETAI*SIN(CK*R1))*COEF2-(ETAI*COS(CK*R1)-ETAR*
     1SIN(CK*R1))*COEF1+COEF3*COS(GAMGI*R1)
      ERR=-ERR
      ERI=(ETAI*COS(CK*R1)-ETAR*SIN(CK*R1))*COEF2+(ETAR*COS(CK*R1)+ETAI*
     1SIN(CK*R1))*COEF1-COEF3*SIN(GAMGI*R1)
      ERI=-ERI
      COCO=COS(GAMI*Z)
      SISI=SIN(GAMI*Z)
      DEX=EXP(-GAMR*(X-Z))
      RE1(J)=RE1(J)+(ERR*COCO-ERI*SISI)*DEX*DV
      COM1(J)=COM1(J)+(ERR*SISI+ERI*COCO)*DEX*DV
8     Z=Z+DV
      IF (D-Q) 10,10,9
9     R1=RA+Q
      COEF1=CK*(PI/2.-ATAN2(R1,H)+R1/H*ALOG(R1/SQRT(R1*R1+H*H)))
      COEF2=(H/R1+R1/H)/SQRT(R1*R1+H*H)-1./H
      COEF3=1./(SIG*R1*R1)*EXP(-GAMGR*R1)
      ERR=(ETAR*COS(CK*R1)+ETAI*SIN(CK*R1))*COEF2-(ETAI*COS(CK*R1)-ETAR*
     1SIN(CK*R1))*COEF1+COEF3*COS(GAMGI*R1)
      ERR=-ERR
      ERI=(ETAI*COS(CK*R1)-ETAR*SIN(CK*R1))*COEF2+(ETAR*COS(CK*R1)+ETAI*
     1SIN(CK*R1))*COEF1-COEF3*SIN(GAMGI*R1)
      ERI=-ERI
      COCO=COS(GAMI*Q)
      SISI=SIN(GAMI*Q)
      DEX=EXP(-GAMR*(Q-EX))
      RE2(NBB)=RE2(NBB)+(ERR*COCO+ERI*SISI)*DEX*DV
      COM2(NBB)=COM2(NBB)+(ERI*COCO-ERR*SISI)*DEX*DV
10    Q=Q+DV
11    CONTINUE
      EX=EX-DX
12    IF (D-X) 16,16,13
13    X=X+DX
      IF (D-X) 14,15,15
14    X=D
15    CONTINUE
16    RETURN
17    FORMAT (F10.2,2E10.3)
      END
```

The following variables must be read into the program on data cards (see table I):

SIG is the conductivity of the earth in mhos per meter.

AA,AB, and AC are the parameters to determine the dielectric constant of the earth. Measurements by Scott of the U.S. Geodetic Survey (reference 12) indicate that the dielectric constant of soil is frequency dependent. His curves of dielectric constant against frequency (see figure 47) indicate a dependence approximated by the relation

$$\frac{\varepsilon_2}{\varepsilon_o} = \left[\left(\frac{AA}{f} \right)^{AB} - 1 \right] \cdot AC$$

where AC is the high frequency level-off value, AB is the exponent of the low frequency fall-off and AA is the frequency where

$$\frac{\varepsilon_2}{\varepsilon_o} = 2\ AC$$

D is the length of the wire in meters.

RA is the distance from the dipole antenna to the nearest end of the wire in meters.

RAA is the radius of the wire in meters.

CMUW is the magnetic permeability of the wire in henrys per meter.

SIGW is the conductivity of the wire in mhos per meter.

DECON is the dielectric constant of the insulating material.

CT is the thickness of the insulation in meters. If the wire is bare, the value will be read in as zero.

SIGI is the conductivity of the wire covering in mhos per meter. If the covering is insulation, this value will be read in as zero.

DX is the incremental distance between the points along the wire, at which the current will be calculated, in meters, starting with the endpoint nearest to the dipole antenna.

DV is the incremental distance in meters used in the integration subroutine for the numerical integration term of the solution. The value used has been 1 meter, which is sufficiently small for CW fields of the frequencies of interest. In general, the wave length of the CW fields must be much greater than DV for an accurate numerical integration by the method used.

AZ1 and BZ1 are the real and imaginary parts of the termination impedance in ohms at the end of the wire nearest the dipole antenna. If these values are read

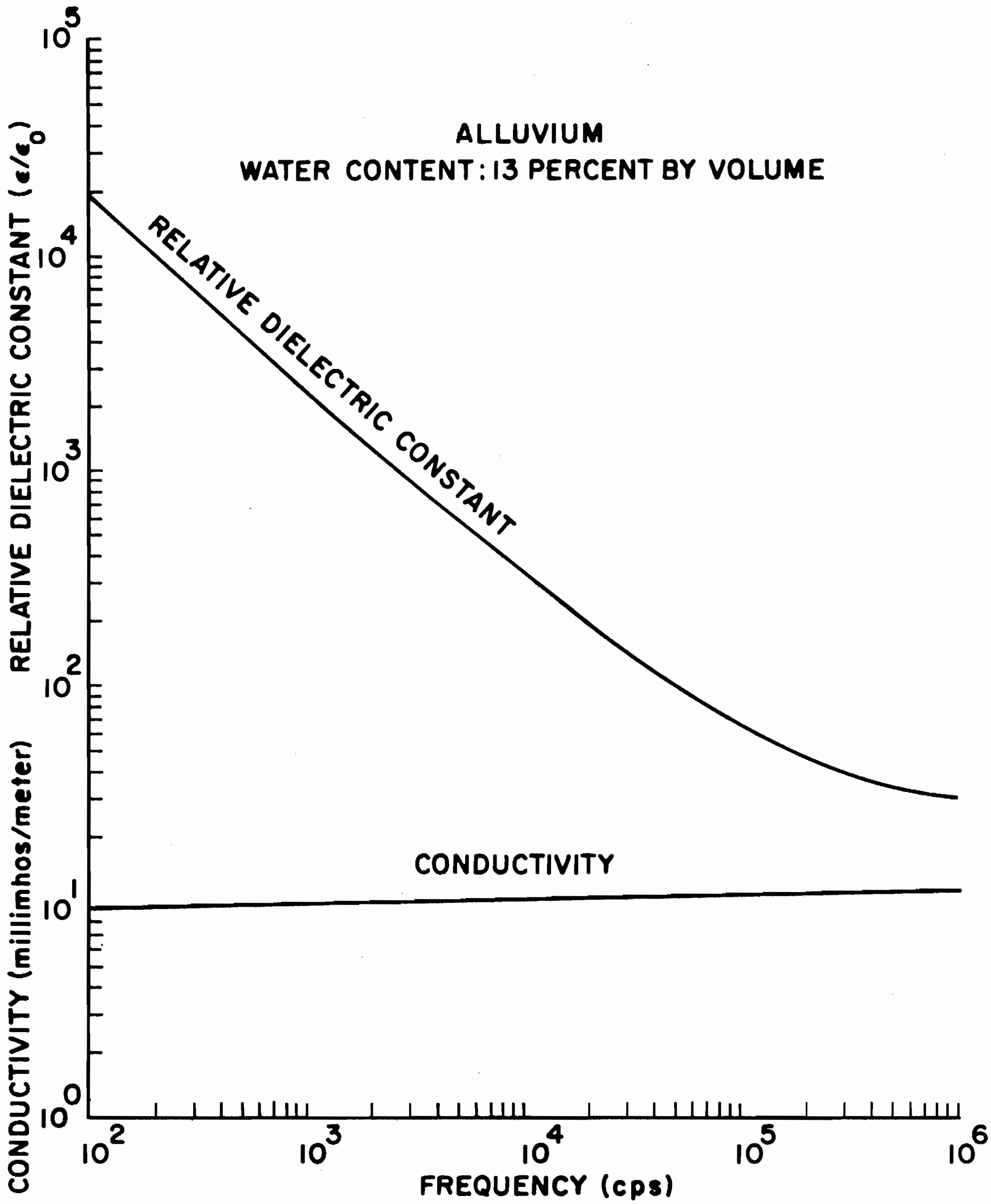

Figure 47. Relative Dielectric Constant and Conductivity Measurements for Alluvium. (Taken from reference 12, page 25.)

in as negative numbers, they will be set equal to the real and imaginary parts of the line impedance of the wire. The wire will then appear electrically to extend to infinity, except that there shall be no driving fields beyond the actual limits of the wire.

AZ2 and BZ2 are the real and imaginary parts of the termination impedance in ohms at the second end of the wire. These may also be set equal to the equivalent components of the line impedance by reading them into the program as negative numbers.

ALTC is a number to arbitrarily change the value of the capacitance of the insulation by $C_i = C/ALTC$, where C is the capacitance calculated from the insulation dimensions and dielectric constant. The purpose of this factor in the program is to attempt to determine the effects of non-ideal electrical contact with the earth. If there is a sizeable discrepancy between the theory and the data in the magnitude of the currents the reason for discrepancy can often be determined by a simple change of the insulation capacitance. This constant will be set equal to 1 for all practical cases of current calculation.

SCAFAC is a scaling factor necessary in the IBM 7044 (which will overflow above 10^{38}), to prevent overflow in the calculation of the reflection terms. This factor is read in as 10^{-5}, unless an overflow readout indicates that a smaller factor is necessary.

W(N) are the frequencies, which are read into the program one card of eight frequencies at a time. Any frequency cards after the first card will be placed at the end of the data deck. After the last frequency on the cards, the number 1×10^{20} will be read in, which will end the program immediately.

For the subroutine:

H in the subroutine is the height of the dipole antenna; 30.5 meters for the SRI antenna.

CA in the subroutine is the effective capacitance of the antenna in farads. The SRI antenna input impedance was determined by measurement to be a practically pure capacitive reactance equivalent to that produced by a 400-picofarad capacitance.

VA is the applied antenna voltage in volts. In the test calculations a voltage of 1 kilovolt was used for simplicity.

ERR and ERI are the real and imaginary components of the electric field, respectively. In this program listing, the electric field is the radial electric field at the surface of the earth produced by a vertical grounded dipole antenna of finite height and infinitesimal thickness. Note that R1 is the distance from the antenna in meters, and Q and Z are the distances from the termination of the cable nearest to the dipole antenna.

Any desired distributed CW electric field may be used in this program by placing it in the proper form in the two places where ERR and ERI are found.

The answers printed out by this program as written here are:

FREQ, the frequency of the CW electromagnetic wave used.

Y, the distance along the cable in meters from the termination of the cable nearest the dipole antenna.

CIA and CIB, the real and imagninary parts of the total current magnitude, including reflections, induced into the cable.

AMAG and PHASE, the magnitude of the total current, including reflections, and its phase with respect to the phase of the antenna voltage.

AF(K) and BK(K), the real and imaginary part of the induced current in the cables, ignoring the reflection terms.

BMAG and BPHASE, the magnitude of the induced current, ignoring reflections, and its phase relative to the phase of the dipole antenna voltage.

These 9 quantities are printed out in a block after the frequency. In the third to the last line of the block, we have printed out:

GAMR and GAMI, the real and imaginary components of the propagation constant Γ for the cable.

In the second to the last line of the block, we have printed out:

EI, the dielectric permittivity in farads per meter of the wire covering, if any covering is present. Otherwise, this number will be ignored.

GI, the conductive admittance in mhos per meter of the wire covering if any covering is present. Otherwise, this number will be ignored.

C, the capacitance per unit length in farads per meter of the wire covering, if any covering is present. Otherwise, the number will be ignored.

RG, the effective resistance from the cable (including covering) to the earth. It is the inverse of GG, the admittance per unit length in mhos per meter from the cable (including covering) to the surrounding earth.

CG, the effective capacitance per unit length in farads per meter between the cable (including covering) and the surrounding earth.

In the final line of print out in each frequency block, we have the following quantities:

CK, the propagation constant of an electromagnetic wave in the air in meters^{-1}.

AZO and BZO, the real and imaginary parts of the effective transmission line impedance of the cable in ohms.

GP, the real part of the transverse admittance per unit length of the cable in mhos per meter (see appendix I).

CP, the imaginary part of the transverse admittance per unit length of the cable divided by the radian frequency of the signal. This quantity will be the effective total capacitance per unit length of the cable in farads per meter.

EG, the dielectric permittivity of the earth, at the given frequency, in farads per meter.

CL, the inductance per unit length of the cable in henries per meter.

R, the longitudinal resistance per unit length of the cable in ohms per meter.

Also a product of the program, as previously stated, is the Tape 4, which contains W(N), RA, I, and all values of Y, AMAG and PHASE. This tape is run into a plot program with the available data, which produces a plot tape. The plot tape is then run through a CALCOMP plot machine to produce the graphs seen in the results of this paper (section IV).

Note that the program as written will give the phase of the currents with respect to the phase of the antenna voltage. The results, however, are stated in terms of a current phase relative to the phase of the vertical electric field. For this purpose statement number 50 must be replaced with the group of statements in table II.

Table II

STATEMENTS TO DETERMINE PHASE WRT
VERTICAL ELECTRIC FIELD

```
      APHASE=ATAN2(CIB,CIA)*360./(2.*PI)
      R2=RA+Y
      AT=ATAN2(R2,H)
      SIZ=R2/SQRT(R2*R2+H*H)
      COZ=H/SQRT(R2*R2+H*H)
      SIX=SIN(CK*R2)
      COX=COS(CK*R2)
      COF1=OM*CMU*(COZ+R2/H*(SIZ-1.))
      COF2=(COZ-COZ**3/3.+R2/(3.*H)*((SIZ**3-1.)))/(OM*EO*R2*R2)
      COF3=ETAA*(PI/2.-AT+SIN(2.*AT)/2.+R2/H*(SIZ*SIZ-1.))/(2.*R2)
      EZ1R=AR*(SIX*(COF1-COF2)+COX*COF3)+AI*(SIX*COF3-COX*(COF1-COF2))
      EZ1R=-EZ1R
      EZ1I=AR*(COX*(COF1-COF2)-SIX*COF3)+AI*SIX*(COF1-COF2)+AI*COX*COF3
      EZ1I=-EZ1I
      EZ1=SQRT(EZ1R*EZ1R+EZ1I*EZ1I)
      PHEZ1=ATAN2(EZ1I,EZ1R)*360./(2.*PI)
      P1=APHASE-PHEZ1
      AMOUR=ABS(P1)
      IF(AMOUR-180.)50,50,51
50    PHASE=P1
      GO TO 54
51    IF(APHASE)52,52,53
52    PHASE=360.+P1
      GO TO 54
53    PHASE=P1-360.
```

REFERENCES

1. E. Hanson and S. K. Waldorf, "An Eight-Year Investigation of Lightning Currents and Preventive Lightning Protection on a Transmission System," AIEE, 63. (May 1944).

2. "EMP: Can it Short Circuit Our Defenses?" Electronic Design, pp. 6-14, (2 March 1964).

3. AFWL-TR-65-39, "Electromagnetic Field Distortions and Currents In and Near Buried Cables and Bunkers," Final Report on Contract AF29(601)-5904 with Stanford Research Institute, (July 1965).

4. F. B. Hildebrand, Advanced Calculus for Engineers, Prentice-Hall, Inc., New Jersey, (1948).

5. J. A. Stratton, Electromagnetic Theory, McGraw-Hill Book Co., Inc., New York (1941).

6. H. Hertz, Ann. Physik, 36, (1888).

7. S. Ramo and J. R. Whinnery, Fields and Waves in Modern Radio, 2nd Edition, John Wiley and Sons, Inc., New York, (1962).

8. R. M. Whitmer, Electromagnetics, Prentice-Hall, Inc., New Jersey, (1952).

9. E. D. Sunde, Earth Conduction Effects in Transmission Systems, D. Van Nostrand and Co., Ltd., New York, (1949).

10. R. D. Carroll and D. R. Cunningham, Ground Conductivity Changes - Dipole Antenna and Small Boy Sites - Nevada Test Site, United States Geological Survey Technical Letter, Special Project - 14, (16 June 1964).

11. J. D. Kraus, Antennas, McGraw-Hill Book Co., Inc., New York, (1950).

12. J. H. Scott, R. D. Carroll, and D. R. Cunningham, Dielectric Constant and Electrical Conductivity of Moist Rock from Laboratory Measurements, United States Geological Survey Technical Letter, Special Projects - 12, (17 August 1964).